arXiv:math-ph/0105048v1 30 May 2001

Copyright by

Jean-Marie Linhart

NUMERICAL INVESTIGATIONS OF SINGULARITY FORMATION IN NON-LINEAR WAVE EQUATIONS IN THE ADIABATIC LIMIT

by

JEAN-MARIE LINHART, B.S., M.A.

DISSERTATION

Presented to the Faculty of the Graduate School of

The University of Texas at Austin

in Partial Fulfillment

of the Requirements

for the Degree of

DOCTOR OF PHILOSOPHY

THE UNIVERSITY OF TEXAS AT AUSTIN

May 1999

NUMERICAL INVESTIGATIONS OF SINGULARITY FORMATION IN NON-LINEAR WAVE EQUATIONS IN THE ADIABATIC LIMIT

	DISSERTATION COMMITTEE:
Supervisor:	

APPROVED BY



Acknowledgments

Lorenzo Sadun, my dissertation supervisor, managed to drag me through this (kicking and screaming, sometimes), and he deserves a great deal of admiration for that difficult feat as well as gratitude from me.

Ivanna Albertin has been my mentor, supervisor and friend while I've been working for Schlumberger Well Services while completing my dissertation. She's helped me to learn about problems in the real world and also that there is a good life beyond the ivory tower. She made it possible for me to work on my dissertation at my own pace. She often reminded me that I better just hang on and get done, and so I have. Every day I am grateful for her guidance and friendship.

My father, George Linhart, has repeatedly come to my aid morally and financially while I have been working on my doctorate; sometimes he gave me help that I needed even when I was insisting that I didn't need it. Dad taught me that it is only important to get it right in the end, and I know he loves me even when I am (considerably) less than perfect. Even when I doubted, he always knew that I had what it takes to get a Ph.D.

My teacher, John Blankenship, reminded me many times that my best is always good enough and that to obtain success all I have to do is to chop the wood and carry the water and chop the wood and carry the water and so forth and so on, ad nauseum. His school provided a place of sanity for me when graduate school was anything but sane. I appreciate his support and the support of all my brothers and sisters (also known as instructors, friends, comrades and flying femmes) at Austin Cha Yon Ryu.

There are many friends who were there for me while I've been working on this degree. Marcia Branstetter, Joanna McDaniel, Heather Caldwell and Eric Hollas all deserve a special mention. NUMERICAL INVESTIGATIONS OF SINGULARITY FORMATION IN NON-LINEAR WAVE EQUATIONS IN THE ADIABATIC LIMIT

Publication No.

Jean-Marie Linhart, Ph.D. The University of Texas at Austin, 1999

Supervisor: Lorenzo Sadun

This dissertation deals with singularity formation in spherically symmetric solutions of the hyperbolic Yang Mills equations in (4+1) dimensions and in spherically symmetric solutions of $\mathbb{C}P^1$ wave maps in (2+1) dimensions. These equations have known moduli spaces of time-independent (static) solutions. Evolution occurs close to the moduli space of static solutions. The evolution is modeled numerically using an iterative finite differencing scheme, and modeling is done close to the adiabatic limit, *i.e.*, with small velocities. The stability of the numerical scheme is analyzed and growth is shown to be bounded, yielding a convergence estimate for the numerical scheme. The trajectory of the approach is characterized, as well as the shape of the profile at any given time during the evolution.

vii

Table of Contents

Acl	cnowle	edgments	\mathbf{V}		
Ab	stract		vii		
List	t of Ta	ables	xi		
List	t of Fi	gures	xii		
Cha	apter	1. Introduction	1		
1.1	Introd	luction to the equations	1		
1.2	Introd	luction to the adiabatic limit	5		
Cha	apter :	2. The 4+1 dimensional model	8		
2.1	Nume	rics for the 4+1 dimensional model	10		
2.2	Predic	etions	12		
2.3	Result	ts	14		
	2.3.1	Evolution of $f(0,t)$	14		
	2.3.2	Characterization of time slices $f(r,T)$: evolution of a horizontal line	17		
	2.3.3	Characterization of time slices $f(r,T)$: evolution of a parabola	23		
Cha	apter :	3. The $\mathbb{C}P^1$ model, charge 1 sector	29		
3.1	Nume	rics for the $\mathbb{C}P^1$ charge 1 sector model	30		
3.2					
3.3	Result	ts	35		
	3.3.1	Evolution of $f(0,t)$	35		
	3.3.2	Characterization of time slices $f(r,T)$	44		

Cha	apter 4. The $\mathbb{C}P^1$ model, charge 2 sector	53				
4.1	Numerics for the $\mathbb{C}P^1$ charge 2 sector model					
4.2	Predictions					
4.3	Results	56				
	4.3.1 Evolution of $f(0,t)$	56				
	4.3.2 Characterization of time slices $f(r,T)$: evolution of a horizontal ine	59				
	4.3.3 Characterization of time slices $f(r,T)$: evolution of a parabola	64				
Cha	apter 5. Conclusions	70				
App	pendices	73				
App	pendix A. Stability and convergence of the 4+1 dimensional model	74				
A.1	Continuum stability: simplified model	75				
A.2	The whole equation	77				
A.3	Discretization scheme	79				
A.4	Outline of the stability analysis	80				
A.5	Stability near zero	81				
A.6	Stability away from zero: simplified model	89				
A.7	The complications	93				
A.8	Convergence estimates	99				
Apj	pendix B. Stability and convergence of the $\mathbb{C}P^1$ model, charge 1 sector	L09				
B.1	Continuum stability: simplified model	109				
B.2	Continuum stability	111				
В.3	Discretization scheme	112				
B.4	Outline of stability analysis	113				
B.5	Stability near zero	113				
B.6	Stability away from zero: simplified model	119				
B.7	The complications	122				
B.8	Convergence estimates	128				

Bibliography	136
Vita	137

List of Tables

2.1	4+1 Dimensional Model, parabolic fit to $f(0,t)$ vs. Initial conditions f_0 and v_0						
2.2	4+1 Dimensional Model, Elliptical Parameters vs. Initial Conditions f_0 and v_0						
3.1	$\mathbb{C}P^1$ model, charge 1 sector: Parameters for best fit line to $f(0,t)$ vs. initial data f_0 and v_0	39					
3.2	$\mathbb{C}P^1$ model, charge 1 sector: c and R vs. $\triangle r$ and $\triangle t$. $f_0 = 1.0$ and $v_0 = -0.01$	40					
3.3	$\mathbb{C}P^1$ model, charge 1 sector: c and R vs. v_0 . $f_0 = 1.0$	41					
3.4	$\mathbb{C}P^1$ model, charge 1 sector: c and R vs. f_0 . $v_0 = -0.01$	42					
3.5	$\mathbb{C}P^1$ model, charge 1 sector: Best fit line to evolution of $-b/a$ slope m and intercept b_i vs. f_0	46					
3.6	$\mathbb{C}P^1$ model, charge 1 sector: Best fit line to evolution of $-b/a$ slope m and intercept b_i vs. v_0	47					
4.1	$\mathbb{C}P^1$ model, charge 2 sector: Parameters for best fit parabola to $f(0,t)$ vs. initial data f_0 and v_0	57					
4.2	$\mathbb{C}P^1$ model, charge 2 sector, Elliptical parameters vs. initial conditions f_0 and v_0	61					
A.1	4+1 dimensional model: Convergence data 1	107					
A.2	4+1 dimensional model: Convergence data 2	107					
A.3	4+1 dimensional model: Convergence data 3	107					
A.4	$4+1$ dimensional model: Convergence data $4.\dots\dots$	108					
B.1	$\mathbb{C}P^1$ model, charge 1 sector: Convergence data 1	134					
B.2	$\mathbb{C}P^1$ model, charge 1 sector: Convergence data 2	134					
B.3	$\mathbb{C}P^1$ model, charge 1 sector: Convergence data 3	134					
B.4	$\mathbb{C}P^1$ model, charge 1 sector: Convergence data 4	135					

List of Figures

2.1	4+1 dimensional model, evolution $f(0,t)$	16
2.2	4+1 Dimensional model, Time Slices $f(r,T)$ evolve an elliptical bump at the origin	19
2.3	$4+1$ dimensional model: elliptical parameter a as a function of time when $f_0=4.0$ and $v_0=-0.01.\ldots$	20
2.4	$4+1$ dimensional model: elliptical parameter b as a function of time when $f_0 = 4.0$ and $v_0 = -0.02$	21
2.5	$4+1$ dimensional model: elliptical parameter k as a function of time when $f_0=2.0$ and $v_0=-0.01.\ldots$	22
2.6	4+1 dimensional model: Time slices of the evolution of a parabola are parabolas	26
2.7	4+1 dimensional model: evolution of parabolic parameter p with time	27
2.8	4+1 dimensional model: Parabolic parameter h as a function of time evolves as $f(0,t)$	28
3.1	$\mathbb{C}P^1$ model, charge 1 sector: Example plot of $f(0,t)$ vs ct as predicted by the effective Lagrangian	34
3.2	$\mathbb{C}P^1$ model, charge 1 sector: Time slices $f(r,T)$	39
3.3	$\mathbb{C}P^1$ model, charge 1 sector: Evolution of $f(0,t)$ is not quite linear	40
3.4	$\mathbb{C}P^1$ model, charge 1 sector: Plot of $1/(\dot{f})^2$ vs $\ln(f)$ and the best fit line to this data	41
3.5	$\mathbb{C}P^1$ model, charge 1 sector: Predicted course of $f(0,t)$ from equation [3.5] and actual course of $f(0,t)$ vs. t	42
3.6	$\mathbb{C}P^1$ model, charge 1 sector: R vs 1/v0 and the best fit parabola.	43
3.7	$\mathbb{C}P^1$ model, charge 1 sector: Time slices evolve hyperbolic bump at origin	46
3.8	$\mathbb{C}P^1$ model, charge 1 sector: Plot of hyperbolic parameter a vs time, $f_0 = 1.0, v_0 = -0.01$	47

3.9	$\mathbb{C}P^1$ model, charge 1 sector: Plot of hyperbolic parameter b vs time, $f_0 = 1.0, v_0 = -0.01$	48
3.10	$\mathbb{C}P^1$ model, charge 1 sector: Plot of hyperbolic parameter k vs time, $f_0 = 1.0, v_0 = -0.01$	49
3.11	$\mathbb{C}P^1$ model, charge 1 sector: Plot of hyperbolic parameter $-b/a$ vs time, $f_0 = 1.0, v_0 = -0.01.$	50
3.12	$\mathbb{C}P^1$ model, charge 1 sector: Plot of slope m vs initial velocity $v_0.$	51
3.13	$\mathbb{C}P^1$ model, charge 1 sector: Plot of intercept b_i vs initial velocity v_0	52
4.1	$\mathbb{C}P^1$ model, charge 2 sector: Evolution of $f(0,t)$ and overlaying fit to parabola	58
4.2	$\mathbb{C}P^1$ model, charge 2 sector: Time slices of $f(r,T)$ evolve an elliptical bump at the origin	59
4.3	$\mathbb{C}P^1$ model, charge 2 sector: Elliptical parameter a as a function of time	61
4.4	$\mathbb{C}P^1$ model, charge 2 sector: Elliptical parameter b as a function of time	62
4.5	$\mathbb{C}P^1$ model, charge 2 sector: Elliptical parameter k as a function of time	63
4.6	$\mathbb{C}P^1$ model, charge 2 sector: Time slices of the evolution of a parabola are parabolas	67
4.7	$\mathbb{C}P^1$ model, charge 2 sector: Evolution of parabolic parameter p with time	68
4.8	$\mathbb{C}P^1$ model, charge 2 sector: Evolution of parabolic parameter h with time, comparison to $f(0,t)$	69

Chapter 1

Introduction

1.1 Introduction to the equations

One of the classic problems of physics is that of the motion of a particle.

In finite dimensions, *i.e.*, in \mathbb{R}^n , we have a particle described by its position \vec{x} and velocity $\dot{\vec{x}}$, and the particle is under the influence of a potential $V(\vec{x})$ (corresponding perhaps to gravity or an electrical potential). The Lagrangian is the kinetic (energy of motion) minus the potential and is given by

$$L = \frac{1}{2}m|\dot{\vec{x}}|^2 - V(\vec{x}).$$

The Euler-Lagrange equations give the equations of motion which are

$$m\ddot{\vec{x}} = -\nabla V(\vec{x}).$$

In field theory, the position of the particle is not given by a vector $\vec{x} \in \mathbb{R}^n$ but rather by a function which is a point in an infinite dimensional vector space. Call this position $f(\vec{x})$ and instead of the inner product on \mathbb{R}^n , the inner product is based on a function space, such as the \mathcal{L}^2 inner product. Using the \mathcal{L}^2 norm as an example, if there is a potential V(f), and

the Lagrangian action is given by:

$$L = \int |\dot{f}(\vec{x})|^2 - V(f(\vec{x})) \, d\vec{x},$$

the calculus of variations gives the equations of motion

$$\ddot{f} = -\frac{\delta V}{\delta f}.$$

We will study two situations similar to this in this dissertation.

First, we address the situation of the Yang Mills Lagrangian in 4 dimensions. The Yang Mills equation is a generalization of Maxwell's equations in a vacuum. We wish our particles to have certain internal and external symmetries, which give rise to the various geometrical objects in the problem. The state of our particles are given by gauge potentials or connections A on \mathbb{R}^4 , where we identify \mathbb{R}^4 as \mathbb{H} , the quarternions. The gauge potentials have values in the Lie algebra of SU(2) which can be viewed as pure imaginary quarternions, $Im(\mathbb{H})$. The curvature $F_{ij} = \partial_i A_j - \partial_j A_i + [A_i, A_j]$ where $[A_i, A_j] = A_i A_j - A_j A_i$ is the bracket in the Lie Algebra, gives rise to the potential $V(A) = \langle F, F \rangle$ which is a nonlinear function of A. The action is:

$$L = \frac{1}{2} \int \langle F_{ij}, F_{ij} \rangle d\vec{x}. \tag{1.1}$$

The local minima of [1.1] are the instantons on 4 dimensional space. These correspond to solutions of Maxwell's equations in the vacuum, if we consider the Yang Mills Lagrangian to be a generalization of Maxwell's equations. We now consider the wave equation generated by this potential with Lagrangian:

$$L = \frac{1}{2} \int \langle \dot{A}_i, \dot{A}_i \rangle - \frac{1}{2} \langle F_{ij}, F_{ij} \rangle d\vec{x}$$
 (1.2)

Here we use the summation convention; however in taking inner products of two forms, we only sum over i < j, and not all i, j, which has here been expressed by dividing by 2 in computing $\langle F_{ij}, F_{ij} \rangle$. Now use the calculus of variations by taking $A \to A + \delta A$, to obtain

$$L(A + \delta A) =$$

$$\int \frac{1}{2} \langle \dot{A}_i, \dot{A}_i \rangle + \langle \dot{A}_i, \delta \dot{A}_i \rangle + \frac{1}{2} \langle \delta \dot{A}_i, \delta \dot{A}_i \rangle -$$

$$\frac{1}{4} \langle \partial_i A_j + \partial_i \delta A_j - \partial_j A_i - \partial_j \delta A_i + [A_i + \delta A_i, A_j + \delta A_j],$$

$$\partial_i A_j + \partial_i \delta A_j - \partial_j A_i - \partial_j \delta A_i + [A_i + \delta A_i, A_j + \delta A_j] \rangle d\vec{x}$$

Using the definition of F, one obtains

$$L(A + \delta A) = \int \frac{1}{2} \langle \dot{A}_i, \dot{A}_i \rangle + \langle \dot{A}_i, \delta \dot{A}_i \rangle + \frac{1}{2} \langle \delta \dot{A}_i, \delta \dot{A}_i \rangle - \frac{1}{4} \langle F_{ij}, F_{ij} \rangle$$
$$+ \frac{1}{2} \langle F_{ij}, \delta F_{ij} \rangle + \frac{1}{4} \langle \delta F_{ij}, \delta F_{ij} \rangle d\vec{x}.$$

One now takes the linear part of the variation,

$$\int \langle \dot{A}_i, \dot{\delta A}_i \rangle + \frac{1}{2} \langle F_{ij}, \delta F_{ij} \rangle d\vec{x},$$

and analyzes it. First work on

$$\int \langle F_{ij}, \delta F_{ij} \rangle = \int \langle F_{ij}, \partial_i \delta A_j \rangle - \langle F_{ij}, \partial_j \delta A_i \rangle + \langle F_{ij}, [\delta A_i, A_j] \rangle + \langle F_{ij}, [A_i, \delta A_j] \rangle
= \int \langle F_{ij}, \partial_i \delta A_j \rangle - \langle F_{ij}, \partial_j \delta A_i \rangle -
\operatorname{Tr}(F_{ij}(\delta A_i A_j - A_j \delta A_i + A_i \delta A_j - \delta A_j A_i))
= \int -2\langle \partial_j F_{ij}, \delta A_i \rangle - \operatorname{Tr}(F_{ij}(\delta A_i A_j - A_j \delta A_i))$$

by integration by parts and the cyclic property of traces:

$$= \int -2\langle \partial_j F_{ij}, \delta A_i \rangle - \text{Tr}(F_{ij}A_j - F_{ij}A_j))\delta A_i$$

$$= \int -2\langle \partial_j F_{ij} + [F_{ij}, A_j], \delta A_i \rangle$$

$$= \int -2\langle \nabla_j F_{ij}, \delta A_i \rangle.$$

Here ∇_j represents the covariant derivative in the j direction. Now integrate the first term by parts to obtain:

$$\int \langle \dot{A}_i, \delta \dot{A}_i \rangle d\vec{x} = -\int \langle \ddot{A}_i, \delta A_i \rangle d\vec{x}.$$

Put these two things together to get

$$\ddot{A}_i = -\nabla_j F_{ij} \tag{1.3}$$

This is our evolution equation for the 4+1 dimensional model.

The second situation to be addressed is that of the $\mathbb{C}P^1$ model in 2+1 dimensions.

In the finite dimensional analog of this case, we consider motion on a manifold under the influence of a potential. The Lagrangian in this case is

$$L = \frac{1}{2}g_{ij}(\vec{x})\dot{x}_i\dot{x}_j - V(\vec{x}),$$

where g_{ij} is the metric tensor that allows us to measure length on the curved space of the manifold. The equations of motion are of the form

$$D_t \dot{\vec{x}} = -\nabla V,$$

where D_t is a covariant derivative with respect to time.

In the $\mathbb{C}P^1$ model we have motion on an infinite dimensional manifold as we consider maps from $\mathbb{R}^{2+1} \to S^2$, to the two sphere, of a particular degree. If $\phi: \mathbb{R}^{2+1} \to S^2$ the Lagrangian is

$$\int_{\mathbb{R}^2} |\dot{\phi}|^2 - |\nabla \phi|^2.$$

Identifying S^2 as $\mathbb{C} + \{\infty\}$, one can consider $u : \mathbb{R}^{2+1} \to \mathbb{C} + \{\infty\}$. The Lagrangian is

$$\int_{\mathbb{R}^2} \frac{|\dot{u}|^2}{(1+|u|^2)^2} - \frac{|\nabla u|^2}{(1+|u|^2)^2}.$$
 (1.4)

One can see this is one again the kinetic minus the potential energy.

The calculus of variations on this Lagrangian in conjunction with integration by parts yields the following equation of motion for the $\mathbb{C}P^1$ model:

$$(1 + |u|^2)(\partial_t^2 u - \partial_x^2 u - \partial_y^2 u) = 2\bar{u}(|\partial_t u|^2 - |\partial_x u|^2 - |\partial_y u|^2)$$
 (1.5)

1.2 Introduction to the adiabatic limit

The origin of the term "adiabatic" seems to be with reversible processes: processes that do not change the entropy of a system and consequently that can be undone. One way of enacting such a reversible process it to make the changes infinitely slowly.

Another way of looking at making changes infinitely slowly is to break space-time into two pieces, space and time. If one then rescales the spatial piece to be extremely small, or the time piece to be extremely large, it then takes correspondingly more time to move from point to point. In the limit as we take the spatial piece to be infinitely small or the time piece to be infinitely large, we are moving infinitely slowly.

Naturally, this sort of rescaling can occur in any problem that can be broken into two pieces. Any space that is a Cartesian product, say an infinite cylinder, $S^1 \times \mathbb{R}$ or a torus $S^1 \times S^1$. Or even any space that locally looks like a product, such as our old friend the Mœbius band, or, if one is even more adventurous and brave, a twisted bundle. The main requirement is that we have a metric on the space that splits into two pieces,

$$g(x,y)\langle x,x\rangle + h(x,y)\langle y,y\rangle.$$

Then one can introduce a parameter λ without changing the topology of the space:

$$g(x,y)\langle x,x\rangle + \lambda h(x,y)\langle y,y\rangle.$$

An adiabatic limit is simply taking the parameter $\lambda \to 0$ or $\lambda \to \infty$, which makes the space Y look either infinitely large or infinitely small. While changing from one finite and nonzero λ to another causes no changes in the topological properties of the space, the limit has no such immunity. Conclusions based on an adiabatic limit must be examined with care, for what happens in the limit $might\ not$ be close to what happens near the limit.

Adiabatic limits take on special meaning in the case of space-time. Taking an adiabatic limit results in moving either infinitely slowly or infinitely quickly, usually infinitely slowly. When we have a partial differential equation with known moduli spaces of static solutions, the adiabatic limit tells us that as velocity tends towards zero, we should get motion along the geodesics of these moduli spaces. We approximate solutions with small velocity with these geodesics, and hence this is called the Geodesic Approximation. Investigating

this phenomenon in the two cases mentioned in the introduction is the concern of this dissertation.

Chapter 2

The 4+1 dimensional model

The first things to identify in this problem are the static solutions to equation [1.3]. These are simply the 4 dimensional instantons investigated in [1]. In [1] the form of all such instantons in the degree one sector is shown to be:

$$A(x) = \frac{1}{2} \left\{ \frac{(\bar{x} - \bar{a})dx - d\bar{x}(x - a)}{\lambda^2 + |x - a|^2} \right\} \qquad x = x_1 + x_2 i + x_3 j + x_4 k \in \mathbb{H}.$$

The curvature F of this potential is computed by F = dA + [A, A] and is:

$$F = \frac{d\bar{x} \wedge dx}{(\lambda^2 + |x - a|^2)^2}.$$

One notices the denominators are radially symmetric about x = a.

An instanton of unit size centered at the origin would be

$$A(x) = \frac{1}{2} \left\{ \frac{\bar{x}dx - d\bar{x}x}{1 + |x|^2} \right\}$$

One motion one can study from these static instantons would be to consider connections the form

$$A(r,t) = \frac{1}{2} \left\{ \frac{\bar{x}dx - d\bar{x}x}{f(r,t) + r^2} \right\} \qquad r = \sqrt{x_1^2 + x_2^2 + x_3^2 + x_4^2}$$

and derive an equation of motion for f(r,t) from [1.3]. This is actually quite computationally extensive.

To get at this, start with connections of the form

$$A(r,t) = \frac{1}{2}g(r,t) \{\bar{x}dx - d\bar{x}x\}.$$

Now we have a formula for F given by F = dA + [A, A]. But F cannot easily be expressed as before. The components can be computed using Maple, with quarternions defined as

$$i = \begin{bmatrix} 0 & i \\ i & 0 \end{bmatrix}, \qquad j = \begin{bmatrix} 0 & -1 \\ 1 & 0 \end{bmatrix}, \qquad k = \begin{bmatrix} i & 0 \\ 0 & -i \end{bmatrix}$$

the usual derivative, and the bracket is that of two matrices: [M, N] = MN - NM. First, computing F one obtains components such as

$$F_{12} = i \left[\frac{x_1^2 g'(r,t) + 2rg(r,t) + x_2^2 g'(r,t)}{r} - 2x_4^2 g(r,t)^2 - 2x_3^2 g(r,t)^2 \right] +$$

$$j \left[\left(\frac{g'(r,t)}{r} + 2g(r,t)^2 \right) (x_2 x_3 - x_1 x_4) \right] +$$

$$k \left[\left(\frac{g'(r,t)}{r} + 2g(r,t)^2 \right) (x_1 x_3 + x_2 x_4) \right]$$

Once F has been obtained one may apply [1.3] to obtain an equation for g(r,t). After much labor, one obtains:

$$\ddot{g} = 12g^2 + \frac{5g'}{r} + g'' - 8g^3r^2. \tag{2.1}$$

It is much less difficult to now compute a differential equation for f(r,t)

if

$$g(r,t) = \frac{1}{f(r,t) + r^2}.$$

It is

$$\ddot{f} = f'' + \frac{5f'}{r} - \frac{8f'r}{f+r^2} + \frac{2}{f+r^2} \left((\dot{f})^2 - (f')^2 \right). \tag{2.2}$$

The static solutions for f(r,t) are simply horizontal lines, f(r,t)=c. The adiabatic limit expects that motion under small velocities should progress from line to line, *i.e.*, f(r,t)=c(t). f(r,t)=0 is a singularity of the system, where the instantons are not well defined. We can use this numerical approximation to the adiabatic limit to observe progression from $f(r,t)=c_0>0$ towards this singularity. Our initial assumption is that $f(\cdot,t)=c(t)$.

2.1 Numerics for the 4+1 dimensional model

A finite difference method is used to compute the evolution of [2.2] numerically. Unless otherwise noted, centered differences are used consistently, so that

$$g'(x) \approx \frac{g(x+\delta) - g(x-\delta)}{2\delta}$$

 $g''(x) \approx \frac{g(x+\delta) + g(x-\delta) - 2g(x)}{\delta^2}$.

In order to avoid serious instabilities in [2.2], the terms

$$f'' + \frac{5f'}{r} \tag{2.3}$$

must be modeled in a special way. Allow

$$f'' + \frac{5f'}{r} = \mathcal{L}f$$

where

$$\mathcal{L} = r^{-5} \partial_r r^5 \partial_r.$$

In Appendix A, we will see that this operator has negative real spectrum, hence it is stable. However the naive central differencing scheme on [2.3] always results in uncontrolled growth near the origin. General wisdom holds

that when one has difficulties with the numerics in one part of a problem one should find a differencing scheme for that specific part in the natural to that specific part. Applying this allowed for the removal of the problem near the origin. Instead of using centered differences on f'' and on f', we difference the operator:

$$\mathcal{L}f = r^{-5}\partial_r r^5 \partial_r.$$

The "natural differencing scheme" is

$$\mathcal{L}f \approx r^{-5} \left[\frac{\left(r + \frac{\delta}{2}\right)^5 \left(\frac{f(r+\delta) - f(r)}{\delta}\right) - \left(r - \frac{\delta}{2}\right)^5 \left(\frac{f(r) - f(r-\delta)}{\delta}\right)}{\delta} \right].$$

With the differencing explained, to derive $f(r, t + \Delta t)$, one always has a guess for $f(r, t + \Delta t)$ given by either the initial velocity, e.g. $f(r, t + \Delta t) = f(r, t) + v_0 \Delta t$, or by $f(r, t + \Delta t) = 2f(r, t) - f(r, t - \Delta t)$. Use this to compute $\dot{f}(r, t)$ on the right hand side of [2.2]. Then solve for $f(r, t + \Delta t)$ in the difference for $\ddot{f}(r, t)$, and iterate this procedure to get a more precise answer. So, one iterates

$$f(r,t+\Delta t) = 2f(r,t) - f(r,t-\Delta t) + (\Delta t)^2 \left[f''(r,t) - \frac{5f'(r,t)}{r} - \frac{2\dot{f}(r,t)^2}{f(r,t)+r^2} - \frac{2f'(r,t)^2}{f(r,t)+r^2} - \frac{8f'(r,t)r}{f(r,t)+r^2} \right],$$

where all derivatives on the right hand side are represented by the appropriate differences.

There remains the question of the boundary conditions. The function f is only modeled out to a value $r=R\gg 0$. Initial data for f(r,0) was

originally a horizontal line. The corresponding boundary conditions are that $f(R,t)=f(R-\triangle r,t),$ and that

$$f(0,t) = \frac{4}{3}f(\triangle r, t) - \frac{1}{3}f(2\triangle r, t)$$

i.e., that f is an even function.

Subsequent investigation of the model indicated that the appropriate form for f(r,t) was a parabola instead of a line, and the f(R,t) boundary condition was changed to reflect this. For the runs with parabolic initial data, we set the boundary condition at R to be:

$$f'(R,t) = f'(R - \triangle r, t) \frac{R}{R - \triangle r}.$$

2.2 Predictions

Equation [1.2] gives us the Lagrangian for the general version of this problem. We are using

$$A = \frac{1}{2} \left\{ \frac{\bar{x}dx - d\bar{x}x}{f + r^2} \right\} \qquad r = \sqrt{x_1^2 + x_2^2 + x_3^2 + x_4^2},$$

and the adiabatic limit says we will move on the moduli space of these solutions. This will give us an effective Lagrangian. The portion of the integral given by

$$-\frac{1}{4} \int_{\mathbb{R}^4} \langle F_{ij}, F_{ij} \rangle d\vec{x}$$

represents the potential energy and integrates to a topological constant, hence it may be ignored. We need to calculate

$$\frac{1}{2} \int_{\mathbb{R}^4} \langle \dot{A}_i, \dot{A}_i \rangle d\vec{x}.$$

First calculate

$$\langle \dot{A}_i, \dot{A}_i \rangle = \frac{3r^2 \dot{f}^2}{(f+r^2)^4}.$$

So the effective Lagrangian is

$$\int_{\mathbb{R}^4} \frac{3r^2 \dot{f}^2}{(f+r^2)^4} d\vec{x},$$

Letting $\vec{y} = \vec{x}/\sqrt{f}$ we can rewrite this integral as

$$\frac{3\dot{f}^2}{f} \int_{\mathbb{R}^4} \frac{|y|^2}{(1+|y|^2)^4} d\vec{y}.$$

The integral with respect to \vec{y} converges, hence we have

$$L = c \frac{\dot{f}^2}{f}.$$

This is purely kinetic energy. Since the potential energy is constant, so is the kinetic energy. We have

$$\frac{\dot{f}^2}{f} = k.$$

Integrating this we get

$$f = (c_1 t + c_2)^2.$$

If f = 0 occurs at time T, we find

$$T = -\frac{c_2}{c_1}$$

hence we rewrite this as

$$f = a(t - T)^2.$$

This is how we predict that f(0,t) will evolve.

2.3 Results

The computer model was run under the condition that $f(r,0) = f_0$ with various small velocities. The initial velocity is $\dot{f}(r,0) = v_0$, other input parameters are $R = r_{max}$, $\triangle r$ and $\triangle t$.

2.3.1 Evolution of f(0,t)

The first question to ask is how does the evolution of the origin occur. We note that equation [2.2] becomes the regular linear wave equation

$$\ddot{f} = f''$$

as $r \to \infty$, and so the interesting nonlinear behavior is at the origin. Consequently we track the evolution of f(0,t).

The evolution of f(0,t) is a parabola of the form:

$$f(0,t) = a(t-T)^2,$$

where

$$a = \frac{v_0^2}{4f_0}$$

and

$$T = \frac{2f_0}{|v_0|}.$$

A typical evolution of f(0,t) is given in Figure 2.1. In this figure, the equation $0.000025(t-200)^2$ neatly overlays the graph of f(0,t). This picture represents the evolution where $f_0 = 1.0$ and $v_0 = -0.01$. Hence $c = \frac{(0.01)^2}{4(1.0)} = 0.000025$ and $T = \frac{2(1.0)}{0.01} = 200$, as predicted.

The time to "blow up" is the parameter T in this equation. Recall that $f_0 = f(r,0)$ is the initial height and $\dot{f}_0(r,0) = v_0$ is the initial velocity. Using a least squares parabolic fit to the origin data obtained after $f(0,t) \leq 0.5 f_0$, one obtains the parameters a and T for a given origin curve. Table 2.1 shows the behavior.

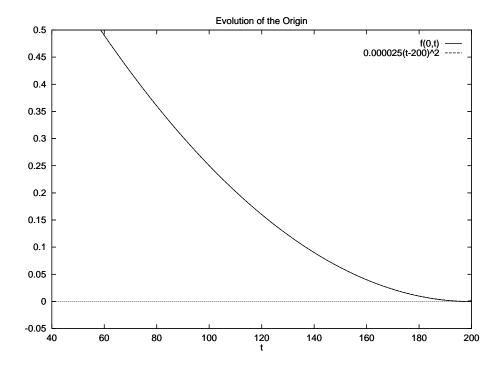


Figure 2.1: 4+1 dimensional model, evolution f(0,t).

Table 2.1: 4+1 Dimensional Model, parabolic fit to f(0,t) vs. Initial conditions f_0 and v_0

f_0	v_0	a	T
1.0	-0.010	0.00002501	200.1
2.0	-0.010	0.00001257	399.4
0.5	-0.010	0.00005166	99.0
4.0	-0.010	0.00000626	799.7
4.0	-0.020	0.00002503	400.1
4.0	-0.005	0.00000157	1599.3

2.3.2 Characterization of time slices f(r,T): evolution of a horizontal line

The most striking immediate result is that the initial line, $f(r,0) = f_0$, evolved an elliptical bump at the origin that grew as time passed. Figure 2.2 shows this behavior.

The elliptical bumps can be modeled as

$$\frac{x^2}{a^2} + \frac{(y-k)^2}{b^2} = 1. (2.4)$$

The question naturally arises as to how the parameters a, b and k evolve. This is straightforward:

$$a = t$$

$$b = \frac{v_0^2}{4f_0}t^2$$

$$k = f_0 + v_0t$$

Table 2.2 shows these values as calculated using least squares fitting (to either a line or parabola). Since the elliptical fit only works before the right end of the ellipse hits the boundary at r = R the fit sometimes needed to be restricted to the portion of the data before this occurred. While the ellipse is small, there is a great deal of noise in finding the elliptical parameters, and to get a good data fit, this noise must often be removed. Here m_a and b_a is the slope and intercept of the line a(t), and likewise m_k and b_k are the slope and intercept of the line k(t). The parameter c is that in $b(t) = ct^2$

A typical evolution for a with $f_0 = 4.0$ and $v_0 = -0.01$ is in Figure 2.3. Note the noise when t < 100.

Figure 2.4 is a typical evolution for b with $f_0 = 4.0$ and $v_0 = -0.02$.

Figure 2.5 is a typical evolution for k with $f_0 = 2.0$ and $v_0 = -0.01$.

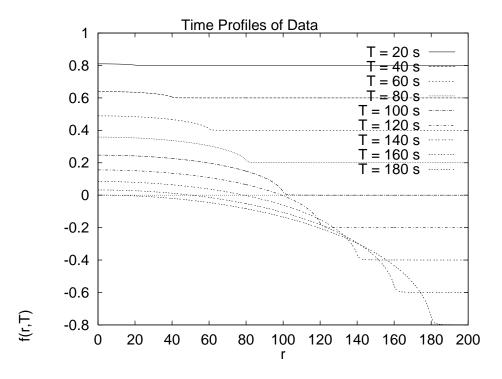


Figure 2.2: 4+1 Dimensional model, Time Slices f(r,T) evolve an elliptical bump at the origin

Table 2.2: 4+1 Dimensional Model, Elliptical Parameters vs. Initial Conditions f_0 and v_0

f_0	v_0	m_a	b_a	c	m_k	b_k
1.0	-0.010	0.999	-0.11	0.00002510	0.0100	-1.00
2.0	-0.010	0.999	0.01	0.00001270	0.0108	-2.00
0.5	-0.010	1.007	-0.420	0.00005653	0.0100	-0.51
4.0	-0.010	1.001	0.764	0.00000626	0.0100	-4.001
4.0	-0.020	0.998	0.177	0.00002527	0.0200	-4.003
4.0	-0.005	1.001	-0.834	0.00000157	0.0050	-4.000

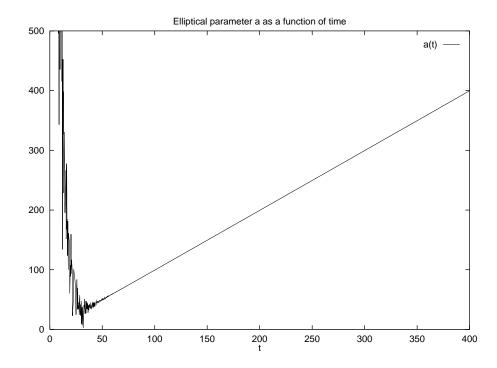


Figure 2.3: 4+1 dimensional model: elliptical parameter a as a function of time when $f_0=4.0$ and $v_0=-0.01$.

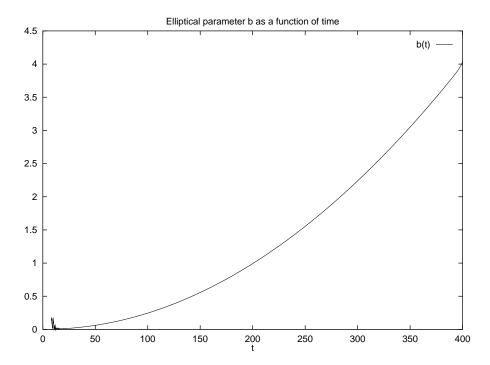


Figure 2.4: 4+1 dimensional model: elliptical parameter b as a function of time when $f_0=4.0$ and $v_0=-0.02$.

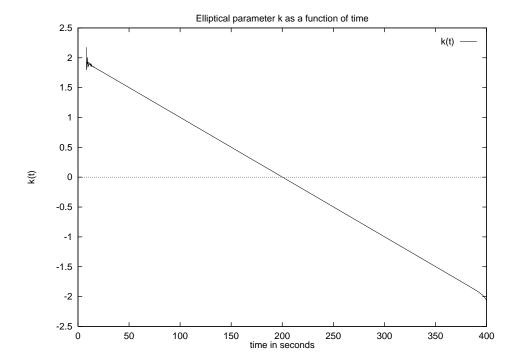


Figure 2.5: 4+1 dimensional model: elliptical parameter k as a function of time when $f_0=2.0$ and $v_0=-0.01$.

2.3.3 Characterization of time slices f(r,T): evolution of a parabola

The elliptical bump that formed in the evolution of a horizontal line and the various configurations that ensued after it bounced off the r=0 and r=R boundary suggested that perhaps the curve was trying to obtain the shape of a parabola. After all, near r=0, ellipses are excellent approximations for parabolas of the form

$$f(r,t) = pr^2 + h. (2.5)$$

To get the parabola, calculate from the general form of our ellipse in [2.4]

$$\frac{dy}{dx} = -\frac{x^2b^2}{(y-k)a^2}$$

so

$$\frac{d^2y}{dx} = \frac{-b^2}{(y-k)a^2} - \frac{xb^2}{(y-k)^2a^2} \frac{dy}{dx}$$

At x = 0, y - k = b and this gives

$$\frac{d^2y}{dx} = \frac{-b}{a^2}.$$

Recall from the previous section that $b=ct^2$ and a=t, so this gives

$$\frac{d^2y}{dx^2} = -c.$$

The identification of c gives

$$\frac{d^2y}{dx^2} = -\frac{v_0^2}{4f_0}.$$

So

$$p = -\frac{1}{2} \frac{d^2 y}{dx^2} = -\frac{v_0^2}{8f_0}$$

When a run is started with this initial data, $\dot{f}_0 = v_0 = -0.01$, $f_0 = f(0,0) = 1.0$ and $p = \frac{v_0^2}{8f_0} = -0.0000125$, the time slices of the data have this same profile. This is shown in figure 2.6.

The curvature of the parabola at the origin, as measured by the parameter p from equation [2.5] changes by less than 1 part in 100 during the course of this evolution, a graph of p over time can be seen in figure 2.7.

The other parameter in equation [2.5] for the parabola, h, should be given by the height of the origin, but this was calculated in the previous section to be $a(t-T)^2$, substituting the expressions for c and T we obtain:

$$h(t) = \frac{v_0^2}{4f_0} \left(t - \frac{2f_0}{|v_0|} \right)^2.$$

This is indeed the correct form, as shown in figure 2.8. The initial conditions were $v_0 = -0.01$ and $f_0 = f(0,0) = 1.0$, hence $h(t) = 0.000025(t - 200)^2$. The plot of the function overlays the data.

Now, using both expressions for p and h, one can get the general form of a parabolic f(r,t), which is

$$f(r,t) = \frac{v_0^2}{8f_0}r^2 + \frac{v_0^2}{4f_0}\left(t - \frac{2f_0}{|v_0|}\right)^2$$
 (2.6)

Substitute this into the partial differential equation [2.2], get a common denominator and simplify to obtain:

$$\begin{split} \frac{v_0^2}{4f_0} \left[-\frac{v_0^2}{4f_0} r^2 + 2\frac{v_0^2}{4f_0} \left(t - \frac{2f_0}{|v_0|} \right)^2 + 2r^2 \right] \stackrel{?}{=} \\ \frac{v_0^2}{4f_0} \left[\frac{v_0^2}{4f_0} r^2 + 2\frac{v_0^2}{4f_0} \left(t - \frac{2f_0}{|v_0|} \right)^2 + 2r^2 \right]. \end{split}$$

Clearly these two sides are not the same, and the error between them is

$$2\left(\frac{v_0^2}{4f_0}\right)^2r^2.$$

Since our concern is the geodesic approximation, $v_0^2/(f_0)$ is always chosen to be less than 1/200. This term is always much smaller than the $2r^2$ term, and since we only have accurate numerics away from the neighborhood of the singularity, the term with $t - 2f_0/|v_0|$ is on the order of magnitude $f_0/|v_0|$, which is large compared to the correction.

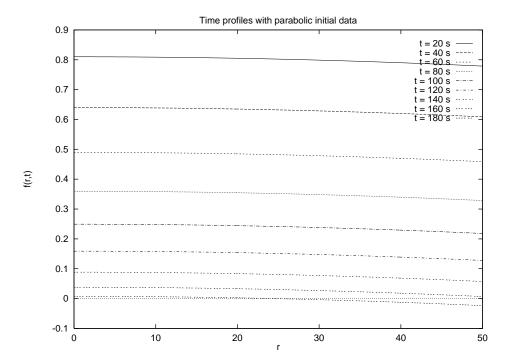


Figure 2.6: 4+1 dimensional model: Time slices of the evolution of a parabola are parabolas.

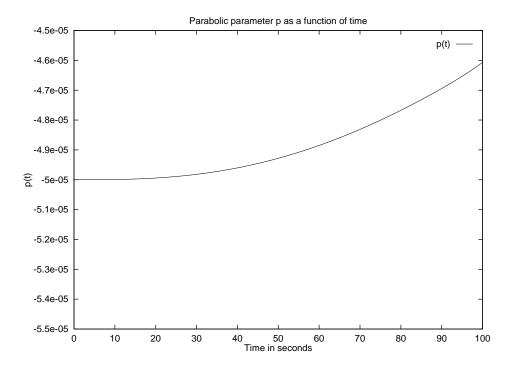


Figure 2.7: 4+1 dimensional model: evolution of parabolic parameter p with time.

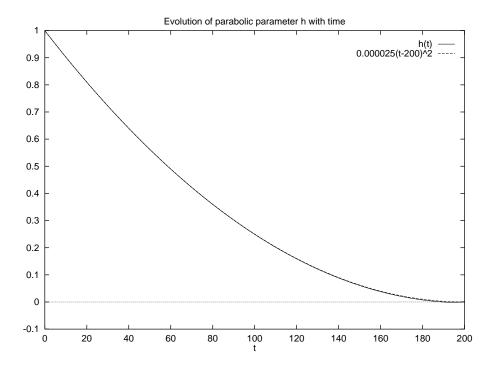


Figure 2.8: 4+1 dimensional model: Parabolic parameter h as a function of time evolves as f(0,t).

Chapter 3

The $\mathbb{C}P^1$ model, charge 1 sector

The first thing to identify in this problem are the static solutions determined by equation [1.5]. These are outlined in [7] among others. The entire space of static solutions can be broken into finite dimensional manifolds \mathcal{M}_n consisting of the harmonic maps of degree n. If n is a positive integer, then \mathcal{M}_n consists of the set of all rational functions of z = x + iy of degree n. For this chapter, we restrict our attention to \mathcal{M}_1 , the charge one sector, on which all static solutions have the form

$$u = \alpha + \beta(z + \gamma)^{-1}. (3.1)$$

In order to simplify, consider only solutions of the form

$$\beta z^{-1}$$

or look for a real radially symmetric function f(r,t) so that this evolution occurs as:

$$\frac{f(r,t)}{z}$$
.

It is straightforward to calculate the evolution equation for f(r,t). It is:

$$\ddot{f} = f'' + \frac{3f'}{r} - \frac{4rf'}{f^2 + r^2} + \frac{2f}{f^2 + r^2} \left(\dot{f}^2 - f'^2 \right). \tag{3.2}$$

The static solutions for f(r,t) are the horizontal lines f(r,t)=c. In the adiabatic limit motion under small velocities should progress from line to line, i.e f(r,t)=c(t). f(r,t)=0 is a singularity of this system, where the instantons are not well defined. We use this to form a numerical approximation to the adiabatic limit to observe progression from $f(r,0)=c_0>0$ towards this singularity.

3.1 Numerics for the $\mathbb{C}P^1$ charge 1 sector model

A finite difference method is used to compute the evolution of [3.2] numerically. As with the 4+1 dimensional model, centered differences are used consistently except for

$$f'' + \frac{3f'}{r}. ag{3.3}$$

In order to avoid serious instabilities in [3.2] this is modeled in a special way. Let

$$\mathcal{L}f = r^{-3}\partial_r r^3 \partial_r f = f'' + \frac{3f'}{r}.$$

In Appendix B it is shown that this operator has negative real spectrum, hence it is stable. The naive central differencing scheme on [3.3] results in unbounded growth at the origin, but the natural differencing scheme for this operator does not. It is

$$\mathcal{L}f \approx r^{-3} \left[\frac{\left(r + \frac{\delta}{2}\right)^3 \left(\frac{f(r+\delta) - f(r)}{\delta}\right) - \left(r - \frac{\delta}{2}\right)^3 \left(\frac{f(r) - f(r-\delta)}{\delta}\right)}{\delta} \right].$$

With the differencing explained, we want to derive $f(r, t + \Delta t)$. We always have an initial guess at $f(r, t + \Delta t)$. In the first time step it is $f(r, t + \Delta t) = f(r, t) + v_0 \Delta t$ with v_0 the initial velocity given in the problem. On subsequent time steps $f(r, t + \Delta t) = 2f(r, t) - f(r, t - \Delta t)$. This can be used to compute $\dot{f}(r, t)$ on the right hand side of [3.2]. Then solve for a new and improved $f(r, t + \Delta t)$ in the differencing for the second derivative $\ddot{f}(r, t)$ and iterate this procedure several times to get increasingly accurate values of f(r, t).

There remains the question of boundary conditions. At the origin f(r,t) is presumed to be an even function, and this gives

$$f(0,t) = \frac{4}{3}f(\triangle r, t) - \frac{1}{3}f(2\triangle r, t).$$

At the r=R boundary we presume that the function is horizontal so $f(R,t)=f(R-\Delta r,t)$.

3.2 Predictions

Equation [1.4] gives us the Lagrangian for the general version of this problem. We are using

$$u = \frac{\beta}{z}$$

for our evolution, and via the geodesic approximation, we restrict the Lagrangian integral to this space, to give an effective Lagrangian. The integral of the spatial derivatives of u gives a constant, the Bogomol'nyi bound, and hence can be ignored. If one integrates the kinetic term over the entire plane, one sees it diverges logarithmically, so if β is a function of time, the soliton has infinite energy.

Nonetheless, this is what we wish to investigate. We cannot address the entire plane in our numerical procedure either, hence we presume that the evolution takes place in a ball around the origin of size R. If $\beta = f(r,t)$ shrinks to 0 in time T, we need R > T. Under these assumptions, up to a multiplicative constant, the effective Lagrangian becomes

$$L = \int_0^R r dr \frac{r^2 \dot{f}^2}{(r^2 + f^2)^2}$$

which integrates to

$$L = \frac{\dot{f}^2}{2} \left[\ln \left(1 + \frac{R^2}{f^2} \right) - \frac{R^2}{f^2 + R^2} \right]$$

Since the potential energy is constant, so is the purely kinetic Lagrangian, and

$$\frac{\dot{f}^2}{2} \left[\ln \left(1 + \frac{R^2}{f^2} \right) - \frac{R^2}{f^2 + R^2} \right] = \frac{c^2}{2},$$

with c (and hence $c^2/2$) a constant. Solving for \dot{f} we obtain

$$\dot{f} = \frac{c}{\sqrt{\left[\ln\left(1 + \frac{R^2}{f^2}\right) - \frac{R^2}{f^2 + R^2}\right]}}.$$
 (3.4)

Since we are starting at some value f_0 and evolving toward the singularity at f = 0 this gives:

$$\int_{f_0}^{f(0,t)} df \sqrt{\ln\left(1 + \frac{R^2}{f^2}\right) - \frac{R^2}{f^2 + R^2}} = \int_0^t cdt.$$
 (3.5)

The integral on the right gives ct. The integral on the left can be evaluated numerically for given values of R, f_0 and f(0,t). A plot can then be generated for ct vs. f(0,t). What we really are concerned with is f(0,t) vs. t, but once the value of c is determined this can be easily obtained. One such plot with

 $f_0 = 1.0$, R = 100 of f(0,t) vs ct is given in Figure 3.1. This curve is almost, but not quite, linear, as seen by comparison with the best fit line to this data which is also plotted in Figure 3.1. The best fit line is obtained by a least squares method.

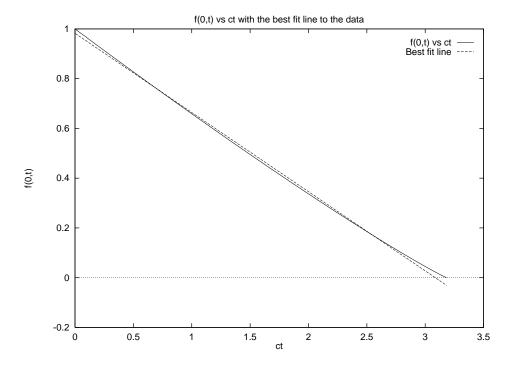


Figure 3.1: $\mathbb{C}P^1$ model, charge 1 sector: Example plot of f(0,t) vs ct as predicted by the effective Lagrangian.

3.3 Results

The computer model was run under the condition that $f(r,0) = f_0$ with various small velocities. The initial velocity is $\dot{f}(r,0) = v_0$, other input parameters are $R = r_{max}$, $\triangle r$ and $\triangle t$.

3.3.1 Evolution of f(0,t)

The primary concern with the evolution of the horizontal line is the way in which the singularity at f(0,t) = 0 is approached, because once again as $r \to \infty$ equation [3.2] reduces to the linear wave equation

$$\ddot{f} = f''$$
,

and so we expect the interesting behavior to occur near r=0. The model is run with initial conditions that $f(r,0)=f_0$, $\dot{f}(r,0)=v_0$. Other input parameters are $R=r_{\rm max}$, $\triangle r$ and $\triangle t$.

The evolution of the initial horizontal line seems to remain largely flat and horizontal, although there is some slope downward as time increases. This is shown in figure 3.2.

We track f(0,t) as it heads toward this singularity, and find that its trajectory is not quite linear, as seen in figure 3.3. This is suggestive of the result obtained in the predictions for this model.

A simple characterization this evolution can be obtained via the slope m of the best fit line (via least squares) and the time T at which f(0,T)=0. Step sizes of $\Delta r=0.01$ and $\Delta t=0.001$ were used with R=100.0. Table 3.1 displays the initial data $f_0=f(r,0)$ and $v_0=\dot{f}(r,0)$ along with the consequent T and m values.

We have

$$T \approx \frac{1.2f_0}{|v_0|}$$

and

$$m \approx \frac{3|v_0|}{4}$$
.

A better method would be to try to use the result from equation [3.5] in chapter 3.2. This requires a determination of the parameters R and c. We already have f_0 and f(0,t). To determine R and c, observe from equation [3.4] that:

$$\frac{1}{\dot{f}^2} = \frac{\left[\ln\left(1 + \frac{R^2}{f^2}\right) - \frac{R^2}{f^2 + R^2}\right]}{c^2} \tag{3.6}$$

Since R is large and f is small

$$\ln\left(1 + \frac{R^2}{f^2}\right) \approx \ln\left(\frac{R^2}{f^2}\right)$$

and

$$\frac{R^2}{f^2 + R^2} \approx 1.$$

Consequently we can rewrite equation [3.6] as

$$\frac{1}{\dot{f}^2} \approx \frac{[\ln(R^2) - \ln(f^2) - 1]}{c^2}.$$

The plot of $\ln(f) = \ln(f(0,t))$ vs $1/\dot{f}^2 = 1/\dot{f}^2(0,t)$ should be linear with the slope $m = 2/c^2$ and the intercept $b = (2\ln(R) - 1)/c^2$. Such a plot is easily obtained from the model, and given slope and intercept, the parameters c and R are easily obtained.

Figure 3.4 is a plot of $\ln(f(0,t))$ vs. $1/\dot{f}^2(0,t)$, with initial conditions $\Delta r = 0.01$, $\Delta t = 0.001$, $f_0 = 1.0$ and $v_0 = -0.01$. It is easily seen that

although the plot of $\ln(f(0,t))$ vs. $1/\dot{f}^2(0,t)$ is nearly straight, it is not quite a straight line. This indicates that the values of R and c are changing with time.

The best fit line y = mx + b has slope m = -2810 and b = 10200. We have

$$c = \sqrt{\frac{-2}{m}}$$

and

$$R = \exp\left(-\frac{b}{m} + \frac{1}{2}\right).$$

This gives values c = 0.0267 and R = 62.1. Using these values of c and R in the calculation of equation [3.5], we obtain the plot of f(0,t) vs t given in Figure 3.5. This is overlayed with the model data for f(0,t) vs. t for comparison. These two are virtually identical.

The next question is how do the parameters c and R vary with the initial conditions. The first piece of bad news is that they are strongly dependent on the size of $\triangle r$ when $\triangle r > 0.01$, however, they appear to converge as $\triangle r \to 0$. Table 3.2 contains data of c, R vs. $\triangle r$ and $\triangle t$ under initial conditions $f_0 = 1.0$ and $v_0 = -0.01$.

Table 3.3 contains the data for c and R vs. change in the initial velocity v_0 , under the initial conditions $f_0 = 1.0$, $\triangle r = 0.01$ and $\triangle t = 0.001$. The data for R varying with v_0 fits well to the parabola

$$-0.00237878x^2 + 0.73551687x + 3.23010905.$$

This fit is shown in figure 3.6. We know this must break down for small initial velocities, because it would send the value of R to $-\infty$. The values of R do

seem to be levelling out. This suggests a direction for further research.

Table 3.4 containing the data for c and R vs. change in f_0 , the initial height. The parameter R varies close to linearly with f_0 , while the parameter c remains nearly constant, changing by less than 7% over the course of the runs.

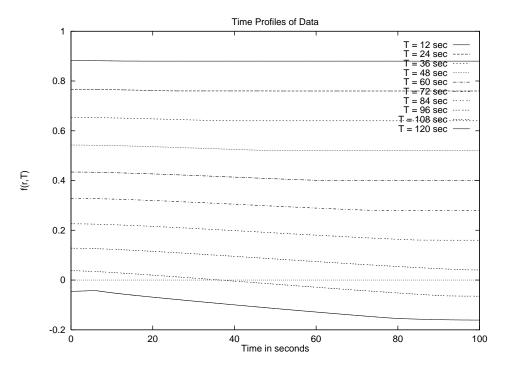


Figure 3.2: $\mathbb{C}P^1$ model, charge 1 sector: Time slices f(r,T)

Table 3.1: $\mathbb{C}P^1$ model, charge 1 sector: Parameters for best fit line to f(0,t) vs. initial data f_0 and v_0

f_0	v_0	T	m
1.0	-0.010	113	-0.00815
2.0	-0.010	228	-0.00811
3.0	-0.010	346	-0.00793
4.0	-0.010	466	-0.00836
5.0	-0.010	588	-0.00828
1.0	-0.020	58	-0.01586
1.0	-0.030	39	-0.02336
1.0	-0.040	30	-0.03069

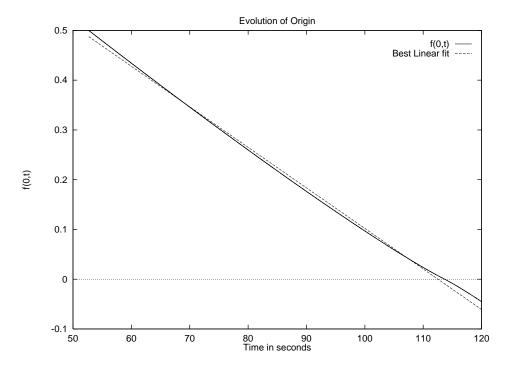


Figure 3.3: $\mathbb{C}P^1$ model, charge 1 sector: Evolution of f(0,t) is not quite linear.

Table 3.2: $\mathbb{C}P^1$ model, charge 1 sector: c and R vs. $\triangle r$ and $\triangle t$. $f_0=1.0$ and $v_0=-0.01$.

	$\triangle r$	$\triangle t$	c	R
0.1	100	0.001	0.0281	101.
0.0	050	0.001	0.0273	76.6
0.0	025	0.001	0.0271	71.0
0.0	020	0.001	0.0271	70.3
0.0	010	0.001	0.0270	69.4
0.1	100	0.002	0.0281	101.
0.1	100	0.004	0.0281	101.
0.1	100	0.005	0.0281	101.

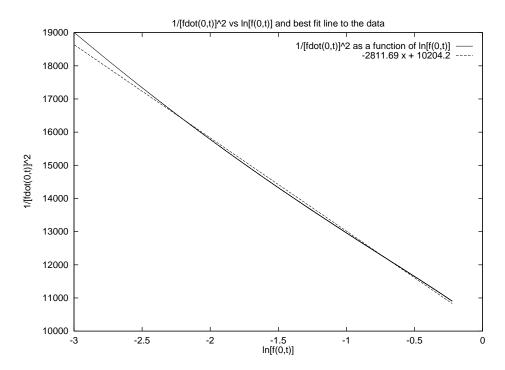


Figure 3.4: $\mathbb{C}P^1$ model, charge 1 sector: Plot of $1/(\dot{f})^2$ vs $\ln(f)$ and the best fit line to this data.

Table 3.3: $\mathbb{C}P^1$ model, charge 1 sector: c and R vs. v_0 . $f_0=1.0$.

v_0	c	R
-0.01	0.0263	53
-0.02	0.0485	34
-0.03	0.0683	25
-0.05	0.104	17
-0.06	0.121	15

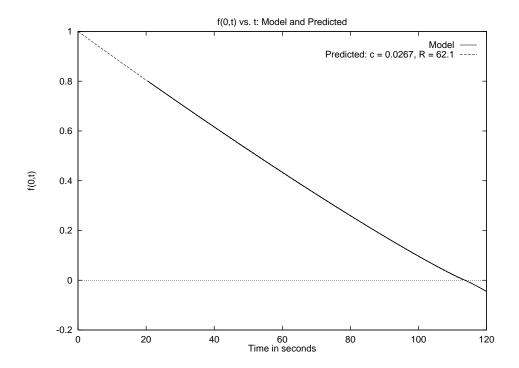


Figure 3.5: $\mathbb{C}P^1$ model, charge 1 sector: Predicted course of f(0,t) from equation [3.5] and actual course of f(0,t) vs. t.

Table 3.4: $\mathbb{C}P^1$ model, charge 1 sector: c and R vs. f_0 . $v_0 = -0.01$.

f_0	c	R
1.0	0.0267	62
2.0	0.0263	108
3.0	0.0260	150
4.0	0.0259	190

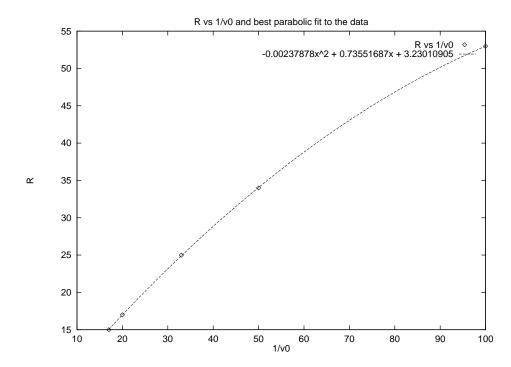


Figure 3.6: $\mathbb{C}P^1$ model, charge 1 sector: R vs 1/v0 and the best fit parabola.

3.3.2 Characterization of time slices f(r,T)

Making a closer inspection of the time profiles f(r,T) with T fixed as in Figure 3.2, one may observe that the initial part of the data is close to a hyperbola as seen in Figure 3.7. The best hyperbolic fit is determined by a least squares method.

The equation for the hyperbola is

$$\frac{(y-k)^2}{b^2} - \frac{x^2}{a^2} = 1.$$

One would naturally ask about the evolution of the hyperbolic parameters a and b with time, however, neither of these is particularly edifying. A simple calculation shows that k should follow f(0,t) closely if b is small, as it is. Figure 3.8 shows an example of a vs. time, Figure 3.9 shows an example of b vs. time, and Figure 3.10 shows an example of k vs. time. In all these figures $f_0 = 1.0$ and $v_0 = -0.01$.

The evolution of -b/a gives the slope of the asymptotic line to the hyperbola, and this evolution is close to linear as seen in Figure 3.11. One might naturally ask how the slope m and intercept b_i of the best fit line to the evolution of the hyperbolic -b/a change with various initial conditions on f_0 and v_0 . The variation of m and b_i with f_0 is shown in Table 3.5. It is easy to see the slope m varies linearly with $1/f_0$, while the intercept b_i changes by only about 2%. The variation of m and b_i with v_0 is shown in Table 3.6. Here m and b_i vary quadratically with the initial velocity. In Figure 3.12 we show the slope m vs. the initial velocity v_0 plotted along with the best parabolic fit $f(x) = -0.11083929x^2 + 0.00009768x + 0.00000220$ to this data. In Figure

3.13 we show the intercept b_i vs. the initial velocity v_0 plotted along with the best parabolic fit $f(x) = -0.77595779x^2 + 0.00943555x + 0.00006655$ to this data.

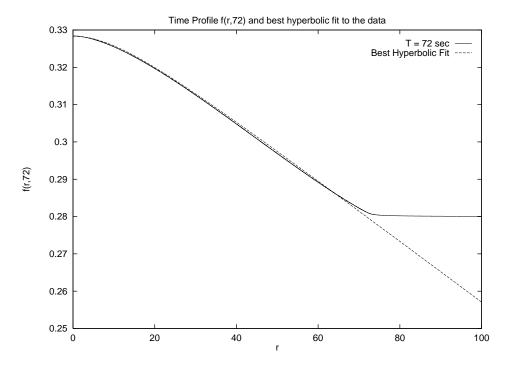


Figure 3.7: $\mathbb{C}P^1$ model, charge 1 sector: Time slices evolve hyperbolic bump at origin.

Table 3.5: $\mathbb{C}P^1$ model, charge 1 sector: Best fit line to evolution of -b/a slope m and intercept b_i vs. f_0 .

f_0	m	b_i
1.0	-0.0000103	-0.000109
2.0	-0.00000516	-0.000108
3.0	-0.00000344	-0.000107
4.0	-0.00000258	-0.000107

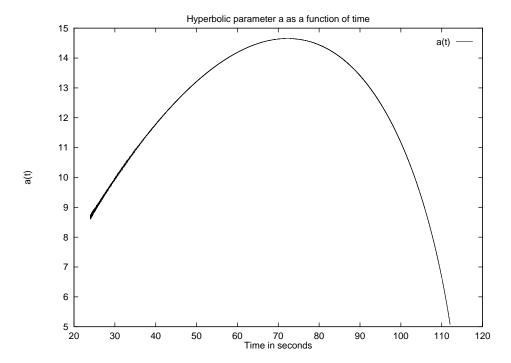


Figure 3.8: $\mathbb{C}P^1$ model, charge 1 sector: Plot of hyperbolic parameter a vs time, $f_0=1.0,\,v_0=-0.01.$

Table 3.6: $\mathbb{C}P^1$ model, charge 1 sector: Best fit line to evolution of -b/a slope m and intercept b_i vs. v_0 .

v_0	m	b_i
-0.01	-0.0000103	-0.000109
-0.02	-0.0000436	-0.000426
-0.03	-0.000100	-0.000916
-0.05	-0.000281	-0.00235
-0.06	-0.000402	-0.00329

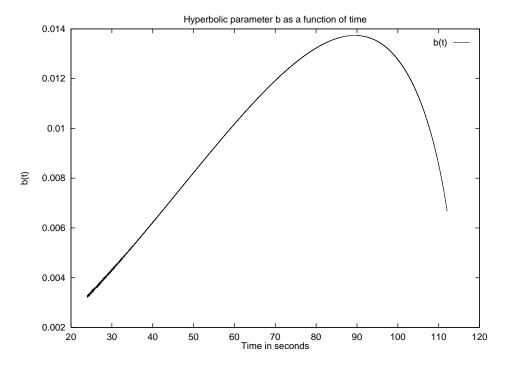


Figure 3.9: $\mathbb{C}P^1$ model, charge 1 sector: Plot of hyperbolic parameter b vs time, $f_0=1.0,\,v_0=-0.01.$

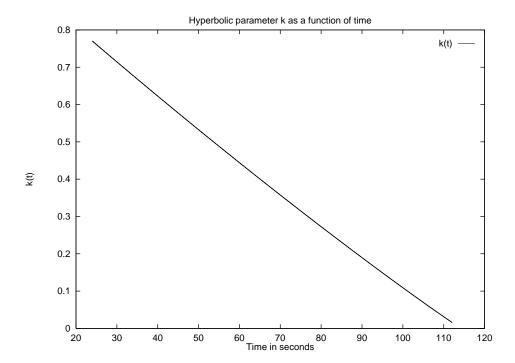


Figure 3.10: $\mathbb{C}P^1$ model, charge 1 sector: Plot of hyperbolic parameter k vs time, $f_0=1.0,\,v_0=-0.01.$

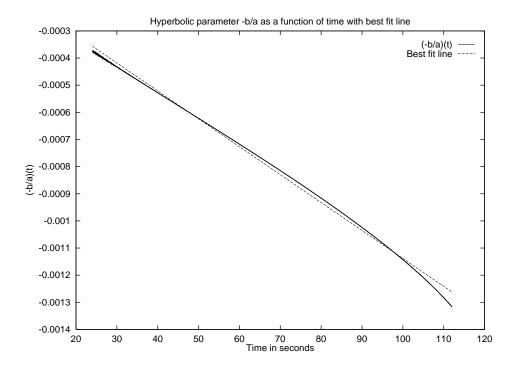


Figure 3.11: $\mathbb{C}P^1$ model, charge 1 sector: Plot of hyperbolic parameter -b/a vs time, $f_0=1.0,\,v_0=-0.01.$

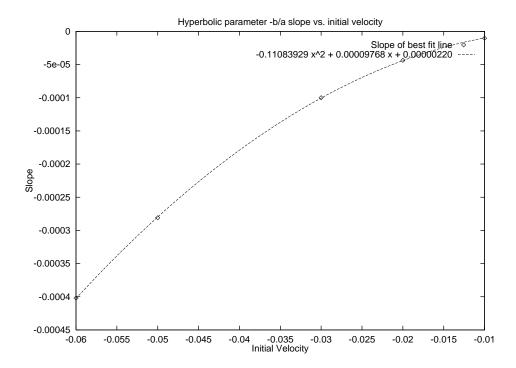


Figure 3.12: $\mathbb{C}P^1$ model, charge 1 sector: Plot of slope m vs initial velocity v_0 .

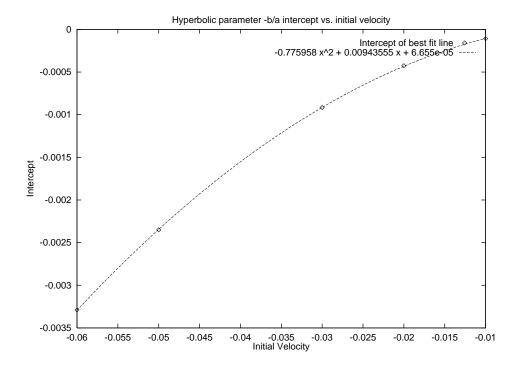


Figure 3.13: $\mathbb{C}P^1$ model, charge 1 sector: Plot of intercept b_i vs initial velocity v_0 .

Chapter 4

The $\mathbb{C}P^1$ model, charge 2 sector

It is thought that the charge 2 sector of the $\mathbb{C}P^1$ model should behave similarly to the 4+1 dimensional instanton model. The charge 2 sector consists of all rational functions of z=x+iy of degree 2. A general static solution is of the form

$$u = \alpha + \frac{\beta z + \gamma}{z^2 + \delta z + \epsilon}$$

depending on the five complex parameters $\alpha, \beta, \gamma, \delta, \epsilon$. To simplify consider only solutions of the form

$$\frac{\gamma}{\gamma^2}$$

with γ real. A straightforward calculation determines the evolution equation for the radially symmetric function $f(r,t) = \gamma$. It is:

$$\ddot{f} = f'' + \frac{5f'}{r} - \frac{8r^3f'}{f^2 + r^4} + \frac{2f}{f^2 + r^4} \left(\dot{f}^2 - f'^2 \right). \tag{4.1}$$

Immediate similarities can be seen with equation [2.2]. The static solutions are f(r,T) = c for T fixed and any constant c. We investigate progression from $f(r,0) = c_0 > 0$ towards the singularity at f(r,T) = 0.

4.1 Numerics for the $\mathbb{C}P^1$ charge 2 sector model

As with the other models, a finite difference method is used to compute the evolution of [4.1] numerically. Centered differences are used consistently except for

$$f'' + \frac{5f'}{r}.$$

A naive central differencing scheme here will yield serious instabilities at the origin. As before, let

$$\mathcal{L}f = r^{-5}\partial_r r^5 \partial r f = f'' + \frac{5f'}{r}.$$

This operator has negative real spectrum, hence it is stable. The natural differencing scheme for this operator is

$$\mathcal{L}f \approx r^{-5} \left[\frac{\left(r + \frac{\delta}{2}\right)^5 \left(\frac{f(r+\delta) - f(r)}{\delta}\right) - \left(r - \frac{\delta}{2}\right)^5 \left(\frac{f(r) - f(r-\delta)}{\delta}\right)}{\delta} \right].$$

This is the differencing scheme used for these terms.

Now with the differencing explained, we derive $f(r, t + \Delta t)$ in exactly the same manner as for the 4+1 dimensional model and the charge 1 sector. We have an initial guess for $f(r, t + \Delta t)$, either given by $f(r, t + \Delta t) = f(r, t) + v_0 \Delta t$ with v_0 the initial velocity given in the problem, or on subsequent time steps $f(r, t + \Delta t) = 2f(r, t) - f(r, t - \Delta t)$. We use this guess to compute $\dot{f}(r, t)$ on the right hand side of [4.1], and then we can solve for a new and improved $f(r, t + \Delta t)$ on the left hand side of [4.1]. Iterate this procedure to get increasingly accurate values of f(r, t).

The boundary condition at the origin is found by requiring that f(r,t) is an even function, hence

$$f(0,t) = \frac{4}{3}f(\triangle r, t) - \frac{1}{3}f(2\triangle r, t).$$

At the r=R boundary the function should be horizontal so $f(R,t)=f(R-\Delta r,t)$.

4.2 Predictions

Equation [1.4] gives us the Lagrangian for the general version of this problem. We are using

$$u = \frac{\lambda}{z^2}$$

for our evolution, and via the geodesic approximation we restrict the Lagrangian integral to this space, to give an effective Lagrangian. The integral of the spatial derivatives of u gives a constant, and hence can be ignored. Under these assumptions, up to a multiplicative constant, the effective Lagrangian becomes

$$L = \int_0^\infty r dr \frac{r^4 \dot{\lambda}^2}{\left(r^4 + \lambda^2\right)^2}$$

which integrates to

$$L = \frac{\dot{\lambda}^2 \pi}{8\lambda}.$$

Since the potential energy is constant, so is the kinetic energy, hence

$$\dot{\lambda} = k\sqrt{\lambda}.$$

Integrating this one obtains

$$\lambda = (c_1 t + c_2)^2.$$

If $\lambda = 0$ occurs at time T, we find

$$T = -\frac{c_2}{c_1},$$

hence we rewrite this as

$$\lambda(t) = a(t - T)^2.$$

Since equation [4.1] tends towards the linear wave equation when $r \to \infty$, the interesting behavior will occur at the origin. This is how we predict that f(0,t) will evolve.

4.3 Results

The computer model was run under the condition that $f(r,0) = f_0$ with various small velocities. The initial velocity is $\dot{f}(r,0) = v_0$, other input parameters are $r_{max} = R$, $\triangle r$ and $\triangle t$.

4.3.1 Evolution of f(0,t)

A typical evolution of f(0,t) is given in Figure 4.1. This is best modeled by a parabola of the form $a(t-T)^2+c$, where c is small and grows smaller as the grid size decreases. This curve in particular is approximated by $0.0000998(t-100.2)^2-0.00102$. This is close to the $a(t-T)^2$ predicted.

We fit f(0,t) to a parabola of the form $a(t-T)^2+c$ for various initial conditions. Table 4.1 gives initial conditions $f_0=f(r,0)$ and $v_0=\dot{f}(r,0)$ and the subsequent T and a when $\Delta r=0.1$ and $\Delta t=0.005$.

We have

$$T \approx \frac{2f_0}{|v_0|}$$

and

$$a \approx \frac{|v_0|^2}{4f_0}.$$

Table 4.1: $\mathbb{C}P^1$ model, charge 2 sector: Parameters for best fit parabola to f(0,t) vs. initial data f_0 and v_0 .

f_0	v_0	T	a
1.0	-0.01	204	0.0000245
1.0	-0.02	102	0.0000978
1.0	-0.03	68	0.000220
1.0	-0.04	51	0.000390
1.0	-0.05	41	0.000609
0.5	-0.01	104	0.0000479
2.0	-0.01	404	0.0000124
3.0	-0.01	604	0.00000828

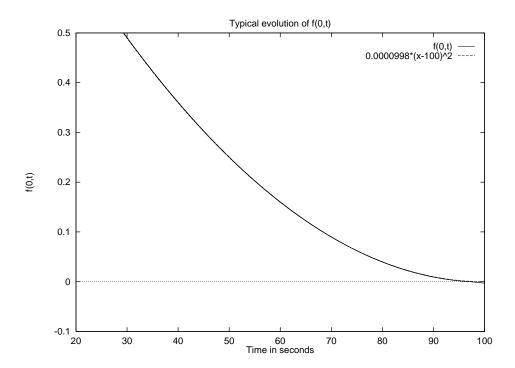


Figure 4.1: $\mathbb{C}P^1$ model, charge 2 sector: Evolution of f(0,t) and overlaying fit to parabola.

4.3.2 Characterization of time slices f(r,T): evolution of a horizontal ine

With the evolution of f(0,t) taken care of, we consider the shape of the time slices f(r,T) for a given fixed T. This is rather striking, as with the 4+1 dimensional model, an elliptical bump forms at the origin, as seen in figure 4.2.

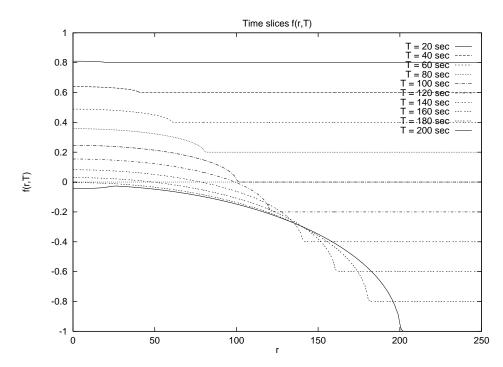


Figure 4.2: $\mathbb{C}P^1$ model, charge 2 sector: Time slices of f(r,T) evolve an elliptical bump at the origin.

As with the 4+1 dimensional model, this elliptical bump has equation

$$\frac{x^2}{a^2} + \frac{(y-k)^2}{b^2} = 1. (4.2)$$

The question naturally arises how the parameters a, b, and k evolve, and they

evolve as they did in the 4+1 dimensional model.

$$a = t$$

$$b = \frac{v_0^2}{4f_0}t^2$$

$$k = f_0 + v_0t$$

Table 4.2 shows these values as calculated using least squares fitting (to either a line or parabola). Since the elliptical fit only works before the right end of the ellipse hits the boundary at r = R the fit sometimes needed to be restricted to the portion of the data before this occurred. While the ellipse is small, there is a great deal of noise in finding the elliptical parameters, and to get a good data fit, this noise must often be removed. Here m_a and b_a is the slope and intercept of the line a(t), and likewise m_k and b_k are the slope and intercept of the line k(t). The parameter c is that in $b(t) = ct^2$

A typical evolution of a with $f_0 = 1.0$ and $v_0 = -0.01$ is in Figure 4.3. Note the initial noise.

Figure 4.4 is a typical evolution for elliptical parameter b as a function of time with $f_0 = 1.0$ and $v_0 = -0.01$.

Figure 4.5 is a typical evolution for elliptical parameter k as a function of time with $f_0 = 1.0$ and $v_0 = -0.01$.

Table 4.2: $\mathbb{C}P^1$ model, charge 2 sector, Elliptical parameters vs. initial conditions f_0 and v_0

f_0	v_0	m_a	b_a	c	m_k	b_k
0.5	-0.01	0.998	0.050	0.0000496	-0.00998	0.500
1.0	-0.01	0.998	0.023	0.0000250	-0.00999	1.000
2.0	-0.01	1.000	-0.138	0.0000125	-0.01000	2.000
3.0	-0.01	0.999	-0.080	0.00000836	-0.01000	3.000
4.0	-0.01	1.000	-0.173	0.00000628	-0.01000	4.000
1.0	-0.02	0.995	0.206	0.000100	-0.01994	1.000
1.0	-0.03	0.989	0.370	0.000224	-0.02983	0.996
1.0	-0.04	0.983	0.507	0.000396	-0.03965	0.993

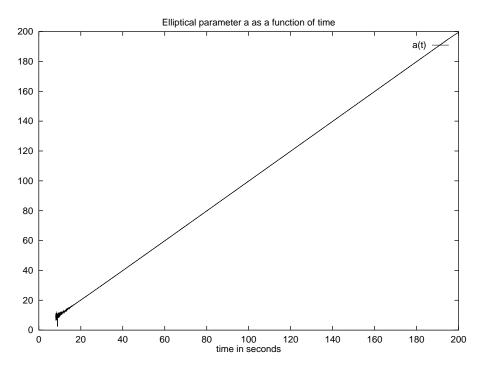


Figure 4.3: $\mathbb{C}P^1$ model, charge 2 sector: Elliptical parameter a as a function of time.

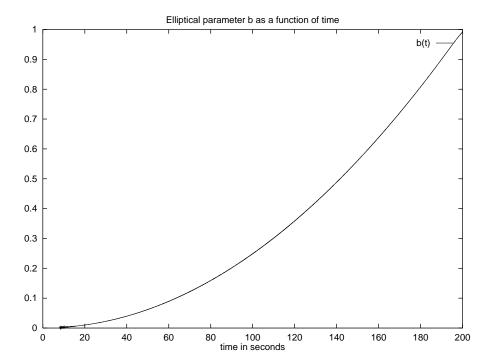


Figure 4.4: $\mathbb{C}P^1$ model, charge 2 sector: Elliptical parameter b as a function of time.

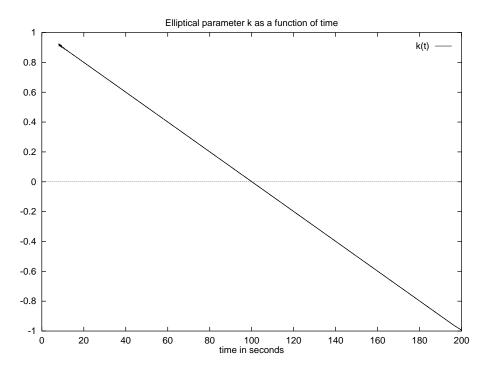


Figure 4.5: $\mathbb{C}P^1$ model, charge 2 sector: Elliptical parameter k as a function of time.

4.3.3 Characterization of time slices f(r,T): evolution of a parabola

As with the 4+1 dimensional model, the evolution of the ellipse suggested the curve was trying to obtain the shape of a parabola of the form

$$f(r,t) = pr^2 + h. (4.3)$$

To get the general form of the parabola, we follow the calculation from the 4+1 dimensional model. From our ellipse equation [4.2]:

$$\frac{dy}{dx} = -\frac{x^2b^2}{(y-k)a^2}$$

SO

$$\frac{d^2y}{dx} = \frac{-b^2}{(y-k)a^2} - \frac{xb^2}{(y-k)^2a^2} \frac{dy}{dx}$$

At x = 0, y - k = b and this gives

$$\frac{d^2y}{dx} = \frac{-b}{a^2}.$$

Recall from the previous section that $b=ct^2$ and a=t, so this gives

$$\frac{d^2y}{dx^2} = -c.$$

The identification of c gives

$$\frac{d^2y}{dx^2} = -\frac{v_0^2}{4f_0}.$$

So

$$p = -\frac{1}{2}\frac{d^2y}{dx^2} = -\frac{v_0^2}{8f_0}$$

When a run is started with this initial data, $\dot{f}_0 = v_0 = -0.02$, $f_0 = f(0,0) = 1.0$ and $p = \frac{v_0^2}{8f_0} = -0.00005$, the time slices of the data have this

same profile. This is shown in figure [4.6]. The parabolic parameter p varies by less than 1 part in 10 during the run as seen in figure [4.7]. The parabolic parameter h evolves close to f(0,t) as seen in figure [4.8].

For a parabola of the form

$$f(r,t) = p(t)r^2 + h(t),$$

we have

$$p(t) = -\frac{v_0^2}{8f_0},$$

i.e. p(t) is constant, and

$$h(t) = \frac{v_0^2}{4f_0} \left(t - \frac{2f_0}{|v_0|} \right).$$

Using the identification of p and h in the parabolic form of f(r,t) and letting

$$\tau = t - \frac{2f_0}{|v_0|}$$

we have

$$f(r,t) = -\frac{v_0^2}{8f_0}r^2 + \frac{v_0^2}{4f_0}\tau^2.$$

Substitute this into the partial differential equation [4.1], get a common denominator, and simplify to obtain

$$\frac{v_0^6}{32f_0^3} \left(\frac{r^4}{4} - r^2 \tau^2 + \tau^4 \right) + \frac{v_0^2}{2f_0} r^4 \stackrel{?}{=}$$
$$-\frac{v_0^6}{32f_0^3} \frac{r^4}{4} + \frac{v_0^6}{32f_0^3} \tau^4 + \frac{v_0^2}{2f_0} r^4.$$

The difference between the two sides is

$$\frac{v_0^6}{64f_0^3}r^4 - \frac{v_0^6}{32f_0^3}r^2\tau^2.$$

As with the 4+1 dimensional mode, our concern is with the geodesic approximation, and so $v_0^2/(f_0)$ is always chosen to be less than 1/200. The correction is then much smaller than the term

$$\frac{v_0^2}{2f_0}r^4.$$

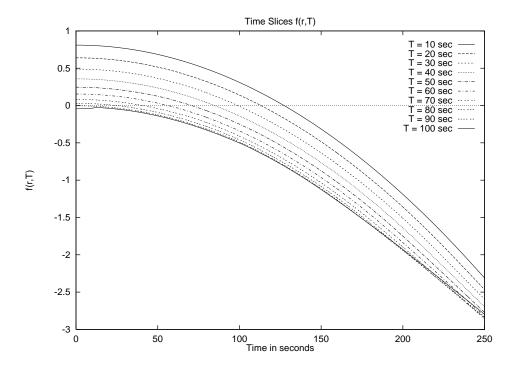


Figure 4.6: $\mathbb{C}P^1$ model, charge 2 sector: Time slices of the evolution of a parabola are parabolas.

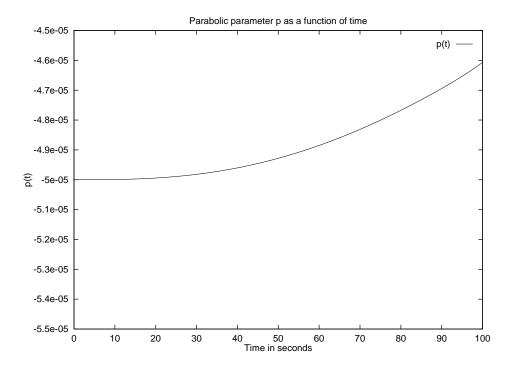


Figure 4.7: $\mathbb{C}P^1$ model, charge 2 sector: Evolution of parabolic parameter p with time.

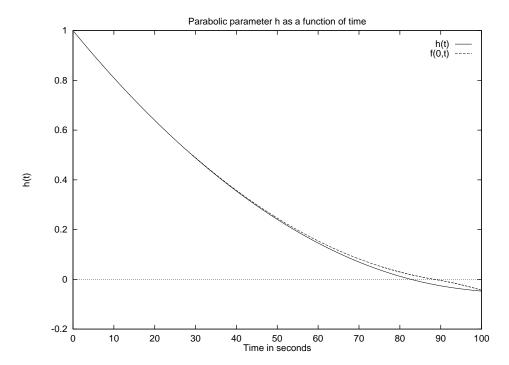


Figure 4.8: $\mathbb{C}P^1$ model, charge 2 sector: Evolution of parabolic parameter h with time, comparison to f(0,t).

Chapter 5

Conclusions

This dissertation investigates the shrinking of solitons in the 4+1 dimensional hyperbolic Yang Mills Lagrangian and the charge 1 and charge 2 sectors of the $\mathbb{C}P^1$ model.

Some theoretical work on the validity of the adiabatic limit for the monopole solutions to the Yang–Mills–Higgs theory on Minkowski space is presented in [6].

Of these models, only the $\mathbb{C}P^1$ model, charge 1 sector has been investigated in any detail in the literature. Many publications [2], [7], [8], [5] are concerned with the translation and scattering of $\mathbb{C}P^1$ solitons. The shrinking of solitons is investigated in [3] and [5]. The stability of solitons is investigated in [4].

In [4], solitons are found to be numerically unstable. A solution of the form

 $\frac{\beta}{z}$

shrinks spontaneously under their numerical procedure. This does not occur in our implementation of any of the three models in this dissertation. The static solutions do not evolve in time unless given an initial rate of shrinking. Further, stability and convergence analysis of two of the numerical procedures is provided in the Appendix.

In [3] the time evolution of the shrinking of solitons was studied. They arbitrarily cut off the Lagrangian outside of a ball of radius R, to prevent logarithmic divergence of the integral for the kinetic energy, and then analyze what happens in the $R \to \infty$ limit. In [5] the problem of the logarithmic divergence in the kinetic energy integral is solved by investigating the model on the sphere S^2 . The radius of the sphere determines a parameter for the size analogous to the parameter R for the size of the ball the Lagrangian is evaluated on in [3].

We use a method analogous to that in [3] of cutting off the Lagrangian outside of a ball of radius R, and we find an explicit integral for the shrinking of the soliton, dependent on two parameters: c which is a function of the kinetic energy, and R which is the size of the ball on which we evaluate the Lagrangian. Once these are specified, this integral gives the theoretical trajectory of the soliton. The dependence on a cut off R is shown to be a feature of the dynamics in the 1+1 dimensional partial differential equation modeled in this dissertation, although the dependence of R on the initial conditions is unclear. The shrinking predicted by the cut off Lagrangian and the shrinking found in the 1+1 dimensional partial differential equation model match.

In [3], via the cut off Lagrangian, an ODE for the evolution is found, and approximate solutions to this ODE were evaluated. A 1+1 dimensional partial differential equation was also solved numerically in [3] for the evolution of the shrinking of solitons, although the initial condition is not a static soliton.

They find the shrinking rate is given by a power law corrected by a small logarithmic term, with the corrections vanishing as $R \to \infty$. In contrast, we find an explicit integral for the shrinking of a soliton where the Lagrangian is cut off outside of the ball of radius R and that the corrections between this and the $R \to \infty$ limit are necessary.

Similar analysis of the predicted shrinking is given in the $\mathbb{C}P^1$ model, charge 2 sector and the 4+1 dimensional model. These two models have no divergences. A prediction is made by evaluating the effective Lagrangian, and the evolution of the 1+1 dimensional partial differential equation is shown to be close to that predicted.

In addition to this, in all of the models, the shape of a time slice f(r,T), with T fixed, is characterized, by elliptical bumps at the origin in the 4+1 dimensional model and the $\mathbb{C}P^1$ model, charge 2 sector or by hyperbolic bumps at the origin in the $\mathbb{C}P^1$ model, charge 1 sector.

In the 4+1 dimensional model and the $\mathbb{C}P^1$ model, a better approximation than the geodesic approximation for solutions to the partial differential equations are found in the evolution of the parabolas.

Appendices

Appendix A

Stability and convergence of the 4+1 dimensional model

In this chapter we analyze the stability of the equation

$$\ddot{f} = f'' + \frac{5f'}{r} + \frac{2\dot{f}^2}{f + r^2} - \frac{2(f')^2}{f + r^2} - \frac{8rf'}{f + r^2},\tag{A.1}$$

and the associated differencing scheme used in finding numerical solutions. Here f=f(r,t), and r is a radial variable, hence r>0. It will be shown that the stability behavior of the differential equation is qualitatively the same as that of the difference equation, and that the difference equation converges to the differential equation as $\Delta r \to 0$ and $\Delta t \to 0$.

The usual Von Neumann stability analysis has one substitute $f(r,t) = f_0(r,t) + \varepsilon e^{i\omega t} e^{i\kappa r}$, where $f_0(r,t)$ is presumed to solve the equation exactly, linearize in ε and then solve the resulting equation for ω in terms of κ . In this case, if ω has a negative imaginary part, then it has a growing mode. The equation is stable if it has no growing modes. This analysis is only valid when $\kappa \gg \frac{1}{\text{length scale}}$ and $\kappa \gg \frac{1}{r}$.

A.1 Continuum stability: simplified model

The first thing to address is the stability of the linear part of the partial differential equation [A.1]. This is:

$$\ddot{f} = f'' + \frac{5f'}{r}.\tag{A.2}$$

Set

$$f(r,t) = e^{i\kappa r}e^{i\omega t},$$

and plug into [A.2] to obtain the equation:

$$\omega^2 = \kappa^2 - \frac{5i\,\kappa}{r}$$

Solving this for ω yields:

$$\omega = \pm \sqrt{\kappa^2 - \frac{5\,i\kappa}{r}}$$

So, by this analysis there is always a solution for ω with a negative imaginary part, and therefore this equation has a growing mode and is not stable.

However, if we consider abstractly the equation

$$\ddot{f} = f'' + \frac{5f'}{r} = \mathcal{L}f$$

where $\mathcal{L}f$ is a linear operator; it is easy to see that

$$\mathcal{L} = r^{-5} \partial_r r^5 \partial_r.$$

and hence that

$$\mathcal{L} = r^{-5/2} (r^{-5/2} \partial_r r^{5/2}) (r^{5/2} \partial_r r^{-5/2}) r^{5/2} = -B^{-1} A^{\dagger} A B$$

where $B = r^{5/2}$ and

$$A = r^{5/2} \partial_r r^{-5/2}.$$

 $A^{\dagger}A$ is hermitian, and so it has real spectrum. Because it is essentially a square, it has positive real spectrum. Consequently $\operatorname{spec}(\mathcal{L}) = \operatorname{spec}(-A^{\dagger}A)$ is real and negative. So the solutions to the equation

$$\ddot{f} = \mathcal{L}f$$

consists of sines and cosines in the time variable multiplying the eigenfunctions of \mathcal{L} , and hence has no growing mode and is strictly stable.

So what gives?

The problem stems from the Von Neuman stability analysis which sets $f(r,t)=e^{i\kappa r}e^{i\omega t}$ instead of using the more general stability analysis where $f(r,t)=g(r)e^{i\omega t}$. The Von Neumann form is used because it results in algebraic equations instead of differential equations, which are much easier to solve. The Von Neumann analysis yielded

$$\omega = \pm \sqrt{\kappa^2 - \frac{5i\kappa}{r}} = \pm \kappa \sqrt{1 - \frac{5i}{\kappa r}}$$

Since in this analysis $\kappa \gg 1/r$, approximate using Taylor's theorem to obtain

$$\omega \approx \pm \kappa \mp \frac{5i}{2r}.$$

Since velocity v is

$$v = -\frac{\partial \omega}{\partial \kappa} \approx \mp 1.$$

then $r \approx r_0 \mp t$, so

$$\exp\left(\int i\omega dt\right) \approx e^{\pm i\kappa t} \exp\left(\pm \int \frac{5}{2(r_0 \mp t)} dt\right)$$

$$= e^{\pm i\kappa t} \exp\left(-\frac{5}{2}\ln(r_0 \mp t)\right)$$
$$= r^{-5/2}e^{\pm i\kappa t}.$$

What happened was that we let $g(r) = e^{i\kappa r}$ and so the $r^{-5/2}$ behavior had no choice but to come out in the $e^{i\omega t}$ portion of the equation.

If, however, we forcibly put the factor of $r^{-5/2}$ into the Von Neumann stability analysis, via

$$f(r,t) = r^{-5/2}e^{i\kappa r}e^{i\omega t}$$

plugging f into [A.1] one obtains the equation:

$$\omega^2 = \kappa^2 + \frac{15}{4r^2}$$

which has solutions,

$$\omega = \pm \frac{1}{2} \frac{\sqrt{15 + 4 r^2 \kappa^2}}{r}$$

So now, ω has only real roots, because the "correct" form for g(r) was used.

A.2 The whole equation

Similarly, any analysis of the general equation [A.1] will have some "growing modes" analogous to the factor of $r^{-5/2}$ found in the linear equation that do not affect the general stability. One can put this factor in explicitly to remove these modes.

Set

$$f(r,t) = f_0(r,t) + \varepsilon r^{(-5/2)} e^{i\kappa r} e^{i\omega t}$$

and linearize [A.1] in ε to obtain the equation:

$$\omega^{2} = \kappa^{2} - \frac{4i \omega \dot{f}_{0}}{f_{0} + r^{2}} + \frac{15}{4r^{2}} + \frac{8r^{2}}{(f_{0} + r^{2})^{2}} - \frac{10(f'_{0} + 2r)}{r(f_{0} + r^{2})} + \frac{4i \kappa (f'_{0} + 2r)}{f_{0} + r^{2}} + \frac{2(f'_{0} + 2r)^{2}}{(f_{0} + r^{2})^{2}} + \frac{2\dot{f}_{0}^{2}}{(f_{0} + r^{2})^{2}}$$

Solutions to this equation are found to be

$$\omega = \frac{1}{2} \left(-4ir\dot{f}_0 \pm \left[-8r^2\dot{f}_0^2 + 4\kappa^2r^6 + 4\kappa^2r^2f_0^2 - 8r^2f_0'^2 + 15f_0^2 - 40rf_0'f_0 + 16ir^4f_0'\kappa + 16ir^2\kappa f_0'f_0 - 72r^3f_0' + 32ir^3\kappa f_0 + 32i\kappa r^5 + 8\kappa^2r^4f_0 + 50f_0r^2 - 65r^4 \right]^{1/2} \right) / (r(f_0 + r^2)),$$

Now address the realm where \dot{f}_0 and f'_0 are small, and κ is large. Use a first order Taylor approximation to the square root to obtain,

$$\omega \approx \frac{-2i\dot{f}_0}{(f_0 + r^2)} \pm \kappa \left[1 + \frac{2i(f_0' + 2r)}{\kappa(f_0 + r^2)} - \frac{5_0'f_0}{\kappa^2 r(f_0 + r^2)^2} - \frac{\dot{f}_0^2 - f_0'^2}{\kappa^2(f_0 + r^2)^2} - \frac{72rf_0' + 50f_0 + 65r^2}{8\kappa^2(f_0 + r^2)^2} + O\left(\frac{1}{\kappa^2}\right) + O\left(\frac{1}{\kappa^4 r^2}\right) \right]$$
(A.3)

There are clearly some negative imaginary parts of ω , but since $\kappa \gg \frac{1}{r}$ they are all bounded.

A.3 Discretization scheme

After much preliminary work on stability with a standard finite differencing scheme, it was discovered that the main stability problems were generated by the linear part of the equation, namely

$$\ddot{f} = f'' + \frac{5f'}{r}$$

as $r \to 0$. Using a naive centered difference scheme for this part of the equation, one has irreconcilable problems with an instability the origin which is not present in the continuum equation. The "general rule of thumb" to use is when you have a problem, discretize the problem in the natural way for its differential operator. Proceeding along these lines:

$$\mathfrak{D}f = f'' + \frac{5f'}{r}$$

and it was shown in section 2.1 that $\mathcal{D}=r^{-5}\partial_r r^5\partial_r$. Discretize with q indexing the space variable r so $q\triangle r=r$ and n indexing the time variable t so $n\triangle t=t$. The discretization for $\mathcal{D}f$ is

$$(q\triangle r)^{-5} \left[\left[\left(q + \frac{1}{2} \right) \triangle r \right]^{5} \left(\frac{f((q+1)\triangle r, n\triangle t) - f(q\triangle r, n\triangle t)}{\triangle r} \right) - \left[\left(q - \frac{1}{2} \right) \triangle r \right]^{5} \left(\frac{f(q\triangle r, n\triangle t) - f((q-1)\triangle r, n\triangle t)}{\triangle r} \right) \right] / \triangle r$$

This differencing scheme removed the problems at the origin completely. Other than this, centered differences are used to discretize the equation [A.1].

A.4 Outline of the stability analysis

The stability analysis for this discretization scheme will be approached in the following way.

First, analyze the stability as $r \to 0$ by linearizing the difference scheme as a matrix \mathcal{L} and finding its eigenvalues and eigenvectors.

Second, use Von Neumann analysis on the difference scheme in the realm where r is bounded away from zero and $f(r,t) = f_0(r,t) + \varepsilon e^{i\kappa q \triangle r} e^{i\omega n \triangle t}$ where $f_0(r,t) \equiv c$, a constant; $f_0(r,t) \equiv c$ does solve the equation exactly. Find ω in terms of κ and show that the growing modes are all bounded.

Third, analyze what happens when f_0 is not presumed to be constant, but the derivatives are presumed to be close to zero. The equation for ω in terms of κ under this new circumstance gains additional dependencies on κ and ω . Given κ , one can show that inverting this map on ω yields contraction maps for ω in balls of radius $|\kappa|/2$ about $\omega = \pm \kappa$. So by the Contraction Mapping Principle, there are solutions for ω in the balls about $\pm \kappa$. From the form of the equation it can be seen that there are two solutions for ω , therefore these are they. Now let ω_0 indicate the solution for ω with f_0 presumed to be constant, and ω_1 indicate the solution for ω with no such assumption, one can use the conclusions of the Contraction Mapping Principle to show that the difference $|\omega_1 - \omega_0|$ is bounded. Hence the negative imaginary part of ω_1 , i.e. the growing mode, is bounded.

A.5 Stability near zero

The Von Neumann stability analysis is not valid for $r \to 0$. To analyze the stability here, let $f = f_0 + \varepsilon \delta f$ and linearize the equation [A.1] in ε . Represent this as

$$\ddot{\delta f} = \mathcal{L}_1(\delta f) + \mathcal{L}_2(\dot{\delta f}),$$

where \mathcal{L}_1 and \mathcal{L}_2 are linear operators, and \mathcal{L}_2 is close to a multiple of the identity matrix, and so one can replace it with cI. Then discretize in space, and find the eigenvalues and eigenvectors of \mathcal{L}_1 , and relate these to the eigenvalues and eigenvectors of

$$\begin{pmatrix} 0 & I \\ \mathcal{L}_1 & cI \end{pmatrix} \begin{bmatrix} \delta f \\ \dot{\delta f} \end{bmatrix} = \begin{bmatrix} \dot{\delta f} \\ \dot{\delta f} \end{bmatrix}. \tag{A.4}$$

This equation is

$$M\vec{v} = \dot{\vec{v}}.$$

if λ is an eigenvalue then one has

$$\dot{\vec{v}} = \lambda v$$
.

We know the solutions to this, for the i^{th} component of \vec{v} we get

$$v_i = A_i e^{\lambda t}.$$

Hence v_i does not grow with time if λ does not have a positive real component.

Now, to relate the eigenvalues and eigenvectors of \mathcal{L}_1 to the eigenvalues of the matrix in [A.4], presume that the vector

$$\left[\begin{array}{c} a \\ b \end{array}\right]$$

is an eigenvector of the matrix in equation [A.4] with eigenvalue λ . Therefore

$$\left(\begin{array}{cc} 0 & I \\ \mathcal{L}_1 & cI \end{array}\right) \left[\begin{array}{c} a \\ b \end{array}\right] = \lambda \left[\begin{array}{c} a \\ b \end{array}\right].$$

The top part of this equation states that $b = \lambda a$. Now one can use this in the bottom part of the equation in the following manner:

$$\mathcal{L}_1 a + cb = \lambda b$$

$$\mathcal{L}_1 a + c\lambda a = \lambda^2 a$$

In particular one sees that a must be an eigenvector of \mathcal{L}_1 , and that if the eigenvalues of \mathcal{L}_1 are equal to α then one can find the eigenvalues of the whole matrix via the equation

$$\alpha a + c\lambda a = \lambda^2 a$$
.

The solutions are

$$\lambda = \frac{c \pm \sqrt{c^2 + 4\alpha}}{2}.$$

So if, as we are about to find, $\alpha < 0$, we have two cases:

$$\left\{ \begin{array}{lll} c < 0 & : & \Re(\lambda) < 0 \\ c > 0 & : & \Re(\lambda) < c \end{array} \right.$$

So any solution of [A.4] can be written as a linear combination of solutions with at worst bounded growth rates.

Now let's turn to showing that $\alpha < 0$ if α is an eigenvalue of \mathcal{L}_1 . Allow $\delta f(q,n)$ to represent $\delta f(q \triangle r, n \triangle t)$ and likewise with $f_0(q,n) \equiv f_0(q \triangle r, n \triangle t)$, compute the following linearized equation, which is discretized in space only:

$$\ddot{\delta f}(q,n) =$$

$$-2\left(\frac{2q\left(\delta f(q+1,n) - \delta f(q-1,n)\right) - \frac{4q^{2}(\Delta r)^{2}\delta f(q,n)}{f_{0}(q,n) + (q\Delta r)^{2}}}{f_{0}(q,n) + (q\Delta r)^{2}}\right)$$

$$+(q\Delta r)^{-5}\left[\left(q + \frac{1}{2}\right)\Delta r\right]^{5}\left(\frac{\delta f(q+1,n) - \delta f(q,n)}{\Delta r}\right)$$

$$-\left[\left(q - \frac{1}{2}\right)\Delta r\right]^{5}\left(\frac{\delta f(q,n) - \delta f(q-1,n)}{\Delta r}\right)\right]/\Delta r$$

$$-8\left(\frac{(q\Delta r)^{2}\delta f(q,n)}{(f_{0}(q,n) + (q\Delta r)^{2})^{2}}\right) - 2\left(\frac{(\dot{f}_{0}(q,n))^{2}\delta f(q,n)}{(f_{0}(q,n) + (q\Delta r)^{2})^{2}}\right)$$

$$+4\left(\frac{\dot{f}_{0}(q,n)\dot{\delta}f(q,n)}{f_{0}(q,n) + (q\Delta r)^{2}}\right)$$

One is concerned about behavior as $r \to 0$, and so the functions $f_0(q\triangle r, n\triangle t)$ and $\dot{f}_0(q\triangle r, n\triangle t)$ can be approximated by $f_0(0, n\triangle t)$ and $\dot{f}_0(0, n\triangle t)$ which shall be called f_0 and \dot{f}_0 . Likewise, $f_0 + (q\triangle r)^2$ will be replaced with f_0 , and this yields the following equation:

$$\ddot{\delta f}(q,n) =
-2 \left(\frac{2q \left(\delta f(q+1,n) - \delta f(q-1,n) \right) - \frac{4q^2(\triangle r)^2 \delta f(q,n)}{f_0}}{f_0} \right)
+ (q\triangle r)^{-5} \left[\left[\left(q + \frac{1}{2} \right) \triangle r \right]^5 \left(\frac{\delta f(q+1,n) - \delta f(q,n)}{\triangle r} \right)
- \left[\left(q - \frac{1}{2} \right) \triangle r \right]^5 \left(\frac{\delta f(q,n) - \delta f(q-1,n)}{\triangle r} \right) \right] / \triangle r$$

$$-8 \left(\frac{(q\triangle r)^2 \delta f(q,n)}{(f_0)^2} \right) - 2 \left(\frac{(\dot{f_0})^2 \delta f(q,n)}{(f_0)^2} \right)$$
(A.5)

$$+4\left(\frac{\dot{f}_0\dot{\delta f}(q,n)}{f_0}\right)$$

Since this analysis is for $r \to 0$,

$$\mathcal{L}_2 = 4 \left(\frac{\dot{f}_0}{f_0} \right) I$$

$$\approx cI$$

is a good approximation.

To find \mathcal{L}_1 use [A.5] and the quadratic fit boundary condition at the origin, i. e.

$$\delta f(0,t) = \frac{4}{3}\delta f(\Delta r, t) - \frac{1}{3}\delta f(2\Delta r, t).$$

If one lets

$$\mathcal{L}_1 = [a_{i,j}],$$

and $f_0(k,t) = f_0(k\Delta r,t)$, then one obtains the following tridiagonal matrix:

$$a_{1,1} = \frac{4}{3} \left(\left(\frac{4}{f_0} \right) + (\triangle r)^{-2} \left[\left(\frac{1}{2} \right)^5 \right] \right)$$

$$+(\triangle r)^{-2} \left[-\left(\frac{3}{2} \right)^5 - \left(\frac{1}{2} \right)^5 \right] - 2 \left(\frac{\dot{f}_0}{f_0} \right)^2$$

$$a_{1,2} = -\frac{1}{3} \left(\left(\frac{4}{f_0} \right) + (\triangle r)^{-2} \left[\left(\frac{1}{2} \right)^5 \right] \right)$$

$$-\left(\frac{4}{f_0} \right) + (\triangle r)^{-2} \left[\left(\frac{3}{2} \right)^5 \right]$$

$$a_{k,k-1} = \frac{4k}{f_0} + k^{-5} (\triangle r)^{-2} \left[\left(k - \frac{1}{2} \right)^5 \right]$$

$$a_{k,k} = k^{-5}(\Delta r)^{-2} \left[-\left(k + \frac{1}{2}\right)^5 - \left(k - \frac{1}{2}\right)^5 \right] - 2\left(\frac{\dot{f}_0}{f_0}\right)^2$$

$$a_{k,k+1} = \left(\frac{-4k}{f_0}\right) + k^{-5}(\Delta r)^{-2} \left[\left(k + \frac{1}{2}\right)^5 \right]$$

One can use Maple to compute the eigenvalues and eigenvectors of this matrix while changing the size of the matrix n, and the values of f_0 , \dot{f}_0 , and $\triangle r$.

Since \dot{f}_0 is always much less than f_0 , the contributions from terms with \dot{f}_0 are negligible. Further, reparametrizing by multiplying a factor p times \dot{f}_0 , $\triangle r$ and p^2 times f_0 yields eigenvalues $1/p^2$ times the originals. In fact, the largest of the terms in any of these matrix elements should be that multiplied by $\triangle r^{-2}$, hence it is to be expected that rescaling $\triangle r$ itself by a factor p should result in the eigenvalues changing by approximately $1/p^2$.

For example, when n = 5, $f_0 = 1$, $\dot{f}_0 = -0.01$, $\triangle r = 0.01$ the matrix

$$\begin{bmatrix} -75828. & 75828. & 0 & 0 & 0 \\ 2381.1 & -32891. & 30510. & 0 & 0 \\ 0 & 4030.7 & -25633. & 21602. & 0 \\ 0 & 0 & 5145.1 & -23149. & 18004. \\ 0 & 0 & 0 & 5925.0 & -22010. \end{bmatrix}.$$

It has eigenvalues with multiplicity m and eigenvectors given by:

is:

Now rescale by p=5 and use parameters $f_0=25,\ \dot{f}_0=-0.05,\ \triangle r=0.05,\ n=5$ to get the matrix:

$$\begin{bmatrix} -3033.1 & 3033.1 & 0 & 0 & 0 \\ 95.243 & -1315.6 & 1220.4 & 0 & 0 \\ 0 & 161.23 & -1025.3 & 864.08 & 0 \\ 0 & 0 & 205.80 & -925.96 & 720.17 \\ 0 & 0 & 0 & 237.00 & -880.40 \end{bmatrix}.$$

This has eigenvalues with multiplicity m and eigenvectors:

These are 1/25th of those of the previous case, as expected.

Now, vary \dot{f}_0 , using parameters $f_0=1,\ \dot{f}_0=-0.1,\ \triangle r=0.01,\ n=5$ and get the matrix:

$$\begin{bmatrix} -75828. & 75828. & 0 & 0 & 0 \\ 2381.1 & -32891. & 30510. & 0 & 0 \\ 0 & 4030.7 & -25633. & 21602. & 0 \\ 0 & 0 & 5145.1 & -23149. & 18004. \\ 0 & 0 & 0 & 5925.0 & -22010. \end{bmatrix}$$

With eigenvalues:

These are unchanged to this level of precision from those found with $\dot{f}_0 = -0.01$. The contribution of the terms with \dot{f}_0 is negligible, as expected.

Now, rescale $\triangle r = 0.1$ while leaving $f_0 = 1$ and $\dot{f}_0 = -0.01$ and get the matrix and eigenvalues:

$$\begin{bmatrix} -753.00 & 753.00 & 0 & 0 & 0 \\ 31.731 & -328.91 & 297.18 & 0 & 0 \\ 0 & 52.187 & -256.33 & 204.14 & 0 \\ 0 & 0 & 67.291 & -231.49 & 164.20 \\ 0 & 0 & 0 & 79.050 & -220.10 \end{bmatrix}$$

So rescaling $\triangle r$ by a factor of 10 rescales the eigenvalues by approximately a factor of $1/100^{\rm th}$, with the scaling best closest to the origin. This is consistent with the original equations.

Lastly, check to see what effect rescaling n or the size of the matrix has. Ideally since we want to explore behavior near r=0 we would want to take $n\to\infty$ as $\Delta r\to 0$ and $n\Delta r\to 0$, but this isn't possible, so instead, simply double the size of n to n=10. The matrix and eigenvalues are:

г	-									_
l	-75828.	75828.	0	0	0	0	0	0	0	0
l	2381.1	-32891	. 30510.	0	0	0	0	0	0	0
l	0	4030.7	-25633	21602.	0	0	0	0	0	0
l	0	0	5145.1	-23149.	18004.	0	0	0	0	0
l	0	0	0	5925.0	-22010.	16085.	0	0	0	0
l	0	0	0	0	6496.2	-21394.	14897.	0	0	0
	0	0	0	0	0	6931.7	-21023.	14091.	0	0
	0	0	0	0	0	0	7273.9	-20783.	13509.	0
l	0	0	0	0	0	0	0	7550.2	-20618.	13068.
l	0	0	0	0	0	0	0	0	7777.8 -	-20501.

Eigenvalue	m	Eigenvector					
-79898.	1	[8.8170,	47043,	.036302,	0034177,		
		.00035827,	000049446,	$.35708 \times 10^{-5}$	44969×10^{-5} ,		
-42854.	1	[2.0301,	.88204,	44662,	.19165,		
		082308,	.036070,	016080,	.0071721,		
		0030613,	.0010666]				
	-	6539×10^{-6} , -	92087×10^{-6}]				
-39076.	1	[7.1614,	3.4681,	-1.2625,	.13923,		
		.23670,	30248,	.25528,	17811,		
		.10369,	043440]				
-34796.	1	[9.2387,	4.9953,	-1.0334,	49271,		
		.61276,	30607,	.00732,	.14346,		
		15312,	.08324]				
-29191.	1	[-19.285,	-11.852,	.068578,	2.1976,		
		75346,	47022,	.57537,	10236,		
		24492,	.21945]				
-22916.	1	[9.1374,	6.3726,	1.3700,	-1.0152,		
		40642,	.39472,	.13659,	21252,		
		04067,	.13029]				
-16554.	1	[-3.3235,	-2.5963,	-1.1309,	.00853,		
		.32669,	.10839,	10703,	08724,		
		.03047,	.059846]				
-10673.	1	[8.5362,	7.3303,	4.6724,	1.8693,		
		040111,	71838,	50033,	014049,		
		.25853,	.20488]				
-5754.	1	[1.7509,	1.6167,	1.3015,	.89606,		
		.49400,	.16895,	03811,	12426,		
		11777,	062081]				
-2158.	1	[.57440,	.55752,	.51684,	.45759,		
		.38593,	.30774,	.22905,	.15526,		
		.090760,	.038476]				

As before, all eigenvalues are negative. The modes localized near zero don't change. The eigenvalues increase towards zero as n increases because there are growing modes of this equation away from r = 0.

One can conclude that the eigenvalues of this matrix under reasonable initial conditions will always all be negative, as required. This differencing scheme does not have any instabilities generated at the origin.

A.6 Stability away from zero: simplified model

In this section the stability of difference equation derived from [A.1] with the differencing scheme outlined in section 2.1 under the special condition that $f(r,t) = f_0(r,t) + \varepsilon e^{i\kappa q \triangle r} e^{i\omega n \triangle t}$ where $f_0(r,t) \equiv c$, a constant, will be addressed.

An astute reader will note that the factor of $r^{-5/2}$ is missing in this analysis. Its explicit inclusion makes the resultant expression for ω far uglier than even it is now. A part of the growing mode is analogous to the $r^{-5/2}$ term, but not exactly the same.

Plug into [A.1] and linearize in ε to obtain the following equation:

$$\frac{e^{i\omega\Delta t} + e^{-i\omega\Delta t} - 2}{(\Delta t)^2} = + \frac{\left(q + \frac{1}{2}\right)^5 \left(e^{i\kappa\Delta r} - 1\right) - \left(q - \frac{1}{2}\right)^5 \left(1 - e^{-i\kappa\Delta r}\right)}{q^5(\Delta r)^2} - \frac{4q(e^{-i\kappa\Delta r} - e^{i\kappa\Delta r})}{f_0 + (q\Delta r)^2}.$$
(A.6)

Let $x = e^{i\omega \Delta t}$ and

$$J = -\frac{4q(e^{-i\kappa\Delta r} - e^{i\kappa\Delta r})}{f_0 + (q\Delta r)^2} + \frac{\left(q + \frac{1}{2}\right)^5 \left(e^{i\kappa\Delta r} - 1\right) - \left(q - \frac{1}{2}\right)^5 \left(1 - e^{-i\kappa\Delta r}\right)}{q^5(\Delta r)^2}.$$

Hence J represents the right hand side of the equation. One can reduce equation [A.6] to

$$x^2 - (2 + J\triangle t^2)x + 1 = 0$$

and so it has two solutions if we try to solve for $x = e^{i\omega t}$. Hence it has two (logarithmic) solutions for ω . These are obtained via the quadratic formula

$$x = e^{i\omega \triangle t} = 1 + \frac{J\triangle t^2}{2} \pm \sqrt{J}\triangle t\sqrt{1 + \frac{J\triangle t^2}{4}}$$

SO

$$\omega = \frac{-i \ln \left(1 + \frac{J \triangle t^2}{2} \pm \sqrt{J} \triangle t \sqrt{1 + \frac{J \triangle t^2}{4}} \right)}{\triangle t}$$

Clearly the biggest concern is determining exactly how big $J\triangle t^2$ is. Let $\kappa\triangle r=\theta$, then reduce exponentials to sines and cosines appropriately, and expand the factors of $q\pm 1/2$, and simplify using such information as $q=r/\triangle r$, to obtain

$$J = \frac{-8i\kappa r}{f_0 + r^2} \left(\frac{\sin\theta}{\theta}\right) + \kappa^2 \left(\frac{2\cos\theta - 2}{\theta^2}\right) + \frac{5i\kappa}{r} \left(\frac{\sin\theta}{\theta}\right)$$
$$+ \frac{5\kappa^2 \triangle r^2}{2r^2} \left(\frac{2\cos\theta - 2}{\theta^2}\right) + \frac{5i\kappa \triangle r^2}{2r^3} \left(\frac{\sin\theta}{\theta}\right)$$
$$+ \frac{5\kappa^2 \triangle r^4}{16r^4} \left(\frac{2\cos\theta - 2}{\theta^2}\right) + \frac{i\kappa \triangle r^4}{16r^5} \left(\frac{\sin\theta}{\theta}\right)$$

Analyze the behavior as $\triangle r \to 0$ and $\triangle t \to 0$, under the assumption that r > 0 is fixed and that $\triangle t \ll \triangle r$. One also knows that $\kappa \triangle r < \pi$. Consequently, all terms go to zero as $\triangle r \to 0$ except the following:

$$\frac{-8i\kappa r}{f_0 + r^2} \left(\frac{\sin \theta}{\theta} \right) + \kappa^2 \left(\frac{2\cos \theta - 2}{\theta^2} \right) + \frac{5i\kappa}{r} \left(\frac{\sin \theta}{\theta} \right) + \frac{5\kappa^2 \triangle r^2}{2r^2} \left(\frac{2\cos \theta - 2}{\theta^2} \right).$$

The trigonometric part is strictly bounded, and the simple condition that $\triangle t \ll c\triangle r$ with c chosen sufficiently small, implies that $\kappa\triangle t^2$ or $(\kappa\triangle t)^2 \ll (c\pi)^2$ can be made as small as one likes.

In particular, one may use the Taylor approximation to the square root.

Then one may then use the Taylor approximation to the logarithm, and with some cancellation between the first and second term, one obtains:

$$\omega \approx \frac{-i \ln \left[\frac{J \triangle t^2}{2} \pm \sqrt{J} \triangle t \left(1 + \frac{J \triangle t^2}{8} + O(J^2 \triangle t^4) \right) \right]}{\triangle t}$$

$$\approx \frac{-i \left[\pm \sqrt{J} \triangle t + O\left((\sqrt{J} \triangle t)^3\right) \right]}{\triangle t}$$

$$\approx \left[\pm i \sqrt{J} + O\left(\sqrt{J}^3 \triangle t^2\right) \right]$$

Recall, as $\triangle r \rightarrow 0$ all of the terms in J go to 0 except for

$$\frac{-8i\kappa r}{f_0+r^2}\left(\frac{\sin\theta}{\theta}\right)+\kappa^2\left(\frac{2\cos\theta-2}{\theta^2}\right)+\frac{5i\kappa}{r}\left(\frac{\sin\theta}{\theta}\right)+\frac{5\kappa^2\triangle r^2}{2r^2}\left(\frac{2\cos\theta-2}{\theta^2}\right).$$

So one has

$$\sqrt{J} \approx \sqrt{\left[\frac{-8i\kappa r}{f_0 + r^2} \left(\frac{\sin\theta}{\theta}\right) + \kappa^2 \left(\frac{2\cos\theta - 2}{\theta^2}\right) + \frac{5i\kappa}{r} \left(\frac{\sin\theta}{\theta}\right)\right]} + \frac{5\kappa^2 \triangle r^2}{2r^2} \left(\frac{2\cos\theta - 2}{\theta^2}\right) + O(\triangle r).$$

Since κ is large while $\triangle r$ is small, the largest term here should be the κ^2 unmultiplied by $\triangle r$, and so approximating the square root this can be modified to:

$$\sqrt{J} \approx i\kappa \sqrt{\frac{2 - 2\cos\theta}{\theta^2}} \left[1 + \frac{4ir}{\kappa(f_0 + r^2)} \left(\frac{\sin\theta}{\theta} \right) \left(\frac{\theta^2}{2 - 2\cos\theta} \right) \right]$$

$$-\frac{5i}{2\kappa r} \left(\frac{\sin \theta}{\theta} \right) \left(\frac{\theta^2}{2 - 2\cos \theta} \right) - \frac{5\triangle r^2}{4r^2} + O\left(\frac{1}{\kappa^2} \right) \right].$$

Therefore the leading order term of \sqrt{J} is of size $O(\kappa)$. Recalling $\kappa \triangle r < \pi$ one can make the correction $O\left(\sqrt{J}^3 \triangle t^2\right)$ as small as one likes by requiring that $\triangle t < c \triangle r^{3/2}$ and choosing the factor c appropriately. And given this choice of $\triangle t$, then one has that

$$\omega \approx \pm \sqrt{\frac{2 - 2\cos\theta}{\theta^2}} \left[\kappa + \frac{4ir}{(f_0 + r^2)} \left(\frac{\sin\theta}{\theta} \right) \left(\frac{\theta^2}{2 - 2\cos\theta} \right) - \frac{5i}{2r} \left(\frac{\sin\theta}{\theta} \right) \left(\frac{\theta^2}{2 - 2\cos\theta} \right) \right]$$
bounded terms
$$-\frac{5\kappa\Delta r^2}{4r^2} + O\left(\frac{1}{\kappa} \right) + O\left(\kappa\sqrt{J}^3\Delta t^2\right) \right].$$
terms that go to zero

Furthermore it is clear that if one permitted $r \to 0$ that the dominant piece would be

$$\omega \approx \pm \kappa \sqrt{\frac{2 - 2\cos\theta}{\theta^2}} - \frac{5i}{2r} \left(\frac{\sin\theta}{\theta}\right) \left(\frac{\theta^2}{2 - 2\cos\theta}\right)$$

and as $\theta \to 0$ this goes to

$$\omega \approx \pm \kappa \mp \frac{5i}{2r}$$

or exactly what we obtained in appendix A.1 that was so often "corrected" by the addition of a factor of $r^{-5/2}$.

A.7 The complications

Now we must deal with the reality that we have thus far assumed $f_0 \equiv c$, and in general this is not so. We need to know that when f_0 is a function with small bounded derivatives, that the growing modes remain close to those in the previous analysis.

In the previous section we let $f(r,t) = f(q\triangle r, n\triangle t) = f_0(r,t) + \varepsilon e^{i\kappa q\triangle r}e^{i\omega n\triangle t}$ under the assumption that $f_0 \equiv c$. Call the solution for ω in terms of κ in this analysis ω_0 . The equation solved to do this was

$$\frac{e^{i\omega\Delta t} + e^{-i\omega\Delta t} - 2}{(\Delta t)^2} = + \frac{\left(q + \frac{1}{2}\right)^5 \left(e^{i\kappa\Delta r} - 1\right) - \left(q - \frac{1}{2}\right)^5 \left(1 - e^{-i\kappa\Delta r}\right)}{q^5(\Delta r)^2} - \frac{4q(e^{-i\kappa\Delta r} - e^{i\kappa\Delta r})}{f_0 + (q\Delta r)^2}.$$

Characterize this equation as

$$g(\omega) = \text{old}(\kappa).$$

If one does not assume that $f_0 \equiv c$ then one gets the equation

$$\frac{e^{i\omega\Delta t} + e^{-i\omega\Delta t} - 2}{(\Delta t)^2} = + \frac{\left(q + \frac{1}{2}\right)^5 \left(e^{i\kappa\Delta r} - 1\right) - \left(q - \frac{1}{2}\right)^5 \left(1 - e^{-i\kappa\Delta r}\right)}{q^5 (\Delta r)^2}
- \frac{4q(e^{-i\kappa\Delta r} - e^{i\kappa\Delta r})}{f_0 + (q\Delta r)^2} - \frac{4f'_0}{f_0 + r^2} \left(\frac{e^{i\kappa\Delta r} - e^{-i\kappa\Delta r}}{2\Delta r}\right)
+ \frac{2(f'_0)^2}{(f_0 + r^2)^2} + \frac{8rf'_0}{(f_0 + r^2)^2} - \frac{2\dot{f}_0^2}{(f_0 + r^2)^2}
+ \frac{4\dot{f}_0}{f_0 + r^2} \left(\frac{e^{i\omega\Delta t} - e^{-i\omega\Delta t}}{2\Delta t}\right)$$
(A.7)

This equation is quadratic in $e^{i\omega\Delta t}$; hence it has two solutions for $e^{i\omega\Delta t}$, and hence two solutions for ω for each branch of the logarithm. We wish to get a handle on these two solutions for ω . Equation [A.7] can be characterized as

$$g(\omega) = \text{old}(\kappa) + \text{new}_1(\kappa) + \text{new}_2(\omega)$$
 (A.8)

with

$$\operatorname{new}_{1}(\kappa) = -\frac{4f'_{0}}{f_{0} + r^{2}} \left(\frac{e^{i\kappa \triangle r} - e^{-i\kappa \triangle r}}{2\triangle r} \right) + \frac{2(f'_{0})^{2}}{(f_{0} + r^{2})^{2}} + \frac{8rf'_{0}}{(f_{0} + r^{2})^{2}} - \frac{2\dot{f}_{0}^{2}}{(f_{0} + r^{2})^{2}}$$
(A.9)

 $\quad \text{and} \quad$

$$\text{new}_2(\omega) = \frac{4\dot{f}_0}{f_0 + r^2} \left(\frac{e^{i\omega\Delta t} - e^{-i\omega\Delta t}}{2\Delta t} \right). \tag{A.10}$$

Here \dot{f}_0 is substituted for the finite difference

$$\frac{f_0(q\triangle r, (n+1)\triangle t) - f_0(q\triangle r, (n-1)\triangle t)}{2\triangle t},$$

and likewise with f'_0 and the centered difference equivalent in the r variable.

Now note that

$$g(\omega) = \frac{2\cos\omega\Delta t - 2}{\Delta t^2},\tag{A.11}$$

and

$$\omega_0 = g^{-1}(\operatorname{old}(\kappa))$$

and

$$\omega_1 = g^{-1}(\text{old}(\kappa) + \text{new}_1(\kappa) + \text{new}_2(\omega_1)).$$

Further if one lets

$$\omega_s = g^{-1}(\text{old}(\kappa) + s(\text{new}_1(\kappa) + \text{new}_2(\omega_s)))$$

then

$$|\omega_{1} - \omega_{0}| = \left| \int_{0}^{1} \frac{\partial \omega_{s}}{\partial s} ds \right|$$

$$\leq \int_{0}^{1} \left| \left[(g^{-1})' \right] (\operatorname{new}_{1}(\kappa) + \operatorname{new}_{2}(\omega_{s})) \right| ds$$

$$\leq \max \left(\left| (g^{-1})' \right| \right) \max \left(\left| \operatorname{new}_{1}(\kappa) + \operatorname{new}_{2}(\omega_{s}) \right| \right) \quad (A.12)$$

So finding a bound on ω in terms of κ will allow one to find a bound for $|\omega_1 - \omega_0|$ in terms of κ .

Now we will show that the map

$$T(\omega) = g^{-1}(\text{old}(\kappa) + \text{new}_1(\kappa) + \text{new}_2(\omega))$$

is a contraction mapping on the ball $|\omega - \kappa| < |\kappa|/2 = B(\kappa, \kappa/2)$. Using [A.11], one finds that

$$g'(\omega) = \frac{-2\sin(\omega \triangle t)}{\triangle t}.$$

We've already stated one needs to choose $\triangle t < c \triangle r^{3/2}$ so specifically, one can make $\triangle t < \triangle r/150$. Then since $|\kappa \triangle r| < \pi$ and $|\omega| < 3|\kappa|/2$ this implies that $|\omega \triangle t| < \pi/100$ and one has

$$|g'(\omega)| = |2\omega| \left| \frac{\sin(\omega \Delta t)}{\omega \Delta t} \right| > 1.98|\omega|.$$

Now if ω_1 and ω_2 are in $B(\kappa, \kappa/2)$ then assign y_1 and y_2 as follows and find that

$$y_1 = \operatorname{old}(\kappa) + \operatorname{new}_1(\kappa) + \operatorname{new}_2(\omega_1)$$

$$y_2 = \operatorname{old}(\kappa) + \operatorname{new}_1(\kappa) + \operatorname{new}_2(\omega_2)$$

$$y_2 - y_1 = \operatorname{new}_2(\omega_2) - \operatorname{new}_2(\omega_1).$$

Letting,

$$y(s) = y_1 + s(y_2 - y_1),$$

calculate

$$|T(\omega_{2}) - T(\omega_{1})| =$$

$$|g^{-1}(y_{2}) - g^{-1}(y_{1})| = \left| \int_{0}^{1} (g^{-1})'(y(s))(y_{2} - y_{1})ds \right|$$

$$\leq \int_{0}^{1} \max \left| (g^{-1})'(y(s)) \right| \left| (y_{2} - y_{1}) \right| ds$$

$$\leq \max \left| (g^{-1})'(y(s)) \right| \left| (y_{2} - y_{1}) \right|.$$
(A.13)

Simple calculus yields:

$$(g^{-1})'(g(\omega)) = \frac{1}{g'(\omega)}.$$

By choice of y_1 and y_2 and $\omega_1, \omega_2 \in B(\kappa, \kappa/2)$,

$$\max |(g^{-1})'(y(s))| = \frac{1}{1.98|\omega|} \le \frac{2}{1.98|\kappa|}.$$
 (A.14)

Since $|\omega_1|, |\omega_2| \leq 3|\kappa|/2$ and $|\omega_1 \triangle t|, |\omega_2 \triangle t| < \pi/100$, we have

$$|\operatorname{new}_{2}(\omega_{2}) - \operatorname{new}_{2}(\omega_{1})| = \left| \frac{4\dot{f}_{0}}{f_{0} + r^{2}} \left(\frac{i \sin(\omega_{2} \Delta t)}{\Delta t} - \frac{i \sin(\omega_{1} \Delta t)}{\Delta t} \right) \right|$$

$$= \left| \frac{4\dot{f}_{0}}{f_{0} + r^{2}} \right| \left| \left(\frac{\sin(\omega_{2} \Delta t)}{\Delta t} - \frac{\sin(\omega_{1} \Delta t)}{\Delta t} \right) \right|$$

$$= \left| \frac{4\dot{f}_{0}}{(f_{0} + r^{2})} \right| \left| \int_{\omega_{1}}^{\omega_{2}} \cos(s \Delta t) ds \right|$$

$$\leq \left| \frac{4\dot{f}_{0}}{(f_{0} + r^{2})} \right| |\omega_{2} - \omega_{1}|. \tag{A.15}$$

Now plug [A.14] and [A.15] into [A.13], to obtain:

$$|T(\omega_2) - T(\omega_1)| = |g^{-1}(y_2) - g^{-1}(y_1)| \le \frac{2}{1.98|\kappa|} \left| \frac{4\dot{f}_0}{(f_0 + r^2)} \right| |\omega_2 - \omega_1|.$$

The quantity

$$\left| \frac{\dot{f}_0}{f_0 + r^2} \right|$$

defines the time scale for the problem. In order for this entire analysis to make sense one expects

$$\kappa \gg {\rm time\ scale} \qquad {\rm and} \qquad \kappa \gg {\rm length\ scale}.$$

Therefore, this is sufficient to show that T(w) is a contraction map from $B(\kappa, \kappa/2)$ to itself. So by the Contraction Mapping Principle, one concludes that there exists a fixed point of T in $B(\kappa, \kappa/2)$. Clearly this argument holds just as well for -T and $B(-\kappa, \kappa/2)$, so there is a fixed point for -T in $B(-\kappa, \kappa/2)$. Since the left hand side of [A.7] is quadratic in $e^{i\omega \Delta t}$, there are two solutions for ω and these are they.

Lastly, we finish estimating in equation [A.12]. We already have a perfectly good estimate for $(g^{-1})'$ from [A.14]. We merely need to estimate

$$|\text{new}_1(\kappa) + \text{new}_2(\omega)|$$
.

Replacing the exponentials with their trigonometric forms in [A.9] and [A.10] to get:

$$\operatorname{new}_{1}(\kappa) = -\frac{4f'_{0}}{f_{0} + r^{2}} \left(\frac{2i\sin(\kappa \triangle r)}{2\triangle r} \right) + \frac{2(f'_{0})^{2}}{(f_{0} + r^{2})^{2}} + \frac{8rf'_{0}}{(f_{0} + r^{2})^{2}} - \frac{2\dot{f}_{0}^{2}}{(f_{0} + r^{2})^{2}}$$

and

$$\operatorname{new}_{2}(\omega) = \frac{4\dot{f}_{0}}{f_{0} + r^{2}} \left(\frac{2i\sin\omega\Delta t}{2\Delta t} \right). \tag{A.16}$$

Recall also that $\kappa \gg 1/r$ so $\kappa r \gg 1$. Now if θ is real,

$$|\sin \theta| \le \theta$$
,

and if θ is complex with $|\theta|$ sufficiently small, as it would be if $\theta = \omega \triangle t$, then

$$|\sin \theta| \le 1.01 |\theta|,$$

one has

$$|\text{new}_{1}(\kappa) + \text{new}_{2}(\omega)| \le \left| \frac{4f'_{0}}{f_{0} + r^{2}} \right| |\kappa| + \left| \frac{2(f'_{0})^{2}}{(f_{0} + r^{2})^{2}} \right| + \left| \frac{8rf'_{0}}{(f_{0} + r^{2})^{2}} \right| + \left| \frac{2\dot{f}_{0}^{2}}{(f_{0} + r^{2})^{2}} \right| + \left| \frac{4\dot{f}_{0}}{f_{0} + r^{2}} \right| |1.01\omega|$$

By my previous arguments about κ and the length and time scales, the three central terms are much much smaller than the others. Plugging $|\omega| \leq 3|\kappa|/2$ and this and [A.14] into [A.12] one concludes that under these assumptions

$$|w_{1} - w_{0}| \leq \frac{2}{1.98|\kappa|} \left(\left| \frac{4f'_{0}}{f_{0} + r^{2}} \right| |\kappa| + \left| \frac{2(f'_{0})^{2}}{(f_{0} + r^{2})^{2}} \right| + \left| \frac{8rf'_{0}}{(f_{0} + r^{2})^{2}} \right| + \left| \frac{2\dot{f}_{0}^{2}}{(f_{0} + r^{2})^{2}} \right| + \left| \frac{4\dot{f}_{0}}{f_{0} + r^{2}} \left| \frac{3.03|\kappa|}{2} \right).$$

Hence, $|\omega_1 - \omega_0|$ is bounded, which implies in turn that the imaginary part of ω_1 is bounded since the imaginary part of ω_0 was. Once again the growing modes are bounded.

Further, if we compare with equation [A.3], we see analogues between the terms in these two equations.

$$\frac{2}{1.98} \left| \frac{4f_0'}{f_0 + r^2} \right| \leftrightarrow \frac{2i(f_0' + 2r)}{f_0 + r^2}$$

and

$$\frac{3.03}{1.98} \left| \frac{4\dot{f_0}}{f_0 + r^2} \right| \longleftrightarrow \frac{-2i\dot{f_0}}{f_0 + r^2}.$$

A.8 Convergence estimates

This section contains an analysis of the convergence of the differencing scheme for the equation

$$\ddot{f} = f'' + \frac{5f'}{r} + \frac{2\dot{f}^2}{f + r^2} - \frac{2(f')^2}{f + r^2} - \frac{8rf'}{f + r^2}.$$
 (A.17)

We will show that as $\triangle r \to 0$ and $\triangle t \to 0$ that the solution found for f(r,t) converges to an actual solution of the partial differential equation.

First consider the scheme to forward integrate the equation and the error in it. Substitute the appropriate differences in [A.17] then solve for $f(r, t + \Delta t)$ in the difference for \ddot{f} i.e. solve:

$$f_c(r, t + \Delta t) = 2f_c(r, t) - f_c(r, t - \Delta t)$$

$$+ \Delta t^2 \left(f_c'' + \frac{5f_c'}{r} + \frac{2\dot{f}_c^2}{f_c + r^2} - \frac{2(f_c')^2}{f_c + r^2} - \frac{8rf_c'}{f_c + r^2} \right).$$

Here f_c is used instead of f to indicate that this is the numerically calculated value rather than the one that is a solution to the PDE. Also assume the derivatives are represented by the appropriate differences. Approximate $f_c(r, t + \Delta t)$ for use in \dot{f}_c^2 by using first $f_c(r, t + \Delta t) = 2f_c(r, t) - f_c(r, t - \Delta t)$, and then one iterates 6 times, finding a new $f_c(r, t + \Delta t)$ from solving the equation with the previous value. Using greater numbers of iterations on $f_c(r, t + \Delta t)$ does not change the answer to the numerical precision on the computer, so this will not be considered as a source of error.

The error comes from the discretizations. Let $\Delta t^2 C_1$ be the error in the difference used for \ddot{f} , and C_2 be the accumulated error in the differences for the left hand side of [A.17], then one can see that the error is of the form

$$|f(r, t + \triangle t) - f_c(r, t + \triangle t)| = |\triangle t^2 C_1 + \triangle t^2 C_2| \le \triangle t^2 (|C_1| + |C_2|).$$

The error in going 2 steps would be

$$|f(r, t + 2\triangle t) - f_c(r, t + 2\triangle t)| \le 2\triangle t^2 (|C_1| + |C_2|) + e^{W\triangle t} [\triangle t^2 (|C_1| + |C_2|)].$$

With the term involving $e^{W \triangle t}$ coming from the stability analysis, with $W \ge |\Re(i\omega)|$. One knows from the stability analysis that the negative imaginary part of ω is bounded, hence W is. The error in going n steps would therefore be:

$$|f(r, t + n\Delta t) - f_c(r, t + n\Delta t)| \le n\Delta t^2 (|C_1| + |C_2|)$$

 $+ \sum_{j=1}^n e^{Wj\Delta t} [\Delta t^2 (|C_1| + |C_2|)].$

And one also knows that

$$\sum_{j=1}^{n} e^{Wj\triangle t} \le \int_{1}^{n} e^{Wj\triangle t} dj = \frac{e^{Wn\triangle t} - e^{W\triangle t}}{W\triangle t}$$
(A.18)

Since W was strictly bounded, one represents the above as $\frac{C_3}{\Delta t}$. Now see that the error in going n steps is

$$|f(r, t + n\Delta t) - f_c(r, t + n\Delta t)| \le n\Delta t^2 (|C_1| + |C_2|) + \Delta t C_3 (|C_1| + |C_2|).$$

Since C_3 is bounded, one merely needs to show that C_1 and C_2 are bounded to know that as $\Delta t \to 0$ clearly this error goes to zero.

Now we use Taylor's Theorem to find the errors in using the differences, i. e. to find C_1 and C_2 .

We use a generic function h(x) and approximate to fourth order:

$$h(x+\delta) = h(x) + \delta h'(x) + \frac{\delta^2}{2}h''(x) + \frac{\delta^3}{6}h'''(x) + \frac{\delta^4}{24}h^{(4)}(\zeta_1)$$
$$h(x-\delta) = h(x) - \delta h'(x) + \frac{\delta^2}{2}h''(x) - \frac{\delta^3}{6}h'''(x) + \frac{\delta^4}{24}h^{(4)}(\zeta_2).$$

Here $\zeta_1 \in [x, x + \delta]$, $\zeta_2 \in [x - \delta, x]$. Use a third order approximation, subtracting, plus a little algebra, to obtain:

$$\frac{h(x+\delta)-h(x-\delta)}{2\delta}-\frac{\delta^2}{6}h'''(\xi_1)=h'(x).$$

where $\xi_1 \in [x - \delta, x + \delta]$ and replaced $h'''(\zeta_1) + h'''(\zeta_2) = 2h'''(\xi_1)$. Likewise, using the fourth order approximation, add the equations, and do some algebra to obtain:

$$\frac{h(x+\delta) + h(x-\delta) - 2h(x)}{\delta^2} - \frac{\delta^2}{12}h^{(4)}(\xi_2) = h''(x).$$

Applying this to equation [A.17], one has

$$\ddot{f}(r,t) = \frac{f(r,t+\Delta t) + f(r,t-\Delta t) - 2f(r,t)}{\Delta t^2} - \frac{\Delta t^2}{12} \frac{\partial^4 f}{\partial t^4}(r,\eta_1)$$

$$\frac{2\dot{f}^2(r,t)}{f(r,t) + r^2} = \frac{(f(r,t+\Delta t) - f(r,t-\Delta t))^2}{2\Delta t^2 (f(r,t) + r^2)}$$

$$-2\left(\frac{f(r,t+\Delta t) - f(r,t-\Delta t)}{\Delta t (f(r,t) + r^2)}\right) \left(\frac{\Delta t^2}{6} \frac{\partial^3 f}{\partial t^3}(r,\eta_2)\right)$$

$$+ \frac{2}{f(r,t) + r^2} \left(\frac{\Delta t^2}{6} \frac{\partial^3 f}{\partial t^3}(r,\eta_2)\right)$$

$$\frac{2(f'(r,t))^2}{f(r,t)+r^2} = \frac{(f(r+\Delta r,t)-f(r-\Delta r,t))^2}{2\Delta r^2(f(r,t)+r^2)}
-2\left(\frac{f(r+\Delta r,t)-f(r-\Delta r,t)}{\Delta r(f(r,t)+r^2)}\right)\left(\frac{\Delta r^2}{6}\frac{\partial^3 f}{\partial r^3}(\xi_1,t)\right)
+\frac{2}{f(r,t)+r^2}\left(\frac{\Delta r^2}{6}\frac{\partial^3 f}{\partial r^3}(\xi_1,t)\right)
\frac{8rf'(r,t)}{f(r,t)+r^2} = \frac{4(f(r+\Delta r,t)-f(r-\Delta r,t))}{\Delta r(f(r,t)+r^2)}
+\frac{8r}{f(r,t)+r^2}\left(\frac{\Delta r^2}{6}\frac{\partial^3 f}{\partial r^3}(\xi_1,t)\right).$$

The first of these equations says that if

$$\frac{\partial^4 f}{\partial t^4}(r,\eta_1)$$

is bounded then the error C_1 goes to zero as $\triangle t^2 \to 0$.

If f(r,t) is chosen in C(4,4), the space of functions with four bounded space/time derivatives, all of these differences have bounded errors.

Now attending to the discretization for

$$f''(r,t) + \frac{5f'(r,t)}{r} \approx \left[\left[r + \frac{1}{2} \triangle r \right]^5 \left(\frac{f((r+\triangle r,t) - f(r,t))}{\triangle r} \right) - \left[r - \frac{1}{2} \triangle r \right]^5 \left(\frac{f(r,t) - f(r-\triangle r,t)}{\triangle r} \right) \right] / (r^5 \triangle r),$$
(A.19)

one needs to find an approximation of the error on this. Start with $h(r) = r^5 f'(r)$. Consequently:

$$h'(r) = 5r^4 f'(r) + r^5 f''(r) = r^5 \left(f''(r) + \frac{5f'(r)}{r} \right)$$

$$h''(r) = 20r^3 f'(r) + 10r^4 f''(r) + r^5 f'''(r)$$

$$h'''(r) = 60r^2 f'(r) + 60r^3 f''(r) + 15r^4 f'''(r) + r^5 f^{(4)}(r).$$

By taking a Taylor series for h(r), obtain:

$$h\left(r + \frac{\triangle r}{2}\right) = h(r) + \frac{\triangle r}{2}h'(r) + \frac{\triangle r^{2}}{8}h''(r) + \frac{\triangle r^{3}}{48}h'''(\zeta_{1})$$

$$h\left(r - \frac{\triangle r}{2}\right) = h(r) - \frac{\triangle r}{2}h'(r) + \frac{\triangle r^{2}}{8}h''(r) - \frac{\triangle r^{3}}{48}h'''(\zeta_{2}).$$

Subtracting and doing some algebra as before yields:

$$h'(r) = \frac{h\left(r + \frac{\triangle r}{2}\right) - h\left(r - \frac{\triangle r}{2}\right)}{\triangle r} - \frac{\triangle r^3}{24}h'''(\eta).$$

Now start substituting in definitions for h(r), h'(r), and let

$$\rho_3 \in \left[r - \frac{\triangle r}{2}, r + \frac{\triangle r}{2} \right]$$

etc. to obtain:

$$r^{5}\left(f''(r) + \frac{5f'(r)}{r}\right) = \frac{\left(r + \frac{\triangle r}{2}\right)^{5} f'\left(r + \frac{\triangle r}{2}\right) - \left(r - \frac{\triangle r}{2}\right)^{5} f'\left(r - \frac{\triangle r}{2}\right)}{\triangle r} - \frac{\triangle r^{3}}{24} \left(60r^{2}f'(\rho_{3}) + 60r^{3}f''(\rho_{3}) + 15r^{4}f'''(\rho_{3}) + r^{5}f^{(4)}(\rho_{3})\right). (A.20)$$

A centered difference approximation gives:

$$f'\left(r + \frac{\Delta r}{2}\right) = \frac{f(r + \Delta r) - f(r)}{\Delta r} - \frac{\Delta r^2}{24}f'''(\xi_1),\tag{A.21}$$

and similarly

$$f'\left(r - \frac{\Delta r}{2}\right) = \frac{f(r) - f(r - \Delta r)}{\Delta r} - \frac{\Delta r^2}{24}f'''(\xi_2) \tag{A.22}$$

So substituting [A.21] and [A.22] into [A.20], one has the difference equation and approximation for [A.19]. Letting $\rho_4 \in [r, r + \triangle r]$ and $\rho_5 \in [r - \triangle r, r]$

$$f''(r,t) + \frac{5f'(r,t)}{r} =$$

$$\left[\left[r + \frac{\Delta r}{2} \right]^{5} \left(\frac{f(r + \Delta r, t) - f(r, t)}{\Delta r} \right) - \left[r - \frac{\Delta r}{2} \right]^{5} \left(\frac{f(r, t) - f(r - \Delta r, t)}{\Delta r} \right) \right] / (r^{5} \Delta r) \\
- \left[\frac{\left(r + \frac{\Delta r}{2} \right)^{5}}{r^{5} \Delta r} \right] \left(\frac{\Delta r^{2}}{24} \frac{\partial^{3} f}{\partial r^{3}} (\rho_{4}, t) \right) + \left[\frac{\left(r - \frac{\Delta r}{2} \right)^{5}}{r^{5} \Delta r} \right] \left(\frac{\Delta r^{2}}{24} \frac{\partial^{3} f}{\partial r^{3}} (\rho_{5}, t) \right) \\
- \frac{\Delta r^{3}}{24r^{5}} \left(60r^{2} \frac{\partial f}{\partial r} (\rho_{3}, t) + 60r^{3} \frac{\partial^{2} f}{\partial r^{2}} (\rho_{3}, t) + 15r^{4} \frac{\partial^{3} f}{\partial r^{3}} (\rho_{3}, t) \right) \\
+ r^{5} \frac{\partial^{4} f}{\partial r^{4}} (\rho_{3}, t) \right).$$

.

Once again, one sees that if f(r,t) is chosen in C(4,4), the error in this difference is bounded. Under this condition, putting all of this information together, we expect the error in

$$|f(r, t + n\triangle t) - f_c(r, t + n\triangle t)| \le K\triangle t,$$

where K is bounded and $K \to 0$ only when both $\Delta t \to 0$ and $\Delta r \to 0$, but not when only one of Δt or Δr go to zero.

To confirm this, convergence tables have been run on this program. f(0, 100) and f(10, 100) are used as indicators.

First, the convergence as $\Delta t \to 0$ is investigated. One run is made with $\Delta r = 0.100$ and $\Delta t = 0.00125$, since we cannot do a run with Δr and Δt infinitely small, and the stability analysis tells us that we must keep $\Delta t \leq C \Delta r^{3/2}$. Call this f_{∞} . Then Δt is allowed to take on a variety of larger values and each time we can find the errors $E0 = |f(0, 100) - f_{\infty}(0, 100)|$,

 $E10 = |f(10, 100) - f_{\infty}(10, 100)|, h = \Delta t - 0.00125$. Then with any two of these one can calculate

$$\ln(E0_a/E0_b)/\ln(h_a/h_b)$$
 and $\ln(E10_a/E10_b)/\ln(h_a/h_b)$ (A.23)

In this problem, this quotient of natural logarithms should be close to 1 since in theory the error is $K\triangle t$.

The complete set of initial conditions are $f(0,t)=1.0,\ R_{\max}=100,$ $\dot{f}(0,t)=-0.01.$ The data is in Table A.1.

In Table A.1, skipping the first row and proceeding downward, calculate Table A.2, where the previous line is the line associated with subscript "a" in equation [A.23], and the current line is associated with subscript "b" in equation [A.23]. It is clear that the quotient of the natural logarithms as in [A.23] is close to one and gets closer as the size of $\triangle t$ decreases, as the theory predicts.

Next, the convergence as $\triangle r \to 0$ is investigated. One run is made with $\triangle r = 0.00625$ and $\triangle t = 0.00125$, since we cannot do a run with $\triangle r$ and $\triangle t$ infinitely small, and consider this to be the value of f_{∞} . Then $\triangle r$ is allowed to take on a variety of larger values. Likewise, we calculate the values in [A.23], but this time, our theory has no prediction for the value, as the error is predicted to decrease as $K\triangle t$.

Again, the complete set of initial conditions are f(0,t) = 1.0, $R_{\text{max}} = 100$, $\dot{f}(0,t) = -0.01$. The data is in Table A.3.

In Table A.3, skipping the first row and proceeding downward, calculate Tabel [A.4], where the previous line is the line associated with subscript "a"

in [A.23], and the curent line is associated with subscript "b" in [A.23]. The quotient of natural logarithms is closest to being an integer when the error caused by Δr is much greater than the error caused by Δt . This is as this sort of analysis would predict when the error is a sum of a piece that goes to zero as $\Delta r \to 0$ and another piece that goes to zero as $\Delta t \to 0$.

Table A.1: 4+1 dimensional model: Convergence data 1.

$\triangle r$	$\triangle t$	f(0, 100)	f(10, 100)
0.100	0.00125	0.247164210997	0.245952971169
0.100	0.05000	0.247225131669	0.246014184991
0.100	0.04000	0.247212637097	0.246001630149
0.100	0.02000	0.247187644555	0.245976517632
0.100	0.01000	0.247175146883	0.245963959986
0.100	0.00500	0.247168897823	0.245957680759

Table A.2: 4+1 dimensional model: Convergence data 2.

h	E0	E10	$\ln \text{ quot. } E0$	ln quot. E10
0.04875	0.000060920672	0.000061213822		
0.03875	0.000048426100	0.000048658980	0.999822247666	0.999835333093
0.01875	0.000023433558	0.000023546463	0.999907462503	0.999894968679
0.00875	0.000010935886	0.000010988817	0.999972932084	0.999944166093
0.00375	0.000004686826	0.000004709590	0.999995539233	0.999975691565

Table A.3: 4+1 dimensional model: Convergence data 3.

$\triangle r$	$\triangle t$	f(0, 100)	f(10, 100)
0.00250	0.00125	0.250239554784	0.248987627424
0.10000	0.00125	0.247164210997	0.245952971169
0.05000	0.00125	0.249463484942	0.248227707633
0.02500	0.00125	0.250046460114	0.248801253159
0.01250	0.00125	0.250192709322	0.248943556603
0.00625	0.00125	0.250229305018	0.248978377699

Table A.4: 4+1 dimensional model: Convergence data 4.

h	E0	E10	ln quot. E0	$\ln \text{ quot. } E10$
0.09750	0.003075343787	0.003034656255		
0.04750	0.000776069842	0.000759919791	1.914735161591	1.925458076682
0.02250	0.000193094670	0.000186374265	1.861663705261	1.880927424171
0.01000	0.000046845462	0.000044070821	1.746545407713	1.778154140081
0.00375	0.000010249766	0.000009249725	1.549300513769	1.591718519800

Appendix B

Stability and convergence of the $\mathbb{C}P^1$ model, charge 1 sector

In this chapter we analyze the stability of the equation

$$\ddot{f} = f'' + \frac{3f'}{r} - \frac{4rf'}{f^2 + r^2} + \frac{2f}{f^2 + r^2} \left(\dot{f}^2 - f'^2 \right)$$
 (B.1)

and the associated differencing scheme used in finding numerical solutions. This analysis will proceed analogously to that of the 4+1 dimensional model outlined in appendix A. Once again f = f(r,t), and r is a radial variable, hence r > 0. It will be shown that the stability behavior of the differential equation is qualitatively the same as that of the difference equation, and that the difference equation converges to the differential equation as $\Delta r \to 0$ and $\Delta t \to 0$.

B.1 Continuum stability: simplified model

As in section A.1, the first thing we will address is the stability of the linear part of the partial differential equation [B.1]. This is:

$$\ddot{f} = f'' + \frac{3f'}{r} \tag{B.2}$$

Setting

$$f(r,t) = e^{i\kappa r}e^{i\omega t},$$

and plugging this into [B.2] yields the equation:

$$\omega^2 = \kappa^2 - \frac{3i\kappa}{r}.$$

Solve this for ω and find that

$$\omega = \pm \sqrt{\frac{\kappa^2 r - 3i\kappa}{r}}.$$

Hence ω always has a negative imaginary part, therefore this equation has a growing mode and is not stable, as we saw before with equation [A.1] in section A.1.

Once again, we can abstractly consider the equation

$$\ddot{f} = f'' + \frac{3f'}{r} = \mathcal{L}f$$

where $\mathcal{L}f$ is a linear operator with

$$\mathcal{L} = r^{-3} \partial_r r^3 \partial_r$$

and hence that

$$\mathcal{L} = r^{-3/2} (r^{-3/2} \partial_r r^{3/2}) (r^{3/2} \partial_r r^{-3/2}) r^{3/2} = -B^{-1} A^{\dagger} A B$$

where $B=r^{-3/2}$ and $A=r^{-3/2}\partial_r r^{3/2}$. And, just as before $A^{\dagger}A$ is hermitian so it has real spectrum, and since it is essentially a square, it has positive real spectrum. Consequently $\operatorname{spec}(\mathcal{L})=\operatorname{spec}(-A^{\dagger}A)$ is real and negative. The solutions of the equation

$$\ddot{f} = \mathcal{L}f$$

consists of sines and cosines in the time variable multiplying the eigenfunctions of \mathcal{L} , and hence has no growing mode and is strictly stable.

This is resolved in exactly the same manner as in section A.1. In this case we find that under the normal operating conditions of $\kappa \gg 1/r$ we have a factor of $r^{-3/2}$ that is not accounted for in the Von Neumann stability analysis that had no choice but to appear in the $e^{i\omega t}$ portion of the equation.

When one forcibly puts this factor of $r^{-3/2}$ into the Von Neumann stability analysis via

$$f(r,t) = r^{-3/2}e^{i\kappa r}e^{i\omega t}$$

and plugs into [B.2], one calculates:

$$\omega^2 = \kappa^2 + \frac{3}{4r^2}.$$

Hence

$$\omega = \pm \frac{\sqrt{3 + 4r^2\kappa^2}}{2r},$$

and ω has no negative imaginary part.

B.2 Continuum stability

The first thing to address is the stability of partial differential equation [B.1].

We set

$$f(r,t) = f_0(r,t) + \varepsilon r^{-3/2} e^{i\kappa r} e^{i\omega t},$$

and plug into [B.1] then linearize in ε to obtain:

$$\omega^{2} = \kappa^{2} + \frac{3}{4r^{2}} + \frac{4i\kappa r - 6}{r^{2} + f_{0}^{2}} - \frac{8f_{0}'f_{0}r}{(r^{2} + f_{0}^{2})^{2}} - \frac{4if_{0}\dot{f}_{0}\omega}{r^{2} + f_{0}^{2}}$$
$$-\frac{6f_{0}f_{0}'}{r(r^{2} + f_{0}^{2})} + \frac{4i\kappa f_{0}f_{0}'}{r^{2} + f_{0}^{2}} - \frac{\left(2 - \frac{4f_{0}^{2}}{r^{2} + f_{0}^{2}}\right)\left(\dot{f}_{0}^{2} - f_{0}'^{2}\right)}{r^{2} + f_{0}^{2}}$$

Solving this for ω yields:

$$\omega = -\frac{2if_0\dot{f}_0}{(r^2 + f_0^2)} \pm \kappa \left[1 + \frac{4if_0^2}{\kappa(r^2 + f_0^2)^2} + \frac{4if_0f_0'}{\kappa(r^2 + f_0^2)} + \frac{3f_0^4}{4\kappa^2r^2(r^2 + f_0^2)^2} - \frac{6f_0^3f_0'}{\kappa^2r(f_0 + r^2)^2} - \frac{2\dot{f}_0^2}{\kappa^2(r^2 + f_0^2)} + \frac{2f_0'^2(r^2 - f_0^2)}{\kappa^2(r^2 + f_0^2)^2} - \frac{14f_0f_0'r}{\kappa^2(r^2 + f_0^2)^2} - \frac{21r^2 + 18f_0^2}{4\kappa^2(r^2 + f_0^2)^2} \right]^{1/2}$$
(B.3)

The imaginary parts are bounded. If we restrict our concern to the realm where κ is large and $\kappa \gg \frac{1}{r}$, we actually have that all of the rest of the terms in the square root are bounded and small.

B.3 Discretization scheme

As in section A.3, it was found that the main stability problems were generated by the linear part of the equation, namely:

$$\ddot{f} = f'' + \frac{3f'}{r}$$

as $r \to 0$. As before we use the natural differential operator

$$\mathfrak{D}f = r^{-3}\partial_r(r^3f) = f'' + \frac{3f'}{r},$$

and we discretize it in the natural way. Letting $q\triangle r=r$ and $n\triangle t=t$, this discretization is

$$(q\triangle r)^{-3} \left[\left[\left(q + \frac{1}{2} \right) \triangle r \right]^3 \frac{f((q+1)\triangle r, n\triangle t) - f(q\triangle r, n\triangle t)}{\triangle r} - \left[\left(q - \frac{1}{2} \right) \triangle r \right]^3 \frac{f(q\triangle r, n\triangle t) - f((q-1)\triangle r, n\triangle t)}{\triangle r} \right] / \triangle r.$$

B.4 Outline of stability analysis

The stability analysis for this equation will be approached in exactly the same way as in section A.4 for the previous model.

B.5 Stability near zero

Once again we follow our previous methodologies. A review of section A.5 might be in order. One has

$$\ddot{\delta f} = \mathcal{L}_1(\delta f) + \mathcal{L}_2(\dot{\delta f}),$$

with \mathcal{L}_1 and \mathcal{L}_2 linear operators. As before \mathcal{L}_1 and \mathcal{L}_2 are linear operators with \mathcal{L}_2 close to a multiple of the identity matrix. The analysis of the eigenvalues proceeds as before, and once again all hinges on showing that if α is an eigenvalue of \mathcal{L}_1 then $\alpha < 0$.

Allow $\delta f(q,n)$ to represent $\delta f(q\triangle r, n\triangle t)$ and likewise with $f_0(q,n) \equiv f_0(q\triangle r, n\triangle t)$, and compute the following linearized equation, discretized in space only:

$$\dot{\delta f}(q,n) = (q \triangle r)^{-3} \left[\left(q + \frac{1}{2} \right)^{3} \triangle r^{3} \left(\frac{\delta f(q+1,t) - \delta f(q,t)}{\triangle r} \right) \right] \\
- \left(q - \frac{1}{2} \right)^{3} \triangle r^{3} \left(\frac{\delta f(q,t) - \delta f(q-1,t)}{\triangle r} \right) \right] / \triangle r \qquad (B.4) \\
+ \frac{4f_{0}(q,t)\dot{f}_{0}(q,t)\dot{\delta f}(q,t)}{q^{2}\triangle r^{2} + f_{0}^{2}(q,t)} + \frac{2f_{0}(q,t)\left(\delta f(q+1,t) - \delta f(q-1,t)\right)}{q\triangle r^{2}\left(q^{2}\triangle r^{2} + f_{0}^{2}(q,t)\right)} \\
+ \frac{2\dot{f}_{0}^{2}(q,t)\delta f(q,t)}{q^{2}\triangle r^{2} + f_{0}^{2}(q,t)} - \frac{4f_{0}^{2}(q,t)\dot{f}_{0}^{2}(q,t)\delta f(q,t)}{\left(q^{2}\triangle r^{2} + f_{0}^{2}(q,t)\right)^{2}}$$

One sees immediately from this that

$$\mathcal{L}_2 = \left(\frac{4f_0\dot{f}_0}{r^2 + f_0^2}\right)I$$

$$\approx cI$$

is a good approximation.

 \mathcal{L}_1 is determined by [B.4] and the quadratic fit boundary condition at the origin, i.e.

$$\delta f(0,t) = \frac{4}{3}\delta f(\Delta r, t) - \frac{1}{3}\delta f(2\Delta r, t).$$

Let $\mathcal{L}_1 = [a_{i,j}]$, and $f_0 = f_0(r,t) = f_0(k\triangle r,t)$ and obtain the following tridiagonal matrix:

$$a_{1,1} = \frac{4}{3} \left(\frac{(1/2)^3}{\triangle r^2} + \frac{2\triangle r}{\triangle r^2 + f_0^2} \right) - \frac{(3/2)^3}{\triangle r^2} - \frac{(1/2)^3}{\triangle r^2} + \frac{2\dot{f}_0^2}{\triangle r^2 + f_0^2} - \frac{4f_0^2\dot{f}_0^2}{\triangle r^2 + f_0^2}$$

$$a_{1,2} = -\frac{1}{3} \left(\frac{(1/2)^3}{\triangle r^2} + \frac{2\triangle r}{\triangle r^2 + f_0^2} \right) + \frac{(3/2)^3}{\triangle r^2} - \frac{2\triangle r}{\triangle r^2 + f_0^2}$$

$$a_{k,k-1} = \frac{(k-1/2)^3}{k^3 \triangle r^2} + \frac{2k^2 \triangle r}{k^2 \triangle r^2 + f_0^2}$$

$$a_{k,k} = -\frac{(k+1/2)^3}{k^3 \triangle r^2} - \frac{(k-1/2)^3}{k^3 \triangle r^2} + \frac{2\dot{f}_0^2}{k^2 \triangle r^2 + f_0^2} - \frac{4f_0^2 \dot{f}_0^2}{(k^2 \triangle r^2 + f_0^2)^2}$$

$$a_{k,k+1} = \frac{(k+1/2)^3}{k^3 \triangle r^2} - \frac{2k^2 \triangle r}{k^2 \triangle r^2 + f_0^2}.$$

One can now use Maple or another program to compute the eigenvalues and eigenvectors of this matrix while changing the size of the matrix n and the values of f_0 \dot{f}_0 and $\triangle r$.

Since \dot{f}_0 is always much less than f_0 , the contributions from the terms with \dot{f}_0 are negligible. One expects that rescaling Δr by a factor p should result in the eigenvalues changing by approximately $1/p^2$, since the largest terms are multiplied by Δr^2 .

Let's see this explicitly. When $n=5, f_0=1, \dot{f}_0=-0.01, \triangle r=0.01$ the matrix is:

$$\begin{bmatrix} -33333.3 & 33333.3 & 0 & 0 & 0 \\ 4218.8 & -23750.0 & 19531.2 & 0 & 0 \\ 0 & 5787.2 & -21666.7 & 15879.4 & 0 \\ 0 & 0 & 6699.5 & -20937.5 & 14238.0 \\ 0 & 0 & 0 & 7290.5 & -20600.0 \end{bmatrix}.$$

This matrix has eigenvalues with multiplicity m and eigenvectors given by

Now rescale $\dot{f}_0 = -0.1$, which is multiplying by a factor of 10. We expect this to have little or no effect.

$$\begin{bmatrix} -33333.3 & 33333.3 & 0 & 0 & 0 \\ 4218.8 & -23750.0 & 19531.2 & 0 & 0 \\ 0 & 5787.2 & -21666.7 & 15879.4 & 0 \\ 0 & 0 & 6699.5 & -20937.5 & 14238.0 \\ 0 & 0 & 0 & 7290.5 & -20600.0 \end{bmatrix}$$

This matrix has eigenvalues with multiplicity m and eigenvectors given by

Now rescale $\triangle r = 0.1$ so that $\triangle r$ is 10 times the original with $f_0 = 1, \dot{f}_0 = -0.01$. This we expect to scale the eigenvalues by a factor of 100. The matrix is:

$$\begin{bmatrix} -333.1 & 333.1 & 0 & 0 & 0 \\ 43.0 & -237.5 & 194.5 & 0 & 0 \\ 0 & 59.5 & -216.7 & 157.1 & 0 \\ 0 & 0 & 69.8 & -209.4 & 139.6 \\ 0 & 0 & 0 & 76.9 & -206.0 \end{bmatrix}.$$

The eigenvalues with multiplicity m and eigenvectors are:

Eigenvalue
$$m$$
 Eigenvector -440.7 1 [$0.945, -0.305, 0.110, -.041, .0136$] -353.0 1 [$-3.145, 0.188, 0.583, -0.576, 0.302$] -243.4 1 [$1.745, 0.470, -0.399, -0.110, 0.226$] -127.6 1 [$2.333, 1.439, 0.298, -0.376, -0.369$] -38.0 1 [$-0.714, -0.633, -0.491, -0.319, -0.146$]

These are indeed scaled by a factor of 100 from the original.

Now rescale so $f_0 = 10$ is 10 times as large with $\triangle r = 0.01, \dot{f}_0 = -0.01$.

The matrix is:

$$\begin{bmatrix} -33333.3 & 33333.3 & 0 & 0 & 0 \\ 4218.8 & -23750.0 & 19531.2 & 0 & 0 \\ 0 & 5787.0 & -21666.7 & 15879.6 & 0 \\ 0 & 0 & 6699.2 & -20937.5 & 14238.3 \\ 0 & 0 & 0 & 7290.0 & -20600.0 \end{bmatrix}$$

The eigenvalues with multiplicity m and eigenvectors are:

Eigenvalue
$$m$$
 Eigenvector -43905.2 1 $[-0.9471, 0.3004, -0.1054, 0.0381, -0.0119]$ -35118.5 1 $[3.3030, -0.1769, -0.6105, 0.5816, -0.2920]$ -24319.3 1 $[-1.7836, -0.4823, 0.3993, 0.1091, -0.2138]$ -12891.5 1 $[2.5037, 1.5354, 0.3128, -0.3867, -0.3657]$ -4053.0 1 $[0.7281, 0.6396, 0.4877, 0.3079, 0.1357]$

These are virtually the same as in the original with $f_0 = 1.0$.

The final rescaling is to reset the matrix size n=10 with $\triangle r=.01$, $f_0=1, \dot{f}_0=-0.01$. The matrix is:

_	_									_
	-33333.	33333.	0	0	0	0	0	0	0	0
	4218.8	-23750.	19531.	0	0	0	0	0	0	0
	0	5787.2	-21667.	15879.	0	0	0	0	0	0
	0	0	6699.5	-20938.	14238.	0	0	0	0	0
	0	0	0	7290.5	-20600.	13310.	0	0	0	0
١	0	0	0	0	7703.3	-20417.	12713.	0	0	0
	0	0	0	0	0	8007.5	-20306.	12299.	0	0
	0	0	0	0	0	0	8241.0	-20234.	11993.	0
l	0	0	0	0	0	0	0	8425.8	-20185.	. 11759.
	0	0	0	0	0	0	0	0	8576.	-20150.

The eigenvalues with multiplicity m and eigenvectors are:

Eigenvalue	m	Eigenvector				
-43977.1	1	[0.9460,	-0.3021,	0.1085,	-0.0423,	
		0.0175,	-0.0075,	0.0033,	-0.0015,	
		0.0006,	-0.0002			
-39218.2	1	[-2.5044,	0.4421,	0.1908,	-0.3720,	
		0.3879,	-0.3388,	0.2660,	-0.1885,	
		0.1156,	-0.0520]			
-35858.2	1	[-3.5682,	0.2703,	0.6032,	-0.6376,	
		0.3843,	-0.0914,	-0.1219,	0.2136,	
		-0.1945,	0.1062]			
-31051.4	1	[6.2021,	0.4246,	-1.4984,	0.7308,	
		0.1859,	-0.5463,	0.3443,	0.0549,	
		-0.2861,	0.2250]			
-25358.7	1	[-2.3840,	-0.5703,	0.5619,	0.0772,	
		-0.2884,	0.0608,	0.1511,	-0.1017,	
		-0.0604,	0.0994]			
-19307.4	1	[-3.8375,	-1.6147,	0.4616,	0.6571,	
		-0.1420,	-0.3737,	0.0534,	0.2477,	
		-0.01757,	-0.1788]			
-13418.0	1	[-4.6228,	-2.7619,	-0.4625,	0.7663,	
		0.6223,	-0.0839,	-0.4233,	-0.1824,	
		0.1872,	0.2384]			
-8177.3	1	[-2.2447,	-1.6940,	-0.8658,	-0.1181,	
		0.3015,	0.3462,	0.1505,	-0.0769,	
		-0.1808,	-0.1295]			
-4002.9	1	[-1.2609,	-1.1095,	-0.8494,	-0.5405,	
		-0.2432,	-0.0072,	0.1381,	0.1877,	
		0.1592,	0.0845]			
-1210.9	1	[0.5060,	0.4876,	0.4534,	0.4063,	
		0.3497,	0.2868,	0.2214,	0.1570,	
		0.0969,	0.0439].			

Once again, all eigenvalues are negative. The modes localized near zero don't change. The eigenvalues increase towards zero as n increases because there are growing modes of this equation away from r = 0.

One can conclude that the eigenvalues of this matrix under reasonable

initial conditions will always be negative, as required. This differencing scheme does not have any instabilities generated at the origin.

B.6 Stability away from zero: simplified model

The analysis in this section shall follow that of section A.6.

In this section the stability of the difference equation derived from [B.1] with the differencing scheme outlined in section 3.1 under the special condition that $f(r,t) = f_0(r,t) + \epsilon e^{i\kappa q \triangle r} e^{i\omega n \triangle t}$ where $f_0(r,t) \equiv c$, a constant, will be addressed.

Explicit inclusion to the factor $r^{-3/2}$ is omitted, because it does not impact this analysis to omit it.

Plug the previous expression for f(r,t) into [B.1] and linearize in ε to obtain the following:

$$\frac{e^{i\omega\Delta t} + e^{-i\omega\Delta t} - 2}{\Delta t^2} = + \frac{\left(q + \frac{1}{2}\right)^3 \left(e^{i\kappa\Delta r} - 1\right) - \left(q - \frac{1}{2}\right)^3 \left(1 - e^{-i\kappa\Delta r}\right)}{q^3 \Delta r^2} - \frac{2q^2 \Delta r \left(e^{i\kappa\Delta r} - e^{-i\kappa\Delta r}\right)}{q^2 \Delta r^2 + f_0^2}.$$
(B.5)

As before let $x = e^{i\omega \triangle t}$ and

$$J = \frac{\left(q + \frac{1}{2}\right)^3 \left(e^{i\kappa\triangle r} - 1\right) - \left(q - \frac{1}{2}\right)^3 \left(1 - e^{-i\kappa\triangle r}\right)}{q^3\triangle r^2} - \frac{2q^2\triangle r \left(e^{i\kappa\triangle r} - e^{-i\kappa\triangle r}\right)}{q^2\triangle r^2 + f_0^2}.$$

Reduce equation [B.5] to

$$x^2 - (2 + J\Delta t^2)x + 1 = 0.$$

This is exactly as in section A.6. As before there are two logarithmic solutions for ω given by

$$\omega = \frac{-i \ln \left(1 + \frac{J \triangle t^2}{2} \pm \sqrt{J} \triangle t \sqrt{1 + \frac{J \triangle t^2}{4}} \right)}{\triangle t}.$$

As in section A.6, the biggest concern is determining exactly how big $J\triangle t^2$ is. Let $\kappa\triangle r=\theta$, then reduce exponentials to sines and cosines appropriately, and expand the factors of $q\pm 1/2$, and simplify using such information as $q=r/\triangle r$, to obtain

$$J = \kappa^2 \left(\frac{2\cos\theta - 2}{\theta^2} \right) + \frac{3i\kappa}{r} \left(\frac{\sin\theta}{\theta} \right) + \frac{3\kappa^2 \triangle r^2}{4r^2} \left(\frac{2\cos\theta - 2}{\theta^2} \right) - \frac{i\kappa\triangle r^2}{4r^3} \left(\frac{\sin\theta}{\theta} \right) - \frac{4ir^2\kappa}{r^2 + f_0^2} \left(\frac{\sin\theta}{\theta} \right).$$

As $\triangle r \rightarrow 0$ one of these terms go to zero but the following do not:

$$\kappa^2 \left(\frac{2\cos\theta - 2}{\theta^2} \right) + \frac{3i\kappa}{r} \left(\frac{\sin\theta}{\theta} \right) + \frac{3\kappa^2 \triangle r^2}{4r^2} \left(\frac{2\cos\theta - 2}{\theta^2} \right) - \frac{4ir^2\kappa}{r^2 + f_0^2} \left(\frac{\sin\theta}{\theta} \right).$$

As before, the trigonometric parts of these terms is strictly bounded, and we are working in the case where r is bounded away from zero. Our only concern is with the size of κ , but we know that $\kappa \triangle r < \pi$ and $\triangle t \ll \triangle r$, hence we can make $\triangle t < c\triangle r$ and with c chosen sufficiently small, we can make $\kappa \triangle t$ as small as we like. In particular we may use the Taylor approximation to the square root and then apply the Taylor approximation to the logarithm. Just as in section A.6, with some cancellations, one obtains:

$$\omega \approx \frac{-i \ln \left[\frac{J \triangle t^2}{2} \pm \sqrt{J} \triangle t \left(1 + \frac{J \triangle t^2}{8} + O(J^2 \triangle t^4) \right) \right]}{\triangle t}$$

$$\approx \frac{-i\left[\pm\sqrt{J}\triangle t + O\left((\sqrt{J}\triangle t)^3\right)\right]}{\triangle t}$$
$$\approx \left[\pm i\sqrt{J} + O\left(\sqrt{J}^3\triangle t^2\right)\right]$$

Recall, as $\triangle r \to 0$ all of the terms in J go to 0 except for

$$\kappa^2 \left(\frac{2\cos\theta - 2}{\theta^2} \right) + \frac{3i\kappa}{r} \left(\frac{\sin\theta}{\theta} \right) + \frac{3\kappa^2 \triangle r^2}{4r^2} \left(\frac{2\cos\theta - 2}{\theta^2} \right) - \frac{4ir^2\kappa}{r^2 + f_0^2} \left(\frac{\sin\theta}{\theta} \right).$$

So one has

$$\sqrt{J} \approx \sqrt{\left[\kappa^2 \left(\frac{2\cos\theta - 2}{\theta^2}\right) + \frac{3i\kappa}{r} \left(\frac{\sin\theta}{\theta}\right) + \frac{3\kappa^2 \triangle r^2}{4r^2} \left(\frac{2\cos\theta - 2}{\theta^2}\right)\right]}$$
$$-\frac{4ir^2\kappa}{r^2 + f_0^2} \left(\frac{\sin\theta}{\theta}\right) + O(\triangle r)\right]}$$

Since κ is large while Δr is small, approximating this square root yields:

$$\sqrt{J} \approx i\kappa \sqrt{\frac{2 - 2\cos\theta}{\theta^2}} \left[1 + \frac{3i}{2\kappa r} \left(\frac{\sin\theta}{\theta} \right) \left(\frac{\theta^2}{2 - 2\cos\theta} \right) + \frac{3\triangle r^2}{8r^2} \right. \\
\left. - \frac{i\triangle r^2}{8\kappa r^2} \left(\frac{\sin\theta}{\theta} \right) \left(\frac{\theta^2}{2 - 2\cos\theta} \right) - \frac{2ir^2}{\kappa (r^2 + f_0^2)} \left(\frac{\sin\theta}{\theta} \right) \left(\frac{\theta^2}{2 - 2\cos\theta} \right) \\
+ O\left(\frac{1}{\kappa^2} \right) \right].$$

As before, the leading order term of \sqrt{J} is $O(\kappa)$. We can make the correction $O(\sqrt{J}^3 \triangle t^2)$ as small as we like by requiring that $\triangle t < c \triangle r^{3/2}$ and choosing the factor c appropriately. Given these choices, one has:

$$\omega \approx \pm \sqrt{\frac{2 - 2\cos\theta}{\theta^2}} \left[\kappa + \frac{3i}{2r} \left(\frac{\sin\theta}{\theta} \right) \left(\frac{\theta^2}{2 - 2\cos\theta} \right) + \frac{3\kappa\Delta r^2}{8r^2} - \frac{i\Delta r^2}{8r^2} \left(\frac{\sin\theta}{\theta} \right) \left(\frac{\theta^2}{2 - 2\cos\theta} \right) - \frac{2ir^2}{(r^2 + f_0^2)} \left(\frac{\sin\theta}{\theta} \right) \left(\frac{\theta^2}{2 - 2\cos\theta} \right) + O\left(\frac{1}{\kappa} \right) + O\left(\sqrt{J}^3 \Delta t^2 \right) \right].$$

It is also clear as in section A.6 that if one permitted $r \to 0$ the dominant piece would be:

$$\omega \approx \pm \kappa \sqrt{\frac{2 - 2\cos\theta}{\theta^2}} \mp \frac{3i}{2r} \left(\frac{\sin\theta}{\theta}\right) \left(\frac{\theta^2}{2 - 2\cos\theta}\right)$$

and as $\theta \to 0$ this goes to

$$\omega \approx \pm \kappa \mp \frac{3i}{2r}$$

or exactly what we obtained in section B.1 that was so often "corrected" by the addition of the factor $r^{-3/2}$.

B.7 The complications

We must now deal with the reality that the assumption $f_0 \equiv c$ is not in general true. We shall, as in section A.7, analyze the difference between the solution for ω when $f_0 \equiv c$, called ω_0 , and the solution for ω when $f_0 \not\equiv c$, called ω_1 .

To find ω_0 we solved [B.5] an equation which can be characterized as

$$g(\omega) = \text{old}(\kappa).$$

It was:

$$\frac{e^{i\omega\Delta t} + e^{-i\omega\Delta t} - 2}{\Delta t^2} = + \frac{\left(q + \frac{1}{2}\right)^3 \left(e^{i\kappa\Delta r} - 1\right) - \left(q - \frac{1}{2}\right)^3 \left(1 - e^{-i\kappa\Delta r}\right)}{q^3 \Delta r^2} - \frac{2q^2 \Delta r \left(e^{i\kappa\Delta r} - e^{-i\kappa\Delta r}\right)}{q^2 \Delta r^2 + f_0^2}.$$

If we do not assume that $f_0 \equiv c$ then the same linearization in ε of [B.1] with $f(q\triangle r, n\triangle t) = f_0(q\triangle r, n\triangle t) + \varepsilon e^{i\kappa q\triangle r} e^{i\omega n\triangle t}$ yields the following equation:

$$\frac{e^{i\omega\Delta t} + e^{-i\omega\Delta t} - 2}{\Delta t^2} = + \frac{\left(q + \frac{1}{2}\right)^3 \left(e^{i\kappa\Delta r} - 1\right) - \left(q - \frac{1}{2}\right)^3 \left(1 - e^{-i\kappa\Delta r}\right)}{q^3 \Delta r^2}$$

$$-\frac{2q^{2}\triangle r(e^{i\kappa\triangle r}-e^{-i\kappa\triangle r})}{q^{2}\triangle r^{2}+f_{0}^{2}} - \frac{8q^{2}\triangle r^{2}f_{0}'f_{0}}{(r^{2}+f_{0}^{2})^{2}} + \frac{\dot{f}_{0}f_{0}(e^{i\omega\triangle t}-e^{-i\omega\triangle t})}{2\triangle t(r^{2}+f_{0}^{2})} - \frac{f_{0}'f_{0}(e^{i\kappa\triangle r}-e^{-i\kappa\triangle r})}{2\triangle r(r^{2}+f_{0}^{2})} + \frac{2(\dot{f}_{0}^{2}-f_{0}'^{2})}{r^{2}+f_{0}^{2}} - \frac{4f_{0}^{2}(\dot{f}_{0}^{2}-f_{0}'^{2})}{(r^{2}+f_{0}^{2})^{2}}.$$
(B.6)

Characterize this equation as

$$g(w) = \text{old}(\kappa) + \text{new}_1(\kappa) + \text{new}_2(\omega)$$

with

$$\operatorname{new}_{1}(\kappa) = -\frac{f'_{0}f_{0}(e^{i\kappa\Delta r} - e^{-i\kappa\Delta r})}{2\Delta r(r^{2} + f_{0}^{2})} - \frac{8q^{2}\Delta r^{2}f'_{0}f_{0}}{(r^{2} + f_{0}^{2})^{2}} + \frac{2(\dot{f}_{0}^{2} - f'_{0}^{2})}{r^{2} + f_{0}^{2}} - \frac{4f_{0}^{2}(\dot{f}_{0}^{2} - f'_{0}^{2})}{(r^{2} + f_{0}^{2})^{2}}$$
(B.7)

and

$$new_2(\omega) = +\frac{\dot{f}_0 f_0 (e^{i\omega\Delta t} - e^{-i\omega\Delta t})}{2\Delta t (r^2 + f_0^2)}$$
(B.8)

Here \dot{f}_0 is substituted for the finite difference

$$\frac{f_0(q\triangle r, (n+1)\triangle t) - f_0(q\triangle r, (n-1)\triangle t)}{2\triangle t},$$

and likewise with f'_0 .

From here we proceed as in section A.7. We have

$$g(\omega) = \frac{2\cos\omega\Delta t - 2}{\Delta t^2},$$

$$\omega_0 = q^{-1}(\text{old}(\kappa)),$$
(B.9)

and

$$\omega_1 = q^{-1}(\text{old}(\kappa) + \text{new}_1(\kappa) + \text{new}_2(\omega_1)).$$

Let

$$\omega_s = g^{-1}(\text{old}(\kappa) + s(\text{new}_1(\kappa) + \text{new}_2(\omega_s)))$$

then

$$|\omega_{1} - \omega_{0}| = \left| \int_{0}^{1} \frac{\partial \omega_{s}}{\partial s} ds \right|$$

$$\leq \int_{0}^{1} \left| \left[(g^{-1})' \right] (\text{new}_{1}(\kappa) + \text{new}_{2}(\omega_{s})) \right| ds$$

$$\leq \max \left(\left| (g^{-1})' \right| \right) \max \left(\left| \text{new}_{1}(\kappa) + \text{new}_{2}(\omega_{s}) \right| \right) \quad (B.10)$$

So finding a bound on ω in terms of κ will allow one to find a bound for $|\omega_1 - \omega_0|$ in terms of κ .

We start by showing that

$$T(\omega) = g^{-1}(\text{old}(\kappa) + \text{new}_1(\kappa) + \text{new}_2(\omega))$$

is a contraction mapping on the ball $|\omega - \kappa| < |\kappa|/2 = B(\kappa, |\kappa|/2)$. Then we will know that there exists a solution for $\omega \in B(\kappa, |\kappa|/2)$ and hence $|\omega| \le 3|\kappa|/2$.

As before using [B.9]

$$g'(\omega) = \frac{-2\sin(\omega \triangle t)}{\triangle t}.$$

We've already stated one needs to choose $\triangle t < c \triangle r^{3/2}$ in section B.6, so specifically, one can make $\triangle t < \triangle r/150$. Then since $|\kappa \triangle r| < \pi$ and $|\omega| < 3|\kappa|/2$ this implies that $|\omega \triangle t| < \pi/100$ and one has

$$|g'(\omega)| = |2\omega| \left| \frac{\sin(\omega \Delta t)}{\omega \Delta t} \right| > 1.98|\omega|.$$

If ω_1 and ω_2 are in $B(\kappa, \kappa/2)$, assign y_1 and y_2 as follows and find that

$$y_1 = \operatorname{old}(\kappa) + \operatorname{new}_1(\kappa) + \operatorname{new}_2(\omega_1)$$

$$y_2 = \operatorname{old}(\kappa) + \operatorname{new}_1(\kappa) + \operatorname{new}_2(\omega_2)$$

$$y_2 - y_1 = \operatorname{new}_2(\omega_2) - \operatorname{new}_2(\omega_1).$$

Letting,

$$y(s) = y_1 + s(y_2 - y_1),$$

calculate

$$|T(\omega_{2}) - T(\omega_{1})| =$$

$$|g^{-1}(y_{2}) - g^{-1}(y_{1})| = \left| \int_{0}^{1} (g^{-1})'(y(s))(y_{2} - y_{1})ds \right|$$

$$\leq \int_{0}^{1} \max \left| (g^{-1})'(y(s)) \right| \left| (y_{2} - y_{1}) \right| ds$$

$$\leq \max \left| (g^{-1})'(y(s)) \right| \left| (y_{2} - y_{1}) \right|. \tag{B.11}$$

Simple calculus yields:

$$(g^{-1})'(g(\omega)) = \frac{1}{g'(\omega)}.$$

By choice of y_1 and y_2 and $\omega_1, \omega_2 \in B(\kappa, \kappa/2)$,

$$\max |(g^{-1})'(y(s))| = \frac{1}{1.98|\omega|} \le \frac{2}{1.98|\kappa|}.$$
 (B.12)

Analyzing since $|\omega_1|, |\omega_2| \leq 3|\kappa|/2$ and $|\omega_1 \triangle t|, |\omega_2 \triangle t| < \pi/100$,

$$|\text{new}_2(\omega_2) - \text{new}_2(\omega_1)| = \left| \frac{f_0 \dot{f}_0}{r^2 + f_0^2} \left(\frac{i \sin(\omega_2 \triangle t)}{\triangle t} - \frac{i \sin(\omega_1 \triangle t)}{\triangle t} \right) \right|$$

$$= \left| \frac{f_0 \dot{f}_0}{r^2 + f_0^2} \right| \left| \left(\frac{\sin(\omega_2 \triangle t)}{\triangle t} - \frac{\sin(\omega_1 \triangle t)}{\triangle t} \right) \right|$$

$$= \left| \frac{f_0 \dot{f}_0}{r^2 + f_0^2} \right| \left| \int_{\omega_1}^{\omega_2} \cos(s \triangle t) ds \right|$$

$$\leq \left| \frac{f_0 \dot{f}_0}{r^2 + f_0^2} \right| \left| \omega_2 - \omega_1 \right|. \tag{B.13}$$

Now plugging [B.12] and [B.13] into [B.11], obtain:

$$|T(\omega_2) - T(\omega_1)| = |g^{-1}(y_2) - g^{-1}(y_1)| \le \frac{2}{1.98|\kappa|} \left| \frac{f_0 \dot{f_0}}{r^2 + f_0^2} \right| |\omega_2 - \omega_1|.$$

The quantity

$$\left| \frac{f_0 \dot{f_0}}{f_0 + r^2} \right|$$

defines the time scale for the problem. In order for this entire analysis to make sense one expects

$$\kappa \gg \text{time scale}$$
 and $\kappa \gg \text{length scale}$.

Therefore, this is sufficient to show that T(w) is a contraction map from $B(\kappa, \kappa/2)$ to itself. So by the Contraction Mapping Principle, one concludes that there exists a fixed point of T in $B(\kappa, \kappa/2)$. Clearly this argument holds just as well for -T and $B(-\kappa, \kappa/2)$, so there is a fixed point for -T in $B(-\kappa, \kappa/2)$. Since the left hand side of [A.7] is quadratic in $e^{i\omega \Delta t}$, there are two solutions for ω and these are they. Lastly, we finish estimating in equation [B.10]. We already have a perfectly good estimate for $(g^{-1})'$ from [B.12]. We merely need to estimate

$$|\text{new}_1(\kappa) + \text{new}_2(\omega)|$$
.

Replacing the exponentials with their trigonometric forms in [B.7] and [B.8] to get:

$$\operatorname{new}_{1}(\kappa) = -\frac{if'_{0}f_{0}}{r^{2} + f_{0}^{2}} \left(\frac{\sin(\kappa \triangle r)}{\triangle r} \right) - \frac{8q^{2} \triangle r^{2} f'_{0} f_{0}}{(r^{2} + f_{0}^{2})^{2}} + \frac{2(\dot{f}_{0}^{2} - f'_{0}^{2})}{r^{2} + f_{0}^{2}} - \frac{4f_{0}^{2}(\dot{f}_{0}^{2} - f'_{0}^{2})}{(r^{2} + f_{0}^{2})^{2}}$$

and

$$\text{new}_2(\omega) = +\frac{\dot{f}_0 f_0}{r^2 + f_0^2} \left(\frac{i \sin(\omega \triangle t)}{\triangle t} \right)$$

Recall also that $\kappa \gg 1/r$ so $\kappa r \gg 1$. Now if θ is real,

$$|\sin \theta| \le \theta$$
,

and if θ is complex with $|\theta|$ sufficiently small, as it would be if $\theta = \omega \triangle t$, then

$$|\sin \theta| \le 1.01 |\theta|,$$

one has

$$|\operatorname{new}_{1}(\kappa) + \operatorname{new}_{2}(\omega)| \leq \left| \frac{f'_{0}f_{0}}{r^{2} + f_{0}^{2}} \right| |\kappa| + \left| \frac{8r^{2}f'_{0}f_{0}}{(r^{2} + f_{0}^{2})^{2}} \right| + \left| \frac{2(\dot{f}_{0}^{2} - f'_{0}^{2})}{r^{2} + f_{0}^{2}} \right| + \left| \frac{4f_{0}^{2}(\dot{f}_{0}^{2} - f'_{0}^{2})}{(r^{2} + f_{0}^{2})^{2}} \right| + \left| \frac{\dot{f}_{0}f_{0}}{r^{2} + f_{0}^{2}} \right| |1.01\omega|$$

By my previous arguments about κ and the length and time scales, the three central terms are much much smaller than the others. Plugging $|\omega| \leq 3|\kappa|/2$ and this and [B.12] into [B.10] one concludes that under these assumptions

$$|w_{1} - w_{0}| \leq \frac{2}{1.98|\kappa|} \left(\left| \frac{f'_{0}f_{0}}{r^{2} + f'_{0}^{2}} \right| |\kappa| + \left| \frac{8r^{2}f'_{0}f_{0}}{(r^{2} + f'_{0}^{2})^{2}} \right| + \left| \frac{2(\dot{f}_{0}^{2} - f'^{2}_{0})}{r^{2} + f'_{0}^{2}} \right| + \left| \frac{4f'_{0}^{2}(\dot{f}_{0}^{2} - f'^{2}_{0})}{(r^{2} + f'^{2}_{0})^{2}} \right| + \left| \frac{\dot{f}_{0}f_{0}}{r^{2} + f'^{2}_{0}} \right| \frac{3.03|\kappa|}{2} \right)$$

Hence, $|\omega_1 - \omega_0|$ is bounded, which implies in turn that the imaginary part of ω_1 is bounded since the imaginary part of ω_0 was. Once again the growing modes are bounded.

Further, if we compare with equation [B.3], we see analogues between the terms in these two equations.

$$\frac{2}{1.98} \left| \frac{f_0' f_0}{f_0^2 + r^2} \right| \leftrightarrow \frac{4i f_0 f_0'}{r^2 + f_0^2} + \frac{4i f_0^2}{(r^2 + f_0^2)^2}$$

and

$$\frac{3.03}{1.98} \left| \frac{\dot{f}_0 f_0}{r^2 + f_0^2} \right| \longleftrightarrow \frac{-2i f_0 \dot{f}_0}{r^2 + f_0^2}.$$

B.8 Convergence estimates

This section contains an analysis of the convergence of the differencing scheme for the equation

$$\ddot{f} = f'' + \frac{3f'}{r} - \frac{4rf'}{f^2 + r^2} + \frac{2f}{f^2 + r^2} \left(\dot{f}^2 - f'^2 \right). \tag{B.14}$$

We will show that as $\triangle r \to 0$ and $\triangle t \to 0$ that the solution found for f(r,t) converges to an actual solution of the partial differential equation. As in this entire chapter, the arguments will essentially mimic those given before in section A.7.

Substituting the appropriate differences into [B.14] and forward integrating the equation one can solve for $f_c(r, t + \Delta t)$, where f_c is used instead of f(r,t) to indicate it is a calculated value (at (r,t)). One obtains

$$f_c(r, t + \Delta t) = 2f_c(r, t) - f_c(r, t - \Delta t)$$

$$+ \Delta t^2 \left[f_c'' + \frac{3f_c'}{r} - \frac{4rf_c'}{f_c^2 + r^2} + \frac{2f_c}{f_c^2 + r^2} \left(\dot{f}_c^2 - f_c'^2 \right) \right].$$

Here we also assume the derivatives are represented by the appropriate differences as outlined in previous sections. Approximate $f_c(r, t + \Delta t)$ for use in \dot{f}_c^2 by using first $f_c(r, t + \Delta t) = 2f_c(r, t) - f_c(r, t - \Delta t)$ and then iterating the solution found for $f_c(r, t + \Delta t)$ six times, finding a new one from solving with the previous value. Using a greater number of iterations on $f_c(r, t + \Delta t)$ does not change the answer to the numerical precision on the computer, so this is not considered a source of error.

The error comes from the discretizations. If we let $\triangle t^2C_1$ be the error in the difference for \ddot{f} and C_2 be the accumulated error in the differences for the left hand side of [B.14], then one may complete the exact same computations as in section A.8 to find the error in n steps is bounded by

$$|f(r,t+n\triangle t) - f_c(r,t+n\triangle t)| \leq n\triangle t^2(|C_1| + |C_2|)$$
$$+\triangle tC_3(|C_1| + |C_2|)$$

where C_3 is a constant.

Taylor's theorem will be applied extensively to the terms of equation [B.14] to show that C_1 and C_2 are constants. We see

$$\ddot{f}(r,t) = \frac{f(r,t+\Delta t) + f(r,t-\Delta t) - 2f(r,t)}{\Delta t^2} - \frac{\Delta t^2}{12} \frac{\partial^4 f}{\partial t^4}(r,\eta_1)$$

$$\frac{4rf'(r,t)}{f^2(r,t) + r^2} = \frac{2(f(r+\Delta r,t) - f(r-\Delta r,t))}{\Delta r(f^2(r,t) + r^2)}$$

$$+ \frac{4r}{f^2(r,t) + r^2} \left(\frac{\Delta r^2}{6} \frac{\partial^3 f}{\partial r^3}(\xi_1,t)\right)$$

$$\frac{2f(r,t)\dot{f}^2(r,t)}{f^2(r,t) + r^2} = \frac{f(r,t)(f(r,t+\Delta t) - f(r,t-\Delta t))^2}{2\Delta t^2(f^2(r,t) + r^2)}$$

$$-\left(\frac{2f(r,t)(f(r,t+\Delta t)-f(r,t-\Delta t))}{\Delta t(f^{2}(r,t)+r^{2})}\right) \times \left(\frac{\Delta t^{2}}{6}\frac{\partial^{3}f}{\partial t^{3}}(r,\eta_{2})\right)$$

$$+\frac{2f(r,t)}{f^{2}(r,t)+r^{2}}\left(\frac{\Delta t^{2}}{6}\frac{\partial^{3}f}{\partial t^{3}}(r,\eta_{2})\right)$$

$$\frac{2f(r,t)f''^{2}(r,t)}{f^{2}+r^{2}} = \frac{f(r,t)(f(r+\Delta r,t)-f(r-\Delta r,t))^{2}}{2\Delta r^{2}(f^{2}(r,t)+r^{2})}$$

$$-\left(\frac{2f(r,t)(f(r+\Delta r,t)-f(r-\Delta r,t))}{\Delta r(f^{2}(r,t)+r^{2})}\right) \times \left(\frac{\Delta r^{2}}{6}\frac{\partial^{3}f}{\partial r^{3}}(\xi_{2},t)\right)$$

$$+\frac{2f(r,t)}{f^{2}(r,t)+r^{2}}\left(\frac{\Delta r^{2}}{6}\frac{\partial^{3}f}{\partial r^{3}}(\xi_{2},t)\right)$$

The first of these equations, for example, says that if

$$\frac{\partial^4 f}{\partial t^4}(r,\eta_1)$$

is bounded then the error $C_1 \to 0$ as $\Delta t^2 \to 0$. If f(r,t) is chosen in C(4,4), the space of functions with five bounded space/time derivatives, all of these differences have bounded errors.

Now we must attend to the discretization error for

$$f''(r,t) + \frac{3f'(r,t)}{r} \approx \left[\left(r + \frac{\triangle r}{2} \right)^3 \left(\frac{f(r+\triangle r,t) - f(r,t)}{\triangle r} \right) - \left(r - \frac{\triangle r}{2} \right)^3 \left(\frac{f(r,t) - f(r-\triangle r,t)}{\triangle r} \right) \right] / (r^3 \triangle r).$$
(B.15)

If we let $h(r) = r^3 f'(r)$ we have:

$$h'(r) = 3r^2f'(r) + r^3f''(r) = r^3\left(f''(r) + \frac{3f'(r)}{r}\right)$$

$$h''(r) = 6rf'(r) + 6r^2f''(r) + r^3f'''(r)$$

$$h'''(r) = 6f'(r) + 18rf''(r) + 9r^2f'''(r) + r^3f^{(4)}(r).$$

Using the appropriate Taylor Series, one can calculate that

$$h'(r) = \frac{h(r + \frac{\triangle r}{2}) - h(r - \frac{\triangle r}{2})}{\triangle r} - \frac{\triangle r^3}{24}h'''(\eta).$$

Now if we allow

$$\rho_1 \in \left[r - \frac{\triangle r}{2}, r + \frac{\triangle r}{2} \right]$$

and substitute, to obtain

$$r^{3}\left(f''(r) + \frac{3f'(r)}{r}\right) = \frac{\left(r + \frac{\triangle r}{2}\right)^{3} f'\left(r + \frac{\triangle r}{2}\right) - \left(r - \frac{\triangle r}{2}\right)^{3} f'\left(r - \frac{\triangle r}{2}\right)}{\triangle r} - \frac{\triangle r^{3}}{24} \left(6f'(\rho_{1}) + 18rf''(\rho_{1}) + 9r^{2}f'''(\rho_{1}) + r^{3}f^{(4)}(\rho_{1})\right)$$
(B.16)

Now calculate central difference approximations for $f'(r + \Delta r/2)$ and $f'(r-\Delta r/2)$ and substitute into [B.16]. Let $\rho_2 \in [r, r+\Delta r]$ and $\rho_3 \in [r-\Delta r, r]$. The resultant equation is

$$f''(r,t) + \frac{3f'(r,t)}{r} = \left[\left(r + \frac{\Delta r}{2} \right)^3 \left(\frac{f(r + \Delta r, t) - f(r,t)}{\Delta r} \right) - \left(r - \frac{\Delta r}{2} \right)^3 \left(\frac{f(r,t) - f(r - \Delta r,t)}{\Delta r} \right) \right] / (r^3 \Delta r) - \left[\frac{\left(r + \frac{\Delta r}{2} \right)^3}{r^3 \Delta r} \right] \left(\frac{\Delta r^2}{24} \frac{\partial^3 f}{\partial r^3} (\rho_2, t) \right) + \left[\frac{\left(r - \frac{\Delta r}{2} \right)^3}{r^3 \Delta r} \right] \left(\frac{\Delta r^2}{24} \frac{\partial^3 f}{\partial r^3} (\rho_3, t) \right) - \frac{\Delta r^3}{24r^3} \left(6f'(\rho_1) + 18rf''(\rho_1) + 9r^2 f'''(\rho_1) + r^3 f^{(4)}(\rho_1) \right).$$

Once again one sees that if f(r,t) is chosen in C(4,4), the error in this difference is bounded. Under this condition, putting all of this information together, we expect the error in

$$|f(r, t + n\triangle t) - f_c(r, t + n\triangle t)| \le K\triangle t$$

where K is bounded and $K \to 0$ only when both $\Delta t \to 0$ and $\Delta r \to 0$, but not when only one of Δt or Δr go to zero.

To confirm this, convergence tables have been created for this program. f(0,60) and f(10,60) are used as indicators.

First, the convergence as $\Delta t \to 0$ is investigated. One run is made with $\Delta r = 0.100$ and $\Delta t = 0.001$, since we cannot do a run with Δr and Δt infinitely small, and the stability analysis tells us that we must keep $\Delta t \leq C\Delta r^{3/2}$. Call this f_{∞} . Then Δt is allowed to take on a variety of larger values and each time we can find the errors $E0 = |f(0,60) - f_{\infty}(0,60)|$, $E10 = |f(10,60) - f_{\infty}(10,60)|$, $h = \Delta t - 0.001$. Then with any two of these one can calculate

$$\ln(E0_a/E0_b)/\ln(h_a/h_b)$$
 and $\ln(E10_a/E10_b)/\ln(h_a/h_b)$ (B.17)

In this problem, this quotient of natural logarithms should be close to 1 since in theory the error is $K\triangle t$.

The complete set of initial conditions are f(0,t) = 1.0, $R_{\text{max}} = 100$, $\dot{f}(0,t) = -0.01$. The data is in Table B.1.

In Table B.1, skipping the first row and proceeding downward, calculate Table B.2, where the previous line is the line associated with subscript "a" in

equation [B.17], and the current line is associated with subscript "b" in equation [B.17]. It is clear that the quotient of the natural logarithms as in [B.17] is close to one and gets closer as the size of $\triangle t$ decreases, as the theory predicts.

Next, the convergence as $\Delta r \to 0$ is investigated. One run is made with $\Delta r = 0.01$ and $\Delta t = 0.001$, since we cannot do a run with Δr and Δt infinitely small, and consider this to be the value of f_{∞} . Then Δr is allowed to take on a variety of larger values. Likewise, we calculate the values in [B.17], but this time, our theory has no prediction for the value, as the error is predicted to decrease as $K\Delta t$.

Again, the complete set of initial conditions are f(0,t) = 1.0, $R_{\text{max}} = 100$, $\dot{f}(0,t) = -0.01$. The data is in Table B.3.

In Table B.3, skipping the first row and proceeding downward, calculate Table B.4, where the previous line is the line associated with subscript "a" in equation [B.17], and the current line is associated with subscript "b" in equation [B.17]. The quotient of natural logarithms is closest to being an integer when the error caused by Δr is much greater than the error caused by Δt . This is as this sort of analysis would predict when the error is a sum of a piece that goes to zero as $\Delta r \to 0$ and another piece that goes to zero as $\Delta t \to 0$.

Table B.1: $\mathbb{C}P^1$ model, charge 1 sector: Convergence data 1.

$\triangle r$	$\triangle t$	f(0, 60)	f(10, 60)
0.1	0.001	0.433979230592	0.431548378650
0.1	0.0025	0.434046902945	0.431616258041
0.1	0.005	0.434159692320	0.431729392396
0.1	0.0075	0.434272484358	0.431842529337
0.1	0.0125	0.434498076252	0.432068810954

Table B.2: $\mathbb{C}P^1$ model, charge 1 sector: Convergence data 2.

h	E0	E10	$\ln \text{ quot. } E0$	ln quot. $E10$
0.0015	0.0000676724	0.0000678794		
0.0040	0.0001804617	0.0001810137	1.000011111	1.000011077
0.0065	0.0002932538	0.0002941507	1.000024846	1.000024070
0.0115	0.0005188457	0.0005204323	1.000040720	0.994688335

Table B.3: $\mathbb{C}P^1$ model, charge 1 sector: Convergence data 3.

$\triangle r$	$\triangle t$	f(0, 60)	f(10, 60)
0.010	0.001	0.434213647771	0.431709360602
0.020	0.001	0.434206452051	0.431707448176
0.025	0.001	0.434201061431	0.431704981289
0.040	0.001	0.434177743230	0.431691546698
0.050	0.001	0.434156269734	0.431677574831
0.100	0.001	0.433979230592	0.431548378650
0.200	0.001	0.433312345450	0.431017145989

Table B.4: $\mathbb{C}P^1$ model, charge 1 sector: Convergence data 4.

h	E0	E10	\ln quot. $E0$	\ln quot. $E10$
0.010	0.0000071957	0.0000019124		
0.015	0.0000125863	0.0000043793	1.37897263	2.043406152
0.030	0.0000359045	0.0000178139	1.512310436	2.024231211
0.040	0.0000573780	0.0000317858	1.629570850	2.012779570
0.090	0.0002344172	0.0001609820	1.735588896	2.000508645
0.190	0.0009013023	0.0006922146	1.802345190	1.952054808

Bibliography

- [1] M. F. Atiyah. *Geometry of Yang-Mills Fields*. Accademia Nazionale Dei Lincei Scuola Normale Superiore, 1979.
- [2] Robert Leese. Low-energy scattering of solitons in the $\mathbb{C}P^1$ model. Nuclear Physics B, 344:33–72, 1990.
- [3] B. Piette and W. J. Zakrzewski. Shrinking of solitons in the (2+1)-dimensional S^2 sigma model. *Nonlinearity*, 9:897–910, 1996.
- [4] Wojciech J. Zakrzewski Robert A. Leese, Michel Peyrard. Soliton stability in the $O(3)\sigma$ model in (2+1) dimensions. *Nonlinearity*, 3:387–412, 1990.
- [5] J. M. Speight. Low-energy dynamics of a $\mathbb{C}P^1$ lump on the sphere. J. Math. Phys., 36:796, 1995.
- [6] D. Stuart. The geodesic approximation for the Yang–Mills–Higgs equations. Commun. Math. Phys., 166:149–190, 1994.
- [7] R. S. Ward. Slowly-moving lumps in the $\mathbb{C}P^1$ model in (2+1) dimensions. Physics Letters, 158B(5):424–428, 1985.
- [8] Wojciech J. Zakrzewski. Soliton-like scattering in the $O(3)\sigma$ model in (2+1) dimensions. *Nonlinearity*, 4:429–475, 1991.

\mathbf{Vita}

Jean-Marie Linhart was born in Melrose Park, Illinois on June 2, 1969, the daughter of Harriet Roeters Linhart and Carl George Linhart. After completing her work at Oak Park and River Forest High School, Oak Park, Illinois, in 1987, she entered The University of Chicago in Chicago, Illinois. She received the degree of Bachelor of Science in Mathematics from the University of Chicago in June 1990. She entered the Graduate School of The University of Texas at Austin in August of 1990. During the summer of 1991 she was employed at Lawrence Livermore National Laboratories in the Global Climate Research group. While working on her Master's degree, she worked as a Teaching Assistant in the Department of Mathematics at the University of Texas at Austin. She received the degree of Master of Arts in Mathematics from the University of Texas in May 1993. She then worked at Lawrence Livermore National Laboratory in the Global Climate Research group until June of 1994. From July of 1994 to October of 1995, she was employed as a Mathematics Instructor at ITT Technical Institute in Austin Texas. In August of 1995, she returned to the Graduate School of The University of Texas. From August 1995 to August 1997, she was employed in the Department of Mathematics at The University of Texas at Austin as a Teaching Assistant and Assistant Instructor. During the summer of 1996 she was employed by Schlumberger Well Services in the Formation Evaluation department. She returned to em-



 $[\]overline{\ ^{\ddagger}\text{LATeX}}$ is a document preparation system developed by Leslie Lamport as a special version of Donald Knuth's TeX Program.